

# **The role of primary visual cortex in visual discrimination**

Chi-Yu Lee

A dissertation submitted in partial fulfilment of the requirements for the degree of

**Master of Philosophy**

Of

**University College London**

University College London

Submitted: September 10<sup>th</sup> , 2021

Revised: February 12<sup>nd</sup> , 2022

Word count: 21486

I, Chi-Yu Lee confirm that the work presented in this thesis is my own. Where information has been derived from other sources, I confirm that this has been indicated in this thesis

**Signature Redacted**

## *Abstract*

Visual discrimination is important for visually guided behaviours. Previous research has suggested the importance of primary visual cortex (V1), among other regions, in visual discrimination. Nevertheless, the role V1 plays in visual discrimination remains largely unclear. Recent advances in techniques such as optogenetics and DREADD (designer receptor exclusively activated by a designer drug), which allow manipulation of a particular region or neuronal population, open opportunities for a better understanding of the role of V1 in visual discrimination. Here I used hM4Di, an inhibitory DREADD, to ask what role V1 plays in mouse visual discrimination, for ethologically valid stimuli.

We virally expressed hM4Di in V1 and examined efficacy of hM4Di manipulation *in vivo* by recording local field potential while presenting a battery of visual stimuli. We found that hM4Di manipulation enhances low-frequency oscillation and visual-evoked responses to slowly flickering grating stimuli. I then performed behavioural experiments after expressing hM4Di, to test if V1 is required for visual discrimination in mice. We found no evidence for an influence of hM4Di on the probability of responding to sweeping (a latent visual threat), or looming (an imminent visual threat) stimuli. In addition, I developed a new visual object recognition (VOR) assay to study spontaneous visual discrimination. Both hM4Di and control groups showed neophilia over novel objects, indicating that hM4Di manipulation in V1 did not disrupt the visual discrimination between novel and familiar objects.

These finding suggests that hM4Di manipulation in V1 does influence activity in V1 but does not disrupt (a) visual detection of visual threats; (b) visual discrimination.

V1's involvement in visual discrimination of ethologically valid stimuli therefore remains to be determined.

## *Impact Statement*

Sensory and motor systems receive information from the environment and support response to the environment. How sensory signals are transformed into motor commands remains largely unknown. We used viruses to insert small molecules (DREADDs) into neurons in the visual part of the cerebral cortex (V1), so that we could repeatedly manipulate the same neural population while monitoring the response of mice under different types of visual tasks. We used hM4Di, an ‘inhibitory’ DREADD that suppresses neural activity. hM4Di is a popular tool but its *in vivo* efficacy in cerebral cortex remains unclear. To address this concern, we made chronic electrophysiological measurements from mice expressing hM4Di in V1 and find evidence for the *in vivo* efficacy in of hM4Di - which enhances low-frequency oscillations and visual-evoked responses to slowly modulated stimuli.

In addition, I provide new behavioural assays, which allowed us to study the effect of expressing hM4Di in V1 on visual discrimination. In one assay, we found limited effects of hM4Di manipulation on the detection of visual threats, suggesting that V1 may not be required for detecting visual threat. In the second assay, I developed a new visual object recognition (VOR) test to study visual discrimination, exploiting neophilia in mice. we found that hM4Di manipulation does not influence visual discrimination in this assay, suggesting that V1 might be required for fine discrimination instead of coarse discrimination.

Thus, this thesis describes new protocols to address the *in vivo* efficacy of hM4Di, and new protocols for measuring visually-guided behaviour. The thesis contributes to our knowledge about the potential role of V1 in visual discrimination for instinctive

behaviours. Finally, these experiments contributed to developing BonVision (Lopes et al., 2021), an open-source graphics programming library to help all researchers study visual neuroscience.

## *Acknowledgement*

I would like to thank *Sam Solomon* and *Aman Saleem* for their continued supervision, support and encouragement in the course of my studies in UCL. Especially I would like to thank *Sam*. We met almost every Tuesday 9:00 over the past two years. I would also like to thank the following people:

*Stefano Zucca, Thomas Wheatcroft, Fabio Rodrigues, Amalia Papanikolaou, and Joanna Holeniewska*, for their continued support throughout my MPhil project.

*Adam Kampff, Catherine Perrodin* for being the member of my thesis committee.

Members of the *Solomon/Saleem lab* and *IBN* for creating a lovely workplace and reminding that I would find a lot of bugs if I kept coding after 22.00.

*Gonzalo Lopez* and *Bonsai* forum for creating an open scientific community.

*Sainsbury Wellcome Centre* for providing financial support. This project would not have been possible without you.

*SWC FabLab* and *UCL Biological Services* for providing me the services to finish this project.

*UCL Student Mediator, Student Support and Wellbeing Adviser, Student Psychological and Counselling Services* and other unsung heroes for career advices.

*UCL statistics consultancy, Virginia Rutten, Fei-Yang Huang, Hung Lo, Wei-Hsiang Lin, Takeru Matsuda, Changle Chen, Ben Grainger and Matthew Edwards* for scientific discussion.

*Chih-Yao Chung, Wenkui Liu, Annie Chen, Kenneth Ho, Anjui Wu, Yuki Akimoto,*

*Yoko Onodera, Lucy Callen, Rachel Valbrun, Elisabeth Gunawan, Izabella Smolicz,*

*Monfans Tai, Selina Maria, Jeffrey Foreman, YM Chen, Ralph Day, Daniel*

*Whitehorn, Inez McGregor, Nick Fitzhenry, Kazuki Shimizu, Sam Robbins, ChaoYi*

*Chang, Wenkai Xu, Heyshiro Kanagawa, Liang Zhou, and Charles Parsons* for bringing joy to London.

*Egzona Morina and XhM foundation* for giving me great teaching opportunities.

Members of the *Pub On Air, Formosa Salon and Goodenough College* for interesting debate and discussion.

*Danbee Kim, Marnie Howlett* and *ghostmyfriend*-positive doodles for being such a great inspiration in London.

And last but not least; my parents and brother for their genuine support.

This research project came out as a surprise. I did not plan to study cortex, but I guess life does not follow a plan. I just took all the surprises as energy for me to grow. In the end, I am glad that I finished it.

## *Contents*

Abstract .....	3
Impact Statement .....	5
Acknowledgement .....	7
Abbreviation List.....	13
Chapter 1: Overview of visual neuroscience .....	14
1.1 Natural behaviours .....	14
1.2 Visual neuroscience .....	15
1.3 Visually guided behaviours .....	16
1.3.1 Collision/predation defensive behaviours .....	17
1.3.2 Vision-based memory tasks .....	18
1.4 Experimental approaches in visual neuroscience .....	19
1.5 Circuits for visual guided behaviour.....	21
1.5.1 Primary visual cortex (V1).....	22
1.5.2 Superior colliculus (SC) .....	24
1.6 Aims of this study .....	25
Chapter 2: Research methods .....	26
2.1 Animals and viruses .....	26
2.2 Stereotaxic surgery.....	26
2.3 LFP recording .....	27
2.4 Visual Stimuli .....	30

2.5 Loom-sweep behavioural assay .....	31
2.6 Visual object recognition assay .....	32
2.7 Histology .....	33
2.8 CNO treatment .....	34
2.9 Data Analysis .....	34
Chapter 3: Physiological evidence for impact of hM4Di manipulation in V1 .....	37
3.1 Introduction .....	37
3.1.1 DREADDs in neuroscience .....	37
3.2 Results .....	39
3.2.1 Confirmation of hM4Di expression in V1 .....	40
3.2.2 Limited effect of hM4Di on VEP waveform shape and amplitude .....	42
3.2.3 No effect of hM4Di on contrast sensitivity .....	46
3.2.4 TF tuning in hM4Di mice .....	48
3.2.5 Tentative increase in low-frequency oscillations during CNO administration .....	52
3.2.6 Limited off-target effects of CNO on delta power .....	53
3.3 Discussion .....	57
3.3.1 Impact of locomotion on VEP amplitude .....	57
3.3.2 Influence of contrast on VEP amplitude and latency .....	57
3.3.3 Limited effects of hM4Di manipulation on VEP amplitude and contrast sensitivity.....	58
3.3.4 TF tuning and baseline harmonic signals in hM4Di mice.....	59

3.3.5 Effects of hM4Di manipulation on harmonic signals and delta power.....	60
3.3.6 Experimental limitations .....	62
3.7 Summary .....	63
Chapter 4: Behavioural impact of hM4Di manipulation in visual discrimination .....	64
4.1 Introduction.....	64
4.2 Results.....	66
4.2.1 hM4Di manipulation in Sweep-Loom assay.....	66
4.2.2 Limited effects of hM4Di manipulation on exploratory behaviours.....	69
4.2.3 Limited effects of hM4Di manipulation on visual detection .....	72
4.2.4 Mice freeze more often than escape in sweep-loom assay.....	72
4.2.5 A new visual object recognition assay .....	77
4.2.6 Limited effects of hM4Di manipulation in the VOR assay .....	82
4.3 Discussion .....	86
4.3.1 Variable responses to looming stimulus .....	86
4.3.2 Limited effects of hM4Di manipulation in visual detection and defensive behaviours .....	88
4.3.3 Establishment of a new VOR assay.....	90
4.3.4 Limited effect of hM4Di on visual discrimination .....	91
4.3.5 Experimental limitations .....	92
4.4 Summary .....	92
Chapter 5: Conclusion.....	94
5.1 Experiments to validate the impact of hM4Di manipulation on V1 function.....	95

5.2 Alternative methods to inhibit V1 output .....	97
5.3 Potential role of V1 in innate visually-guided behaviours .....	98
5.4 Summary .....	100
Chapter 6: Bibliography.....	102

### *Figure List*

#### Chapter 2

Fig. 1: Experimental design of chronic LFP recording.....	29
---	----

#### Chapter 3

Fig. 1: LFP recording in hM4Di-expressing V1.....	41
Fig. 2: hM4Di inactivation of V1 does not increase the VEP amplitude.....	44
Fig. 3: hM4Di inactivation of V1 does not increase the contrast sensitivity.....	47
Fig. 4: hM4Di inactivation of V1 enhances responses to low-frequency gratings....	50
Fig. 5: hM4Di inactivation of V1 increases low-frequency oscillation.....	55

#### Chapter 4

Fig. 1: hM4Di manipulation in sweep-loom assay.....	67
Fig. 2: Mice exploration in the acclimation phase.....	71
Fig. 3: Limited effect of hM4Di manipulation on visually guided behaviours.....	75
Fig. 4: A visual object recognition assay.....	80
Fig. 5: Limited effect of hM4Di manipulation on visual object recognition.....	84

Appendix I hM4Di expression and the location of LFP electrode in different mice..	128
---	-----

## *Abbreviation List*

**AAV** Adeno-Associated Virus

**ANOVA** Analysis of variance

**AP** anterior-posterior

**AUC** area under curve

**CaMKII $\alpha$**  Ca<sup>2+</sup>/calmodulin-dependent  
protein kinase II

**CNO** clozapine-N-oxide

**DAPI** 4',6-diamidino-2-phenylindole

**DC** direct current

**dLGN** dorsal lateral geniculate nucleus  
of the thalamus

**DREADD** Designer receptors  
exclusively activated by designer  
drugs

**EEG** electroencephalogram

**fEPSP** field excitatory postsynaptic  
potential

**GABA** gamma-Aminobutyric acid

**GFP** green fluorescent protein

**GIRK** G-protein inwardly rectifying  
potassium channels

**HA** hemagglutinin

**I.P injection** intraperitoneal injection

**LFP** local field potential

**ML** medial-lateral

**MT/V5** middle temporal visual area

**O.C.T** Optimal cutting temperature  
compound

**PBS** Phosphate-buffered saline

**RSP** Retrosplenial cortex

**SC** superior colliculus

**S.E.M** standard error of the mean

**SRP** stimulus-specific response  
potentiation

**TF** temporal frequency

**V1** primary visual cortex

**VEP** visual evoked potential

**VISP** primary visual cortex

## *Chapter 1: Overview of visual neuroscience*

One of the most fundamental questions in neuroscience is how the nervous system receives information from the environment and responds to that information. While sensory and motor systems are usually studied separately, to characterise the input and output mechanisms of the nervous system, how sensation guides behaviour remains largely understood. The fundamental difficulty is our limited knowledge of what the relevant level of brain organization is for any given behaviour, especially for those behaviours that happen in a sequence, which potentially require context-dependent action. This difficulty calls for the need to study the contribution of brain areas to those complex behaviours.

### *1.1 Natural behaviours*

Classic studies on ecology and biological psychology have accumulated knowledge about natural behaviours such as navigation and foraging across animal species. These behaviours involve actions and goals occurring on different time scales. For example, pursuit behaviours are often studied with appetitive stimuli to induce an action, such as grasping or chasing behaviour, which may occur within as little as one second. But the motivation to grasp or chase an object in response to the appetitive stimulus may have accumulated hours or days before. Thus, studies on natural behaviours span multiple disciplines with the use of various animal models. While some animal species including mice, cats and monkeys have been used to understand the neural mechanisms behind these natural behaviours, other species have been assessed with more complicated behavioural tasks to understand biomechanical mechanisms and ecological impact of animal behaviours (Hein et al., 2020).

Experimental paradigms investigating natural behaviours have two features (Juavinett et al., 2018). One is the ease for animals to adopt the behavioural paradigm. Ethological stimuli tend to elicit stereotypic behaviours that are preserved in the organism's evolutionary history, which may facilitate animals learning a task. However, failure to respond to that stimuli may arise from deficits in detecting the stimuli or reacting to the stimuli rather than engaging in the behavioural paradigm. Secondly, a hypothesis suggesting that neurons at a higher hierarchical structure may respond more reliably to ethological stimuli than other stimuli (Carruthers et al., 2015), as neurons from a higher hierarchical structure of the sensory system such as cortex may form invariant representation of certain sensory stimuli. This property can make animal respond reliably to the stimuli. Thus, understanding why an ethological stimulus becomes ethologically relevant can serve as an important insight of the coding mechanism in those higher hierarchical structure.

## *1.2 Visual neuroscience*

Vision is the best understood sensory modality and provides theoretical foundations for general coding principles in the brain and in artificial neural networks. Early studies in cats and primates revealed a hierarchical of processing in the visual system, such that a serial, feedforward circuit of sensory and relay neurons can account for the firing properties at the next hierarchy (Hubel & Wiesel, 1963 & 1968). Neurons at successive stages in a sensory pathway tend to have larger receptive fields and are tuned to more elaborate features of the sensory stimulus. In studies of patients with focal brain damage, temporal lesions are associated with visual recognition deficits whereas parietal lesions may impair spatial localisation (Newcombe & Russell, 1969). These clinical studies, together with tracing and lesion

experiments on animals, became the basis of theories of two visual pathways, the “what” and “where” pathways (Mishkin et al., 1983).

Several visual tests developed in human subjects have been applied to monkeys, cats and rodents. Some classic behavioural paradigms use visual cues to study other cognitive function such as numerical cognition (Nieder et al., 2002) and self-recognition (Gallup Jr., 1969). In practice, the spatial and temporal properties of visual stimuli can be precisely manipulated with monitor displays. In addition, free open-source software has been developed to create visual stimuli, even in closed-loop experiments (Peirce, 2009; Štih et al., 2019; Lopes et al., 2021). These technical advantages mean that visual stimuli are frequently used to understand physiology and behaviour, even when the scientific question is not about vision.

Primates and cats have been the main models to study vision. However, because of recent advances in genetic tools, shorter research life cycle, and even experimental cost, rodents have become a popular animal model for vision. Despite rodents’ poor visual acuity, the visual cortex of rodents shares features with that of cats and primates, including six-layered structure, retinotopic organization and orientation selectivity in primary visual cortex (V1) (for a review, see Huberman & Niell, 2011).

### *1.3 Visually guided behaviours*

Visual information reveals an object’s size, shape and identity, and these features guide behavioural responses. A classic example is the male stickleback’s aggression response to red spots (Tinbergen, 1951). Tinbergen observed male sticklebacks’ attack pattern during mating session and theorised that this is triggered by the red

spot on another male stickleback's underside. He then tested this hypothesis with wooden models and found that stickled male sticklebacks would react to wooden models only with red spots at their bottom. This experiment clearly showed that aggression behaviour is innate and can be triggered by visual cues. Furthermore, based on clinical studies, visually guided behaviour can be implemented without a phenomenal awareness of visual information. 'Blindsight' patients with damage to the primary visual cortex were able to respond to visual stimuli even in the absence of their (self-reported) perception (Weiskrantz, 2009). In this thesis, visually guided behaviours are defined as vision-based innate behaviours exhibited without learning a rule or receiving external reward or punishment. These behavioural assays are based on animals' incentive to maximise their chances of survival, for example, seeking for food or avoiding danger, and some of them adopt ethological valid sensory stimuli to trigger a certain behaviour. In this thesis, I will focus on collision/predation-based defense and vision-based memory tasks.

### *1.3.1 Collision/predation defensive behaviours*

Collision/predation-based defensive behaviours have been studied across different species. It is important for survival as collision/predation can reduce target animals' fitness or cause lethal damage to animals. To reduce harm from collision or predator, animals need respond timely to decide how to avoid potential physical contact. This impending collision can be predicted based on the movement of objects without prior experience. For example, the size of a moving object over time tells us whether the object is approaching (when its size enlarges over the course of time) or avoiding (when its size shrinks over time) us.

Early studies reported that human infants or monkeys show avoidance behaviour when seeing an object or a shadow of the object approaching their head (Schiff et al., 1962; Ball & Tronick, 1971). In mouse studies, an overhead looming dark spot simulates the silhouette of an approaching predator from the top whereas an overhead sweeping stimulus simulates a potential threat. Mice display a variety of defensive behaviours such as escape and freeze and investigatory behaviours such as rearing behaviours in response to looming stimulus and sweeping stimulus (Yilmaz & Meister, 2013; De Franceschi et al., 2016). In terms of defensive behaviours, the decision to escape or freeze depends on a variety of environmental factors such as whether an escape route is available, distance between the animal and shelter, and the estimated time to predation. Increasing contrast level of looming stimuli or speeding up sweeping stimulus increased escape probability in mice, showing how saliency of the sensory input drives the motor vigour.

### *1.3.2 Vision-based memory tasks*

One of the first visual-based memory tasks was designed to measure visual memory and attention in human infants (Fantz, 1964). In this task, infants were repeatedly exposed to a familiar visual pattern of photographs and their ocular movements were recorded to test whether they pay more attention on the familiar pattern rather than other unfamiliar patterns. Later on, this task was adapted to other non-verbal individuals including monkeys and rats. By exploiting individual attraction to novelty (neophilic behaviours), it has become a common way to measure hippocampus dependent memory (Manns, et al., 2000). In rodent studies, this task is known as novel object recognition test, in which animals spontaneously explore objects in an arena. The standard task consists of two phases, the familiarisation phase and the

test phase (Ennaceur, 2010). During the familiarisation phase, a pair of identical objects is placed in the arena. After the familiarisation phase, one of the identical objects, which are now familiar objects, is replaced with a new (novel) object. Different exploration times for the novel and familiar objects is interpreted as the presence of object memory. The task has involved into different forms. For example, presenting multiple different objects during familiarisation phase (Heyser & Chemero, 2012), switching the location of objects during test phase (Genzel et al., 2019), and using visual stimuli only (Forwood et al, 2007; Romberg et al., 2013; Braida et al., 2013; Cooke et al., 2015; Del Grosso et al, 2017).

In addition, several water mazes have been developed to test rodent's navigation (Morris, 1984) or visual acuity (Prusky et al., 2000). In these mazes, rodents navigate to a hidden platform based on visual landmarks around the maze (for navigation) or around the platform (for visual acuity). By presenting multiple visual cues in the maze, this task can also be transformed to assess visual discrimination. For example, placing a fixed (safe) platform in one colour and a floating platform in another colour (Vorhees & Williams, 2006), or presenting one particular visual cue always on top of the safe route but not the other route (Treviño et al., 2013; 2018). The disadvantages of the water maze are the need to use a large maze and that the animals need to swim in the maze – particularly an issue when recording neural activity at the same time.

#### *1.4 Experimental approaches in visual neuroscience*

Traditionally, experimental approaches to the contribution of a brain region to behaviours can be divided in two categories. The first and oldest approach includes

ablation or clinically-observed lesion cases that cause vision deficits (developmental studies that investigate the consequence of early sensory deprivation on the nervous system are out of the scope of this thesis). This approach led to the discovery of occipital lobe as the hub of vision in monkeys (Munk, 1881). However, the effect of a lesion is irreversible and difficult to replicate across subjects.

Alternative approaches, such as infusing GABA and its receptor agonists (Leventhal et al., 2003) or cooling, can reversibly inhibit a particular brain region. The cooling method has been applied to primates (Przybylski et al., 2000) and cats (Ferster et al., 1996) but it is difficult to evaluate the affected region. By contrast, administration of GABA receptor agonist such as muscimol and baclofen, is widely used in different brain regions across various animals (Purushothaman et al., 2012; Ahmadlou et al., 2018). The diffusion of the muscimol can be visualised by conjugating the drug with fluorescent (Allen et al., 2009) or radioactive molecules (Martin, 1991). It is also possible to examine the effect of inhibition on the brain by comparing neural activity or behaviours during baseline, muscimol injection session and recovery session (Marques et al., 2018). Now, transgenic techniques such as optogenetics and chemogenetics allow targeting of a particular neural population, and manipulation of neural activity at millisecond resolution (in the case of optogenetics). Researchers can use these genetic tools to examine the same animal's behavioural output repeatedly while manipulating their neural activity. I will discuss the use of transgenic techniques further in the following chapters.

The second approach involves recording neural activity during behavioural tasks. By recording neuron activity of interest when the animal performs a vision-based task, we can analyse task-related activity, unravelling neural correlates of visual

performance. A stimulation paradigm can be added to test the causality of the correlation (Ditterich et al., 2003). In addition, task irrelevant movement such as running in a head-fixed condition (Niell & Stryker, 2010) or pupil dynamics (Reimer et al., 2014) can reveal the animal's behavioural state, and drive responses. The precise measure of pupil dynamics also benefits various behavioural tasks. With advances in head-mounted camera system (Wallace et al., 2013; Meyer et al., 2018; Sattler & Wehr, 2020), recent studies have been able to reconstruct the visual scene of freely moving mice (Meyer, et al., 2020; Holmgren et al., 2021; Parker et al., 2022). This would help researchers precisely identify the task related activity, filling the technical gaps between head-fixed and freely moving recordings.

### *1.5 Circuits for visual guided behaviour*

Visual stimuli are transduced at the retina and sent to the brain via several specialized pathways, two of which are of particular relevance here. One reaches V1 via the dorsal lateral geniculate nucleus (LGN) and the other reaches postrhinal and other parts of cortex via superior colliculus (SC). These two pathways provide signals to higher visual regions such as middle temporal area (area MT/V5), a region of extrastriate cortex in primates that is important in processing the direction of visual motion (Newsome & Pare, 1988), and stereoscopic depth perception (Uka & DeAngelis, 2004).

Early studies have revealed particular functions of V1 and SC. V1 is known to be involved in encoding orientation (Hubel & Wiesel, 1963), direction and colour (Livingstone & Hubel, 1984) of visual cues. SC is known to be involved in a variety of visually-guided movements, ranging from in approach and defensive behaviours in

rats (Sahibzada et al., 1986) to saccade movement in monkeys (Mohler & Wurtz, 1977; Feinberg et al., 1978) and is in addition well-known to be a site of multisensory integration (Stanford et al., 2005). Recent studies have focused on the role of SC in vision-based defensive behaviours in rodents (Shang et al., 2015; Wei et al., 2015; Evans et al., 2018). On the other hand, not only visual but motor signals were identified in V1 during navigation (Saleem et al., 2013), revealing a role in multisensory or even cognitive integration. It is therefore clear that V1 is neither the only source projecting to higher visual areas, nor the only sensory area that influences behaviours. Interestingly, V1 project directly to the ipsilateral SC (May, 2006), but there is no direct projection from SC to V1. Indeed, recent rodent studies have found evidence that V1 modulates neural activity in SC (Zhao et al., 2014; Liang et al., 2015) and vice versa (Ahmadlou et al., 2018), though what separate roles these two regions play in behaviours remains largely unclear. Understanding the functional properties and behavioural roles of these two regions and their connections may provide insights into the mechanism underlying visual-guided behaviours.

### *1.5.1 Primary visual cortex (V1)*

V1 has been extensively studied. For scientists studying visual recognition and spatial navigation, V1 projects extensively to the “what” and “where” pathways and is likely to be the main source for integration and relaying of visual information to higher visual areas. For other scientists, the mechanisms that are used to build functional properties, and the interaction of V1 with other cortical and subcortical areas are of great general interest. There have been many databases (Siegle et al., 2021) and tools (Chen et al., 2013; Jun et al., 2017) that have started by focusing on V1. The

diverse projection of V1 to other brain regions such as higher visual cortex, SC, accessory optic system (AOS), pons and ipsilateral cortex (Hallman et al., 1988; Kasper et al., 1994) made it difficult to investigate V1's involvement in visually guided behaviour. Whether there are V1 pathways transmit particular behaviourally relevant information requires the investigation of a battery of visually guided behavioural assay.

Although the classic view of visual cortex originated from Munk's studies where lesions of the occipital lobes resulted in (cortical) blindness, bilateral lesion of the occipital lobes might only cause a mild deficit in vision. As the technical issues in lesion studies remain, it is difficult to replicate these findings. Recent rodent studies showed that inhibiting V1 with muscimol disrupts visual perceptual learning, such that head-fixed mice cannot respond correctly to the motion of random dots (Marques et al., 2018) or form associations between visual stimuli and air puffs (Tang & Higley, 2020) or detect grating stimuli (Bennett et al., 2013).

In freely moving animals, mice with V1 disruption spent more time navigating to a safe platform (Treviño et al., 2018), or estimated wrong distance to jump to distant platforms (Parker et al., 2021). On the other hand, disrupting V1 with muscimol does not prevent animals from escaping from potential visual threats, and only seems to reduce escape speed (Evans et al., 2018). One explanation for this discrepancy may be that V1 is important for learning, hence, it was required for the perceptual learning, where the mice need to associate between visual cues and certain valence but is not required for innate behaviours. Another explanation is that V1 is required for sensing particular visual stimuli and V1 lesions might simply reduce visual acuity

to sense those feature(Dean, 1978). This explanation rises from lesion studies showing that rats with V1 lesion could differentiate large or low-spatial frequency gratings(Dean, 1978 & 1981) but not small, high spatial frequency gratings (Petruno et al., 2013)

### *1.5.2 Superior colliculus (SC)*

The SC is a laminated structure in vertebrate midbrain (May, 2006). One major input to SC is from the retina - the nasal retina projects to contralateral side of the superficial SC and the temporal retina projects to the superficial layers of the ipsilateral SC. Another major input comes from cerebral cortex, including V1 which projects to the ipsilateral superficial layers, and other cortical regions that project to the intermediate and deep layers of the SC (Wang & Burkhalter, 2013). The two major inputs (retinal and cortical), originating from the same part of visual space, might be integrated at the SC for different purposes.

In primates, the SC is known for its role in directing saccadic movements of the eyes and involved in sensory-motor integration. Stimulating rat SC instead generates two classes of innate responses (Dean et al., 1988). One class involves orienting responses, which includes coordinating body movements for tracking or pursuing. The other class includes defensive behaviours such as freezing and flight actions, which have been frequently studied in combination with visual stimuli, particularly over the past decade.

As SC receives inputs directly from the retina, it is intuitive to consider that in SC retina-derived signals are processed before V1-derived signals. Hence, looming-related signals may be transmitted to SC's downstream targets, such as the

periaqueductal gray, to initiate defensive responses without inputs from V1. This would explain why there is only a mild reduction in escape speed in V1-disrupted mice. However, artificial activation of SC-projecting V1 neurons with optogenetics reduced running speed in head-fixed mice (Liang et al., 2015) and increased freeze probability in freely-moving mice (Zingg et al., 2017). In which contexts V1 inputs influences behaviours via SC remains an open question.

### *1.6 Aims of this study*

Over the past few decades, studies in monkey, cats and rodents have elucidated firing properties in V1 cortical neurons. However, the behavioural assays used to study V1 have been limited to head-fixed and learned behaviours. The aim of this study is to draw a stronger conclusion about the role of V1 in innate behaviours. By applying viral genetic techniques to perturb mouse V1 while the mouse performs vision-based behavioural assays, I hope to understand the role of V1 signals in discriminating among visual stimuli and guiding behaviours. I will achieve this by assessing the following hypothesis: V1 is required for innate behaviours under aversive context, such as discrimination between potential visual threats.

## *Chapter 2: Research methods*

### *2.1 Animals and viruses*

For the DREADD experiments, 7- to 8-weeks old male C57BL/6J mice sourced from Charles Rivers. For pilot experiments in the visual object recognition assay, DAT-Cre<sup>-</sup> mice (offspring of male DAT-IRES-Cre and female C57BL/6J) aged between 8 to 10 weeks were used. AP mice (mice originally used by Amalia Papanikolaou) were male adult C57BL/6J mice. They were recorded at the age of 22 weeks, 8 weeks after AP performed experiments on them. All mice were maintained in the animal facility in the Institute of Behavioural Neuroscience at University College London, under a 12h light cycle and with ad libitum access to food and water. All experiments were performed in accordance with the Animals (Scientific Procedures) Act 1986 (United Kingdom) and Home Office (United Kingdom) approved project and personal licenses. Mice were transferred from the cage to the behavioural assay via their paper tube or cardboard house to minimise stress. AAV8-CaMKIIa-HA-hM4D(Gi)-IRES-mCitrine (henceforth referred to as 'hM4Di virus') and AAV8-CaMKIIa-EGFP (henceforth referred to as 'GFP virus') were purchased through Addgene (Plasmid #50467 and #50469).

### *2.2 Stereotaxic surgery*

Anaesthesia was induced with 3% isoflurane, and maintained at approximately 1.5% isoflurane, in constant flow of oxygen. The head was shaved, and mice transferred to the stereotaxic stage. An incision was made after applying betadine and ethanol on the scalp. After the skull was exposed, 6 injection sites were marked to target V1 in each hemisphere. The coordinates were relative to lambda (AP:  $\pm 0.5$  mm, ML:  $\pm 2.5$  mm; AP: 0 mm, ML:  $\pm 2.5$  mm). For animals in which V1 local field potential

(LFP) to be recorded, 3 injections were made at different locations in the left hemisphere, and 4 injections were made in the right hemisphere. The 4 injection sites in the right hemisphere surrounded the subsequent location of the recording electrode at coordinates (AP: 0.5 mm, ML: 2.5 mm; AP: 0 mm, ML: 2.35 mm; AP: 0 mm, ML: 2.65 mm; AP: -0.5 mm, ML: 2.5 mm). 300nl of the hM4Di or GFP virus was injected at each site, 0.6 mm below the brain surface. The injection was performed by a micromanipulator at 30-50 nl/min. The injection pipette remained in place for 4 mins after the injection finished. A LFP recording electrode (Bear lab chronic microelectrode, 30070, FHC, USA) was then inserted 0.6 mm below the cortical surface, 2.5 mm lateral to the lambda, in the right hemisphere.

For animals that were to be used for behavioural testing, three injections were made into each of the left and right hemispheres and the scalp was closed with sutures.

For LFP recording, a reference electrode was implanted over the left prefrontal cortex and a custom-built metal plate was cemented to the skull. Mice were allowed to recover and housed individually after the surgery; each received 20  $\mu$ l Metacam in condensed milk for 3 days post-surgery.

### *2.3 LFP recording*

Mice were awake, and head-fixed above a styrofoam wheel (radius: 10 cm). Mice were provided with 5 days of habituation to the head fixation before recording started. They were allowed to run on the wheel, and the rotation of the wheel was recorded by a rotary encoder. To monitor pupil dynamics, the left eye was imaged by an infra-red video camera (DMK 22BUC03, ImagingSource) through a zoom lens (Computar MLH-10X Macro Zoom Lens). Saline or CNO treatment was delivered via I.P. injection to mice 1 hour prior to the recording. The first batch of LFP recording

was conducted on 4 hM4Di mice, for 10 sessions per mouse, and the second batch of recording was conducted on 2 hM4Di and 3 GFP mice, for 8 sessions per mouse. Each of four sessions is a recording cycle. Within each cycle, saline-saline session pairs and saline-CNO pairs were counterbalanced across animals (Fig. 1a, right).

Except for 9th and 10th session, every 2 sessions were treated as a pair with a 24-hour interval between them (there was a 48-hour interval between 3rd and 4th sessions in 3 hM4Di mice). The 9th and 10th sessions were conducted 5 days after the previous session.

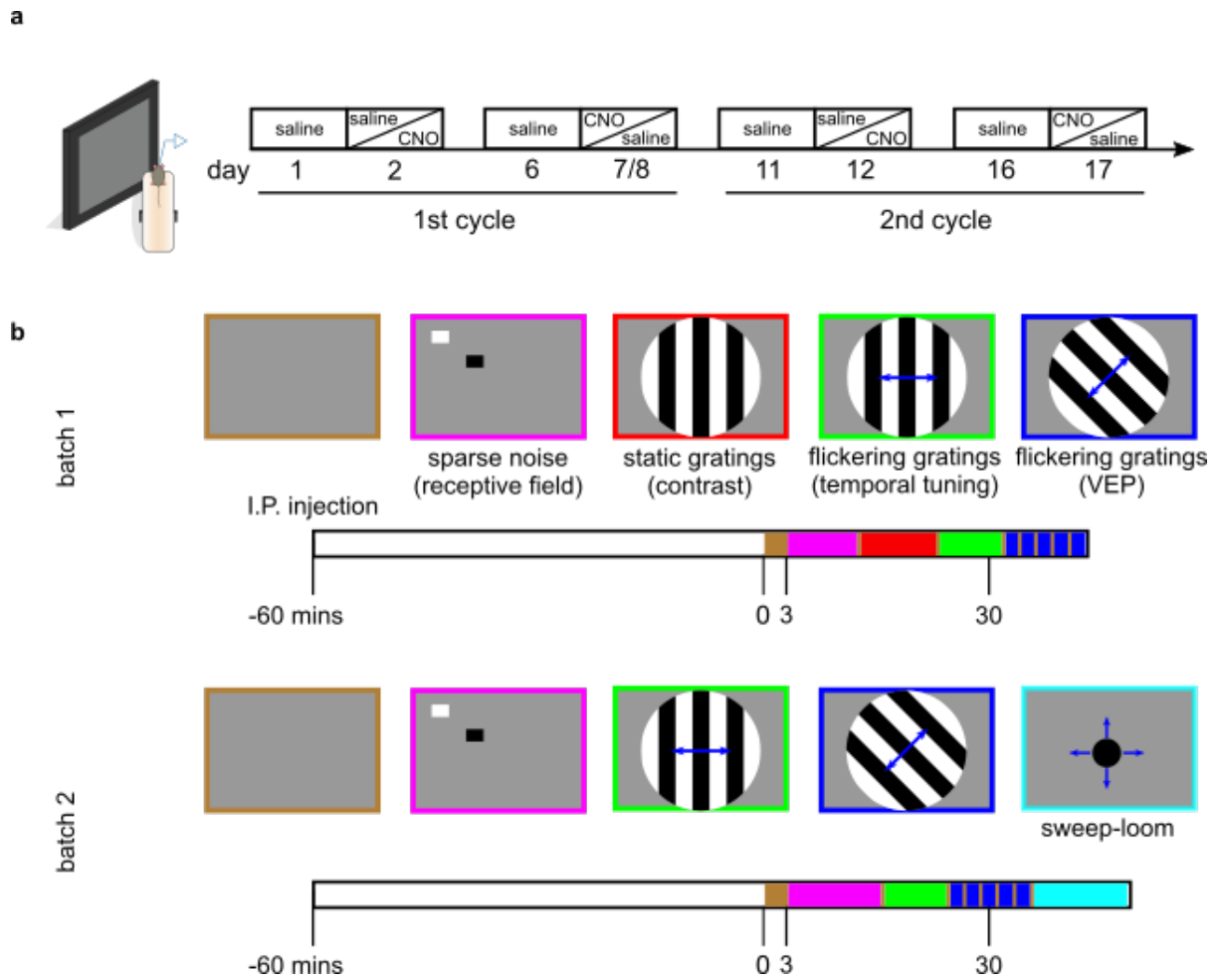


**Fig. 1: Experimental design of chronic LFP recording.**

**a.** Scheme of experimental procedures and treatment. *Left:* diagram denotes a head-fixed mouse sitting in front of a grey screen and above a Styrofoam wheel. *Right:* diagram denotes treatment order given to mice 1 hour prior to LFP recording. For example, 2 mice received saline-saline treatment, and the rest of them received saline-CNO treatment in the first 2 days as shown in the first two rectangle boxes on the timeline. **b.** Scheme of stimulus protocols in recording sessions. Colour in the time bar charts indicates the stimulus type. For instance, in Batch 1, mice first received 3-min grey screen after being head-fixed on the wheel. Then they received sparse noise, static gratings for contrast sensitivity (pink), flickering gratings for TF tuning (green) and flickering gratings for VEP (blue). Except sparse noise, each stimulus protocol proceeded with a 30-sec grey screen (brown).

## 2.4 Visual Stimuli

Visual stimuli were delivered via a PC monitor (ProLite E1980SD, iiyama), which was placed 20 cm from the mouse at a 45° angle (Fig. 1a left), covering the left visual field (contralateral to the recording site in V1). A small stimulus, shielded from the animal, was shown at the edge of the monitor and monitored by a photodiode (PDA25K2, Thorlabs) to provide timing synchronisation.

In the first batch of recordings (Fig. 1b, top), each session started with a 3-min grey screen, followed by presentation of sparse noise, then presentation of static gratings (for contrast sensitivity), then flickering gratings of varying TFs (for TF tuning) and finally flickering gratings of a fixed TF (for visual evoked potentials). In the second batch of recordings (Fig. 1b, bottom), static gratings (for contrast sensitivity) were omitted and were replaced with presentations of sweeping and looming stimuli.

Visual stimuli were generated with BonVision (Lopes et al., 2021). Sparse noise stimuli consisted of 2 white or black squares presented at random locations on a 10x10 grid of positions for 0.5 s without an interstimulus interval. Each square had a width of 8°. Static gratings for studying contrast sensitivity consisted of large sinusoidal gratings with a spatial frequency of 0.05 cycle per degree (cpd) at each of 6 different contrast levels (0 %, 6.25 %, 12.5 %, 25 %, 50 %, and 100 % Michelson contrast). The gratings were presented in pseudo-random order for 1 s, with an inter-stimulus interval of 4 s. Flickering gratings for studying TF tuning consisted of large sinusoidal gratings with a spatial frequency of 0.05 cpd and flickering in counter-phase (sinusoidal temporal modulation) at each of 5 different TF (1 Hz, 2 Hz, 4 Hz, 8 Hz, and 15 Hz). The gratings were presented in pseudo-random order for 2.5 s, with a 2.5 s inter-stimulus interval. Flickering gratings for studying visual evoked

potentials (VEPs) consisted 5 blocks of a large grating of spatial frequency 0.05 cpd, flickering (square wave temporal modulation) at 1 Hz. Each block was preceded by 30s of grey screen, except in 3 hM4Di mice's first 2 sessions. For contrast sensitivity and temporal tuning, the gratings were orientated at 0° from vertical. For VEPs, the gratings were oriented at 45° in the baseline session and -45° in the next day. The sweep-loom stimulus for LFP recording contained 5 blocks of slow loom (expansion speed: 48°/s), fast loom (expansion speed: 192°/s) slow sweep (sweeping speed: 22.5°/s) and slow sweep stimuli (sweeping speed: 56.37°/s). Looming stimulus is a dark spot expanding from 2° to 50°. Sweeping stimulus is a 5° dark spot traveling for 17.7 cm. Each block consists of 10 repeated stimuli of each type of stimuli, presented in pseudo-random order, with 3 s interval stimulus intervals.

AP mice received the stimulus protocol as Batch 1 mice did (Fig. 1b, Top). They had received 45° grating stimuli prior to this experiment so flickering gratings (for VEP) were oriented at -45° in the 1<sup>st</sup> session and 75° in the 2<sup>nd</sup> session.

### *2.5 Loom-sweep behavioural assay*

6 weeks after the virus injection, 8 hM4Di mice and 6 GFP mice were used in the behavioural assay. There were 6 test sessions for each mouse, one session per day, with 3-4 days between each session. In each session the mouse was placed in a 42 x 42cm arena with a 14 cm (wide) x 4.5 cm (high) opening for mice to pass through to a dark nest. Mice were allowed to acclimatise to the arena for 8 mins prior to the first visual stimulus. Two sessions where the mouse became immobile after I.P injection (1 hM4Di/CNO and 1 GFP/Saline session) were removed from analysis. The mouse's position was recorded with an infra-red camera (BlackFly S, FLIR).

Visual stimuli were delivered manually through Bonsai (Lopes et al., 2015) and presented onto a rear projection screen with a projector. The delivery of the stimulus was accompanied by a synchronisation pulse of infrared light, indicating the onset and offset of the stimulus. Stimuli were triggered when the mouse entered the centre of the arena after the 8-min acclimatisation. Up to four visual stimuli were presented in a session in the order sweep, loom, sweep, and loom. If the four visual stimuli had been delivered, the next delivered stimulus was auditory.

Each stimulus was delivered with an inter-stimulus interval of at least 45 s. Mice were removed from the arena under two conditions. (a) The mice had received the five abovementioned stimuli. (b) The mouse was in the arena for more than 30 mins after the 8-min acclimatisation. The looming stimulus was a dark spot expanding from 1.5 cm (visual angle:  $2.2^\circ$ ) to 39 cm (visual angle:  $53^\circ$ ) in 0.25 s and remained the same size for an extra 0.5 s. The sweeping stimulus was a 3.8 cm (visual angle:  $5.5^\circ$ ) black disk that moved from one side of the monitor to the other side at around  $23^\circ/\text{s}$  for 3.4 s. The auditory stimulus is a train of 100ms upswing cosine signals modulated from 17 kHz to 20 kHz over 3 s. The auditory waveform was generated in Matlab by Dr. Catherine Perrodin and delivered with a speaker (Pettersson L60 Ultrasound Speaker) on top of the arena. The Bonsai workflow was created by Dr. Stefano Zucca.

## *2.6 Visual object recognition assay*

In pilot experiments, 12 naïve mice were tested. For the hM4Di manipulation, 9 hM4Di mice and 8 GFP mice were tested 7 months post-surgery. 8 of the hM4Di mice and 5 of the GFP mice were derived from the abovementioned sweep-loom

assay (aged between 33 and 35 weeks). Other mice were derived from the LFP assay (aged between 23 and 24 weeks). Mice subjected to different assays prior to the visual object recognition assay did not show obvious difference in their locomotor activity and exploration time. Hence the data was pooled for analysis. Two mice (1 hM4Di and 1 GFP) became immobile after CNO injection were removed from the analysis. Each mouse was habituated to handling for 5 days before the behavioural assay. Then they were tested in 15 sessions and each session lasted 10 mins. In the first 4 sessions (exploration phase), mice explored an empty arena (37 x 45.5 cm) with two identical transparent cylinders placed 15 cm apart along one wall (7 cm (diameter) x 15 cm (high)). Objects were placed within the cylinders so that the mice could not touch/feel the object, and experienced them predominantly through vision. In the 5<sup>th</sup> session (pre-test phase), mice explored the arena with two different objects put into the transparent cylinders (objects **WX**). From 6<sup>th</sup> to 14<sup>th</sup> session (familiarisation phase), one of the objects was replaced by the copy of the other one (objects **XX**). In the 15<sup>th</sup> session (post-test phase), the initial two different objects were put back to the cylinders (objects **WX**). There was a 24-hr interval between consecutive sessions - though the post-test phase was conducted 4 hrs after the last session. Objects of different shape and colour were selected.

## *2.7 Histology*

Mice were transcardially perfused with saline followed by formalin. Whole mouse brains were removed and post-fixed in formalin for 1 day, followed by dehydration in 30% sucrose at 4°C until the brains sank. Then brains were mounted in O.C.T compound and stored at -20°C before cryo-sectioning. 40 µm coronal brain slices across the entire extent of the V1 were collected using a cryostat. Immunostaining

was performed to better detect hM4Di expression. Brain slices were first rinsed with PBS, permeabilised with PBS with triton (wash buffer) for 10 min and then blocked with blocking buffer, 10% normal goat serum (G9023, abcam) in wash buffer, for 1 hr. Rabbit anti-HA (3724S, Cell Signaling Technology) was applied to the slices (1:400 dilution in blocking buffer) at 4°C overnight. After washing out residual anti-HA with wash buffer, Alexa488-conjugated goat anti rabbit (A-11034, ThermoFisher) were used as secondary antibody and applied to the slices (1:200 dilution in blocking buffer) for 3 hrs at room temperature. Sections were mounted on glass slides with aqueous mounting medium containing DAPI nuclear stain (Vector Laboratories). Florescent images were collected with a Leica Microscope (DMI8 S), equipped with the software Leica Application Suite X (3.7), and camera (DFC7000 Leica Microsystems).

### *2.8 CNO treatment*

10 mg CNO (HB6149, hellobio) was dissolved in 10 ml 0.9% saline, resulting in a 2.4 mM CNO solution, and was kept at -80°C until 1 hr before the injection. Mice were injected at a final concentration of 10 mg/kg, 50-60 min prior to the experiment.

### *2.9 Data Analysis*

Electrical signals were filtered, amplified and converted to digital signals with an Open Ephys acquisition board (via the Intan headstage). Wheel movement signals were obtained from the rotary encoder attached to the treadmill and the speed and direction were estimated with a quadrature encoder. The synchronisation pulse captured by the photodiode was used to define the onset and offset of each stimulus.

Electrical signals, locomotion signals and the synchronisation pulse were all recorded by the Open Ephys acquisition board.

Unless stated otherwise, offline analyses were performed in MATLAB (Mathworks, NA, Release 2019b). The locomotion data was smoothed with a 50ms Gaussian filter. Both the LFP and running signals were down-sampled to 1kHz. Unless otherwise stated, LFP signals were filtered by a band pass filter with a 0.5Hz low cut and 50 Hz high cut frequency prior to further analysis.

*VEP analysis:* the VEPs were averaged across all phase reversals or contrast conditions for a session. The magnitude of VEP was defined as the difference between the trough and the peak of the average VEP response, where peak is the maximum value within the first 250 ms after the stimulus reversal and the trough is the minimum value between the onset of the stimulus and the peak.

*Harmonic analysis:* estimates of harmonic signals were extracted by taking the Fourier transform of individual trials to obtain the power spectra for individual trials. The respective magnitude of first and second harmonic was defined as the amplitude at the stimulus frequency and twice the stimulus frequency.

*Power spectral analysis:* LFP signals were filtered by a band pass filter with a 1.5Hz low cut and 150 Hz high cut frequency to remove arbitrary DC offset. Estimates of spectral power density were extracted using the Chronux toolbox in Matlab (Bokil et al., 2010). I used 3 s sliding window with a 33% overlap and tapers: [3, 5] for all

spectral analysis. Delta power was quantified by taking the AUC for 1.5-4 Hz in the power spectrum.

*Loom-sweep assay:* the centre of the arena was defined as 5 cm away from the wall. Escape was defined as occurring if the mouse reached the nest 2s after the running speed reached 40cm/s. Freeze was defined as occurring if the running speed was slower than 2 cm/s for at least 0.2 s.

*Visual object recognition assay:* the position of the object was defined as the centroid of the transparent cylinder, where I manually annotated the bottom of the cylinder. Object exploration was defined as occurring when the distance between the centroids of mouse nose and the object was shorter than 5cm. The differentiation index was calculated by subtracting the exploration time for the novel object from the exploration time for the familiar object, divided by the exploration time for both objects. The nose position was identified by Deeplabcut (Mathis et al., 2018). Deeplabcut (version 2.1.9) executed under python with NVIDIA-SMI (460.80; CUDA Version: 11.2). To train Deeplabcut's model to recognise mouse's body part, I labelled the nose, cheeks, ears, neck and shoulders, spine and tail. Sessions using different objects were trained in separate models for 1.03 million iterations, causing the overall test errors between 2.77 and 3.01 pixels in those models.

*Statistical analysis:* all repeated measure ANOVA was done under jamovi (version 1.6, retrieved from <https://www.jamovi.org>). Repeated measure correlation was done under rmcrrShiny (Marusich & Bakdash, 2021). In all figures, significance levels are indicated with black asterisks: \*0.05  $\geq$  P-value; #0.1  $\geq$  P-value  $\geq$  0.05.

## *Chapter 3: Physiological evidence for impact of hM4Di manipulation in*

### *V1*

#### *3.1 Introduction*

In Chapter 1, I reviewed several of the experimental approaches possible in visual neuroscience. Among them, genetic manipulation approaches such as optogenetics and chemogenetics, which can precisely manipulate a particular region or neuronal population, have now become widely used in rodent studies. Optogenetics and chemogenetics are genetic methods in which proteins are modified to interact with light and chemical actuators respectively. Optogenetics has the advantage of allowing modulation by optical stimulus at fine temporal resolution, but it is technically challenging to introduce to freely moving animals navigating an environment (for a review, see Deisseroth, 2015). Chemogenetics, by contrast, provides ease of delivering chemical actuators to the brain. It makes broader spatial coverage or long-term manipulation of neural circuits possible. The advantages of using chemogenetics over other pharmacological approaches are that (a) with chemogenetics, the same neural population can be repeatedly manipulated by the actuators, thus allowing stronger conclusions about the role of that neural population, and (b) administration of the actuators to the brain does not require intracerebral injection, so there is no need to anaesthetise animals to prior to the behavioural assay. These two advantages make chemogenetics a popular technique in behavioural neuroscience (for a review, see Campbell & Marchant, 2018).

##### *3.1.1 DREADDs in neuroscience*

Designer receptors exclusively activated by designer drugs (DREADDs), are popular chemogenetic tools whereby muscarinic receptors (Gq-DREADD, Gi-DREADD) are

engineered to be sensitive to clozapine-N-oxide (CNO), a pharmacologically inert drug-like compound (Armbruster et al., 2007). In principle, only neurons expressing DREADDs are affected by CNO and alternative actuators including Compound 21 (Thompson et al., 2018), Olanzapine (Weston et al., 2019) or Deschloroclozapine (Nagai et al., 2020), leaving other nearby neural populations more or less unaltered, at least directly. Muscarinic-based DREADDs are G-coupled receptors that can initiate a variety of intracellular signalling. For example, Gq-DREADDs increase intracellular calcium and thereby activate neurons. Gi-DREADDs, instead, seem to inhibit neuronal activity via two mechanisms, namely (a) opening inwardly rectifying potassium channels (GIRKs) to cause hyperpolarisation, and (b) inhibiting presynaptic release of neurotransmitters (Roth, 2017).

hM4Di is a Gi-DREADD, (Armbruster et al., 2007) that has been widely used in multiple cortical regions including entorhinal cortex (Miao et al., 2015), orbitofrontal cortex (Gremel & Costa, 2013; Ward et al., 2015; Meyer & Bucci, 2016), medial prefrontal cortex (Richards et al., 2014) and insular cortex (Sano et al., 2014; Vetere et al., 2017). While hM4Di has become a popular tool, most of the cortical studies examine its effect *in vitro*, either by recording hM4Di-expressing cells in brain slices (Richards et al., 2014; Robinson et al., 2014; Sano et al., 2014; Chiou et al., 2016;; Doron et al., 2020; Sheng et al., 2020; Vale et al., 2020; Y.-C. Wang et al., 2020; Devienne et al., 2021) or immunostaining against immediate-early genes to examine what portion of cells are active or inactive (Koike et al., 2016; Vetere et al., 2017; Fucich et al., 2018; Dobrzanski et al., 2020; C. Wang et al., 2020; Bubb et al., 2021). *In vivo* studies verifying the efficacy of hM4Di manipulation are limited. Two local field potential (LFP) studies showed an increase in field excitatory postsynaptic

potentials (fEPSP) in entorhinal cortex (Madroñal et al., 2016) or motor cortex (Natale et al., 2021) upon application of CNO, but another study showed a decrease in fEPSP in motor cortex (Y.-C. Wang et al., 2020). In terms of spiking activity, studies with limited number of mice per condition have suggested that hM4Di-expressing manipulation reduces firing rate in insular cortex (Sano et al., 2014) or in retrosplenial cortex (Vale et al., 2020).

As we are interested in what visual properties can be affected by hM4Di manipulation and previous studies have demonstrated that pharmacological inhibition of V1 results in a reduction in the visual evoked potential (VEP) (Cooke et al., 2015; Gu & Cang, 2016), we decided to establish the efficacy of hM4Di in V1 by recording VEPs in awake animals.

### 3.2 Results

Our goal was to express hM4Di virus in V1 and examine the efficacy of hM4Di-expressing V1 *in vivo*. To do so, we implanted an LFP electrode into the injection site in the right hemisphere, and bilaterally injected AAV8-CaMKIIa hM4Di virus or AAV8-CaMKIIa-GFP virus into deep layers of V1 (Fig. 1a). We used an AAV8-CaMKIIa virus vector because its preferential expression in excitatory neurons (Nathanson et al., 2009).

6 weeks after surgery to introduce the virus, mice were first habituated to head-fixation above a Styrofoam wheel, on which they were allowed to run, and visual stimuli were presented to the left visual field via a computer monitor. We designed a series of stimulus protocols to test VEP, contrast sensitivity, temporal frequency (TF)

tuning (see *Visual stimuli* in Chapter 2 for more details). As we did not have setup to deliver CNO within a recording session (such as intra-cortical drug delivery), we designed a two-session protocol (see *LFP recording* in Chapter 2 for more details) in which animals received saline via I.P. injection 1 hour before an initial recording session (Day n-1 session, n=2, 7, 12, 17), and either another saline or a CNO injection in another recording session the next day (Day n session).

### 3.2.1 Confirmation of hM4Di expression in V1

I first established expression of the hM4Di virus by ex-vivo imaging of brain slices through V1. An example is shown in Fig 1b: I found that the virus (stained against HA-tag shown in green) was expressed in the deep layers of cortex, with some labelling along the injection needle tracks. To identify where the LFP electrode was in the brain, a small lesion was created before sacrificing the mouse. I found the electrode side in layer 5, 100-200 um away from the main patterns of virus expression in this case (Fig. 1b). On one hand, virus expression can be identified in hM4Di mice's layer 5, with some labelling extended to their layer 4 and layer 6. On the other hand, the electrode side was identified only in 3 of the hM4Di mice, which were all implanted in layer 5. I could not identify any potential electrode side for the other 3 hM4Di mice (see Appendix I for details).

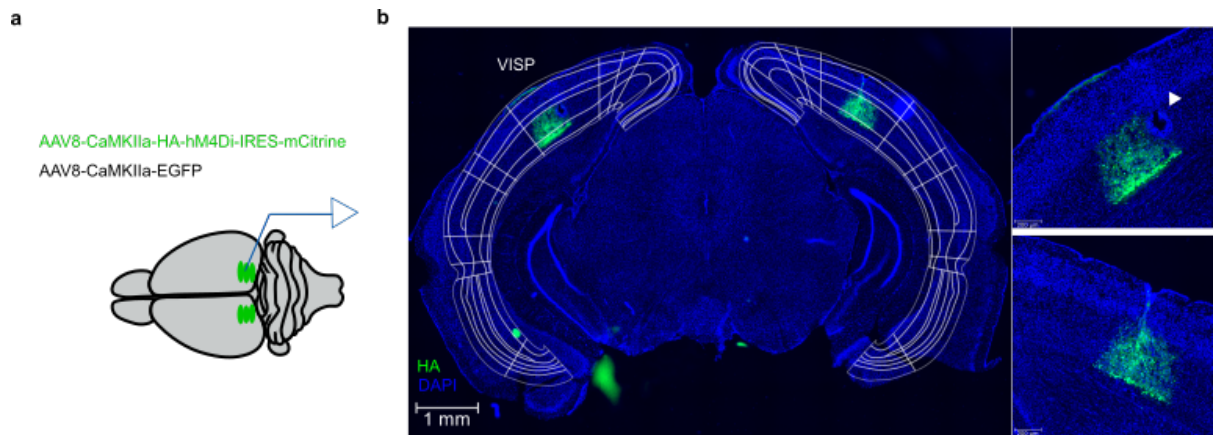


**Fig. 1 LFP recording in hM4Di-expressing V1.**

**a.** Scheme of virus expression strategy in V1. Blue line denotes chronic implant of LFP electrode in V1. Green denotes AAV-CaMKIIa-HA-hM4Di virus in V1. **b.**

Representative image showing HA-hM4Di expression (green) in V1. Layout of V1 (VISP) is modified from Allen Brain Atlas ([portal.brain-map.org](http://portal.brain-map.org)). *Top right:* zoom-in image of right hemisphere. White triangle denotes the electrode site. *Bottom right:* zoom-in image of left hemisphere.

### 3.2.2 Limited effect of hM4Di on VEP waveform shape and amplitude

We asked whether hM4Di manipulation affected VEP amplitude by presenting full-screen flickering gratings. I recorded LFP over 5 blocks of visual stimulation. Each block started with 30-second grey screen followed by presentation of the flickering grating for 100s (2 reversals/s, with a square-wave temporal profile; Fig. 2a).

Visual responses in V1 are known to be modulated by locomotion. In these experiments, we found that mice spent about 80% of their time stationary (speed < 5cm/s); this varied across animals and sessions but there was no clear difference during CNO and the counterpart saline sessions (i.e. Day n sessions; Fig. 2b). I therefore split the VEP responses into epochs in which the mouse was stationary and epochs in which the mouse was running, and averaged within sessions to quantify stationary and running VEPs. Inspection of the VEP waveforms showed some variability in shape and amplitude between animals but little difference during saline and CNO administration (Fig. 2c). I extracted the positive and negative peaks in the VEP and calculated the difference between them to provide an estimate of VEP amplitude. We found that the VEP amplitude was larger in stationary than running VEP epochs (Fig. 2d). As mice were more likely to be stationary ( $77.5 \pm 1.85\%$  of the time across 72 sessions), we focused on the stationary VEP amplitude (Fig. 2e).

I noted that VEP amplitude in GFP mice was smaller than VEP amplitude in hM4Di mice (Fig. 2f, left). Due to this between-group variance, I conducted the statistical testing for each group separately to examine the effect of CNO on their VEP amplitude. VEP amplitude obtained for Day n sessions were subjected to a two-way repeated measures ANOVA with treatment type (CNO or saline) and time (1<sup>st</sup> cycle

or 2<sup>nd</sup> cycle) as fixed factors. The ANOVA revealed no significant main effect of treatment type in either hM4Di group ( $F=0.553$ ;  $p=0.491$ ) or GFP group ( $F=0.070$ ;  $p=0.816$ ), suggesting that there is no effect of the hM4Di manipulation on VEP amplitude. In addition to VEP amplitude, I also observed a gradual increase in VEP amplitude across sessions (Fig. 2f, left), suggesting the gratings in this protocol induced stimulus-specific response potentiation (SRP) in V1 (cf. Cooke et al., 2015). I therefore calculated the proportional change in VEP amplitude from day1 to the last 2 sessions (Fig. 2f, right). There was variability in the effect of SRP between animals, but there was no evidence that the hM4Di manipulation affected this potentiation.

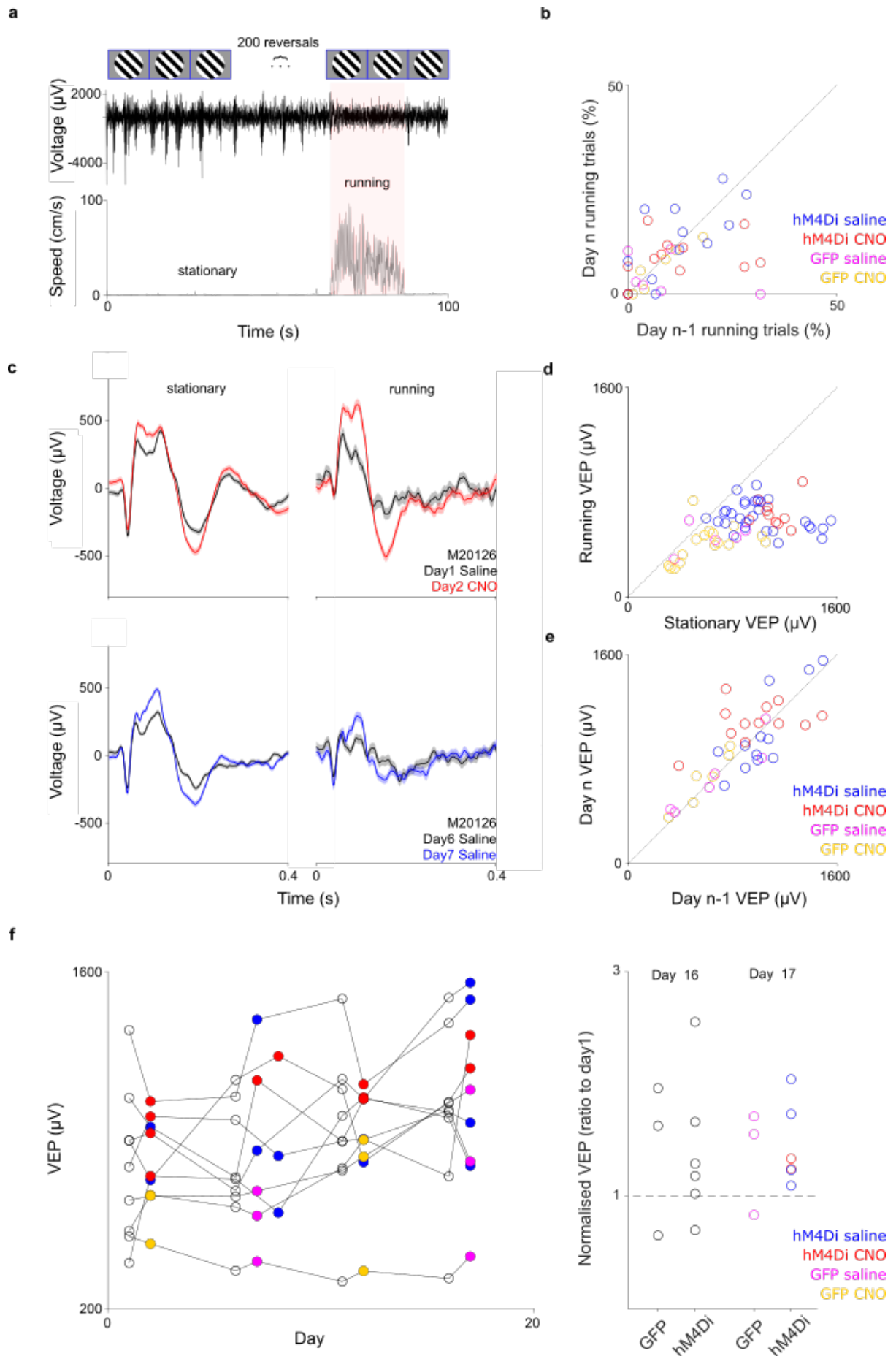


**Fig. 2: hM4Di inactivation of V1 does not increase the VEP amplitude.**

**a.** *Top:* diagram of 2-Hz flicker gratings. *Bottom:* example of raw LFP trace during gratings and running speed of a mouse. **b.** Scatter plot of ratio of running trials in the hM4Di mice (n=6, 42 sessions) and GFP mice (n=3, 24 sessions). Each data point represents a pair of sessions. **c.** Examples of averaged VEP waveform from one mouse. Data are shown as mean  $\pm$  S.E.M. **d.** Scatter plot of VEP amplitude during running versus stationary states in the hM4Di mice (n=6, 42 sessions) and GFP mice (n=3, 24 sessions). Each data point represents a pair of sessions. **e.** Scatter plot of amplitude of stationary VEPs during saline and CNO sessions. Each data point represents a pair of sessions. **f.** *Left:* Trajectory of individual mouse's VEP amplitude over sessions. Different lines are different mice. Fill colour represents the treatment type. *Right:* normalised VEP amplitude of mice on the last 2 sessions. Black dots are VEP amplitudes from day 16 whereas colour dots are from day 17.

### 3.2.3 *No effect of hM4Di on contrast sensitivity*

We next asked whether hM4Di manipulation affects the contrast sensitivity of the VEP. We presented brief, static, gratings of varying contrast and observed similar VEP waveform to those found for the flickering grating described above. Therefore, I used the same method to calculate VEP amplitude (Fig. 3a). Again, I focused on the stationary VEP amplitude, and now also extracted the latency of the positive peak and the latency of the negative trough, at each contrast. We found a decrease in VEP amplitude and an increase in VEP latency for low-contrast stimuli (Fig. 3b-c). To quantify contrast sensitivity for VEP amplitude, I calculated the area-under-contrast curve (AUC) for each session (Fig. 3d). Similar to the abovementioned statistical tests, AUC values from Day n sessions were subjected to a repeated measures ANOVA with treatment type and time as fixed factors. The ANOVA revealed no significant main effect of treatment type in the hM4Di group ( $F=0.630$ ,  $p=0.510$ ), suggesting hM4Di manipulation does not affect contrast sensitivity of the VEP.

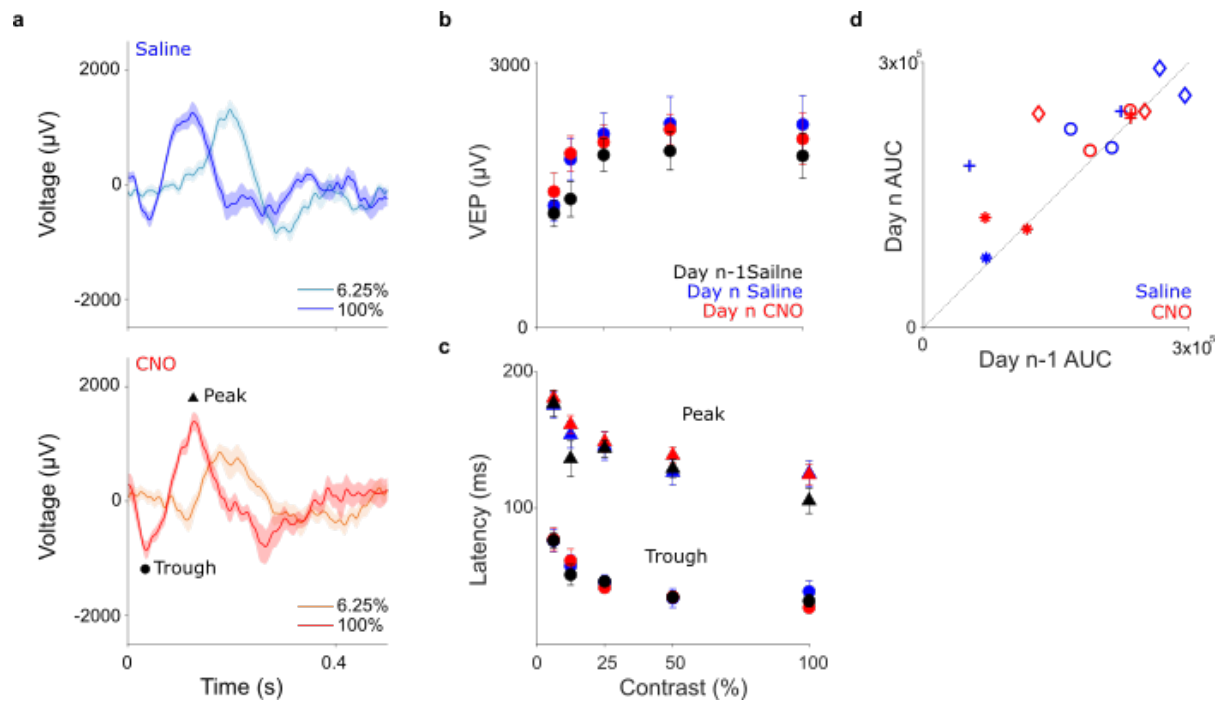


**Fig. 3: hM4Di inactivation of V1 does not increase the contrast sensitivity.**

**a.** Examples of average VEP response from one mouse in response to low- and high-contrast stimuli. Data are shown as mean  $\pm$  S.E.M. **b.** Contrast-amplitude curves of hM4Di mice (Day n-1: 15 sessions; Day n (saline): 7 sessions; Day n (CNO): 8 sessions). Data points are means of trials pooled across mice, error bars are S.E.M. **c.** Contrast-latency curves of hM4Di mice. The latencies of trough are presented as circles whereas the latencies of peak are presented as triangles. **d.** AUC of contrast-amplitude curves during Day n-1 and Day n sessions. Different markers are different mice.

### 3.2.4 TF tuning in hM4Di mice

We next asked whether hM4Di manipulation affects the temporal sensitivity of V1. We presented flickering gratings of varying temporal frequency (TF) to mice and found, as expected, periodic signals during stimulation (Fig. 4a). To quantify the periodic signals, we used LFP responses during stationary periods. To avoid VEPs, we analysed LFP signals from 0.5 sec after the stimulus onset until the end of stimulus presentation. We applied a Fast Fourier Transform to the LFP waveforms obtained on each trial and extracted the power at the stimulus frequency (the '1st harmonic' signal) and that at twice the stimulus frequency (the '2nd harmonic' signal), for each stimulus frequency. In both saline and CNO session, we found that both 1<sup>st</sup> and 2<sup>nd</sup> harmonic signals showed preference for low TFs with at around 2 Hz for most of the animals, and response gradually reduced at higher TFs (Fig. 4b). Preferred frequencies were slightly higher for the 1st harmonic signals (1 to 4Hz) than the 2<sup>nd</sup> harmonic signals (1 to 2Hz). Similar to VEP responses on the Day 1 (Fig. 3f, left), harmonic responses in GFP mice were smaller than hM4Di mice (Fig. 4b), for reasons that are unclear. To visualise the effect of CNO, we normalised the signals of each Day n session to that of their corresponding Day n-1 session (Fig. 4c, e). We found that animals in the hM4Di group showed an increase in response to low TFs during CNO. We therefore focused our statistical analysis on responses to 1 Hz and 2 Hz stimulus frequencies (Fig. 4d, f). The amplitudes of the harmonic signals from Day n sessions were subjected to a two-way repeated measures ANOVA with treatment type and time as fixed factors. First, the ANOVA revealed that a significant main effect of treatment type in the 1<sup>st</sup> harmonic signals of hM4Di group (1Hz:  $F=8.005$ ,  $p=0.037$ ; 2Hz:  $F=10.90$ ,  $p=0.021$ ) but not GFP group (1Hz:  $F=0.276$ ,  $p=0.652$ ; 2Hz:  $F=0.004$ ,  $p=0.956$ ). Second, there was no significant main

effect of treatment type in the 2<sup>nd</sup> harmonic signals (hM4Di group: 1Hz:  $F=0.097$ ,  $p=0.768$ ; 2Hz:  $F=0.011$ ,  $p=0.921$ ; GFP group:  $F=5.700$ ,  $p=0.140$ ; 2Hz:  $F=3.717$ ,  $p=0.194$ ). The 1st harmonic signals were then subjected to a three-way between subject (hM4Di or GFP group) repeated measures ANOVA with treatment type and time as fixed factors, to determine if there is a statistically significant interaction effect between treatment type and virus type. However, the interaction was not significant (1Hz:  $F=2.590$ ,  $p=0.152$ ; 2Hz:  $F=4.896$ ,  $p=0.063$ ). Failure to detect a significant interaction effect might be due to the between-group variance and unbalanced sample size in the harmonic signals (Fig. 4b). As a result, although we saw an enhanced harmonic response when the stimulus was delivered to hM4Di mice at 1 Hz or 2 Hz during CNO treatment, whether statistically there was an interaction effect between CNO and hM4Di group requires further investigation.

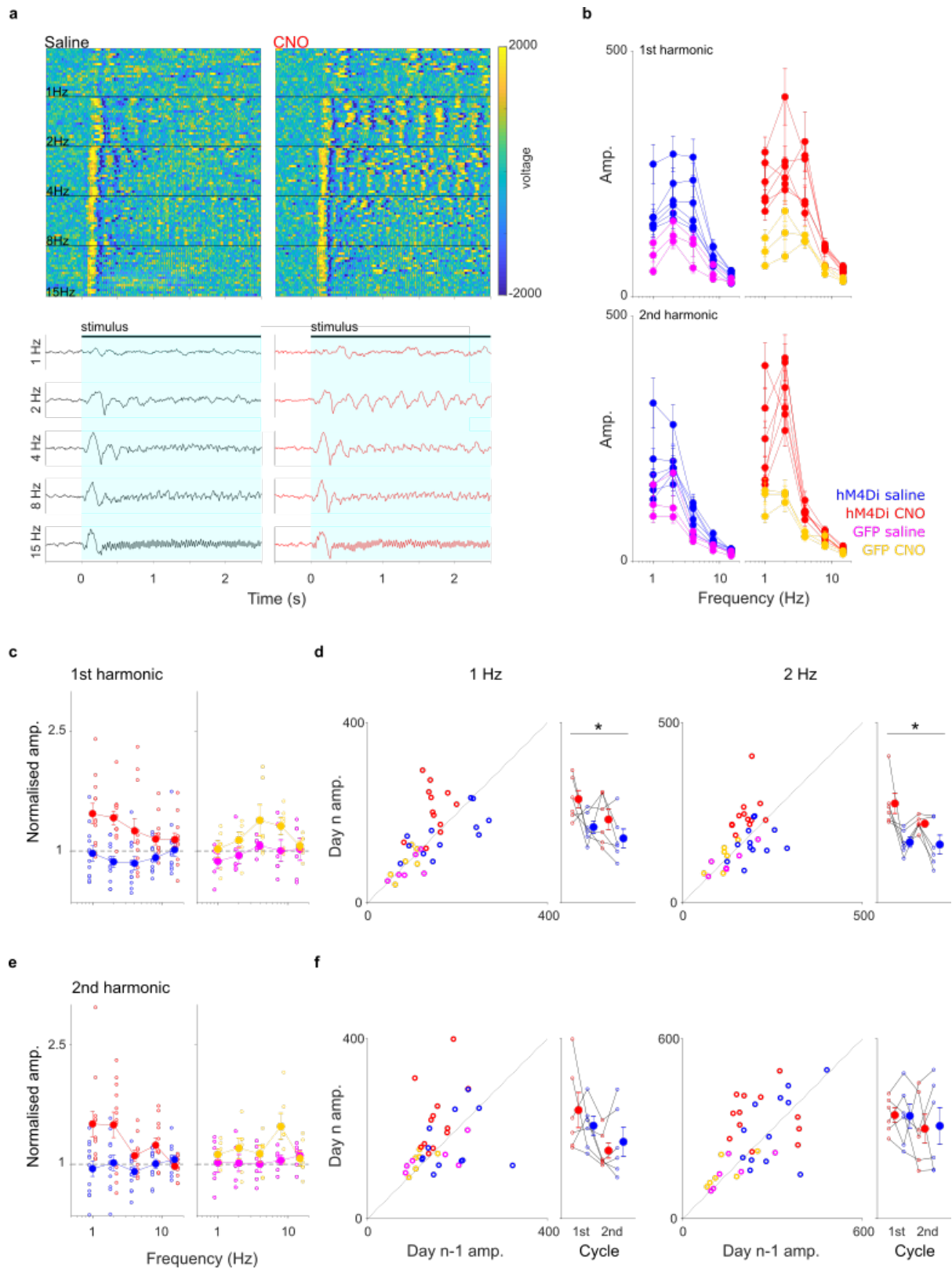


**Fig. 4: hM4Di inactivation of V1 enhances responses to low-frequency gratings.**

**a.** *Top:* Raster plots of single-trial traces from one example mouse. Each row indices one trial. Trials are sorted by stimulus frequency. *Bottom:* Average VEP response from the same TF. Shaded areas show the stimulus presentation. **b.** Individual mouse's TF response in the first CNO session and their previous sessions. Different dotted lines represent different mice. Data are shown as mean  $\pm$  S.E.M. **c.** Normalised amplitude of 1<sup>st</sup> harmonic signals (Day n/ Day n-1) in the hM4Di mice (n=6, 48 sessions) and the GFP mice (n=3, 24 sessions). Open circles denotes individual mouse's response. Closed circles denotes the average response. Data are shown as mean  $\pm$  S.E.M. **d.** *Left:* Scatter plots of 1<sup>st</sup> harmonic signals in response to 1 Hz gratings between Day n-1 and Day n sessions. *Right:* Scatter plots of 1<sup>st</sup> harmonic signals in response to 2 Hz gratings between Day n-1 and Day n sessions. Each data point represents a pair of sessions. Trajectories of hM4Di mice's response during Day n sessions are present at the right of each scatter plot group (1Hz:  $p=0.037$ ; 2Hz:  $p=0.021$ , main effect: CNO vs. saline, repeated measure ANOVA). Different dotted lines represent different mice. Open circles denote individual mouse's response. Closed circles denote the average response. **e-f** Same as **c-d** for responses at 2<sup>nd</sup> harmonic signals.

### 3.2.5 Tentative increase in low-frequency oscillations during CNO administration

To further explore the effect of CNO on responses to low-frequency gratings, we performed power spectral analysis on responses to the 2-Hz flickering gratings that were used to measure VEP amplitude (Fig. 2a). We focused on the power spectrum obtained during stationary state (Fig. 5a). When we averaged the power spectra in hM4Di and GFP mice, we found an increase in the low-frequency band (delta band, 1.5-4 Hz) in hM4Di mice (Fig. 5b-c). To quantify this, I calculated the AUC under delta band. The AUC values from Day n sessions were subjected to a two-way repeated measures ANOVA with treatment type and time as fixed factors. The ANOVA analysis suggested that there was a marginal but no significant main effect of CNO treatment in hM4Di group ( $F= 4.904$ ;  $p=0.080$ ). I wondered this is due to the small sample size and larger variance in these mice (Fig. 5d, right) so I instead used a non-parametric repeated measure ANOVA to examine the effect of CNO and saline on hM4Di mice. The ANOVA suggested hM4Di mice had a difference in their delta power under CNO and Saline treatment (Friedman's test,  $p=0.021$ ).

The mechanism through which hM4Di manipulation affects LFP responses to slowly flickering gratings is not clear. We hypothesised that in these mice there may be a general increase in spontaneous oscillations, which contributed to the enhanced visual responses to 1- and 2-Hz flickering gratings. Therefore, we applied the same analysis to LFP activity during the 30-sec grey screen periods that preceded each block of stimuli (inter-block grey screen, Fig. 5e-5f) as well as the 30-sec grey screen before TF stimulus (pre-TF grey screen). Similar to the power spectra during stimulus presentation, hM4Di mice had an increase under delta band in both grey screen periods (inter-block grey screen: Fig. 5g; pre-TF grey screen: Fig. 5h). 3 hM4Di mice did not have inter-block grey screen in their first 2 sessions, therefore I

applied statistical analysis on the response during pre-TF grey screen. The two-way repeated measure ANOVA (treatment x time) suggested that there is a marginal but not significant main effect between CNO and saline treatment in hM4Di ( $F=6.229$ ,  $p=0.055$ ) but not in GFP group ( $F=0.309$ ,  $p=0.634$ ). This statistical analysis was similar to mice's response during stimulus presentation. Similar to before, a non-parametric repeated measure ANOVA to examine the effect of CNO and saline on hM4Di mice was used. The ANOVA suggested hM4Di mice had a difference in their delta power under CNO and Saline treatment (Friedman's test,  $p=0.004$ ).

### *3.2.6 Limited off-target effects of CNO on delta power*

Emerging studies have raised concerns about CNO's off-target effects in the brain. It is known that CNO has moderate permeability through blood brain barrier and is metabolised to clozapine within 30 mins (Manvich et al., 2018). Clozapine is an antipsychotic drug that serves as an antagonist for a variety of receptors expressed in the brain (Meltzer, 1994). EEG recordings from both awake rats and humans found an increase in delta power after clozapine administration (Knott et al, 2001; MacCrimmon et al., 2012; Sebban, Tesolin-Decros et al., 1999). As I only had 3 GFP mice as control, I ran an additional LFP recording on C57BL/6J mice under saline and CNO treatment to exclude the possibility of CNO's off-target effect on delta power. A postdoc researcher in the lab (Amalia Papanikolaou, 'AP'), had done an LFP recording on 7 C57BL/6J mice receiving 2-Hz flickering gratings. Her mice (AP mice) had LFP electrode implanted in their layer 4 but no virus injection (see *Animals* in Chapter 2 for more details). I assigned AP mice into two groups based on their delta power during habituation phase to balance out any uneven delta power (data not shown) and the two groups were subjected to a counterbalanced design of

treatments (Fig. 5I, Top). One group received saline in the first session and CNO in the second session. The other group received CNO in the first session and saline in the second session. I used the same stimulus protocols as before (sparse noise followed by static gratings for contrast, flickering gratings for TF and flickering gratings for VEP) and set the orientation of grating stimuli different from what AP had used (see *Visual Stimuli* in Chapter 2 for more details). I ran the same power spectral analysis as abovementioned methods and calculated AUC value for these mice's delta power under CNO and saline treatment. While most of the data points for delta power were at similar range as hM4Di and GFP mice, one AP mouse which ran throughout the grey screen period (95.7% of the time) had a substantial large delta power during grey screen. I reckoned that large delta power is due to lack of stationary data points during grey screen, as (a) no other mice ran as much as this mouse during grey screen (b) this mouse spent less time running during stimulus presentation (81%) and no deviation in delta power was not found. Due to the apparent outlier, I used non-parametric repeated measure ANOVA to examine the effect of CNO and saline on AP mice. The ANOVA suggested that in both grey screen and stimulus presentation, there was no difference in the delta power under CNO and Saline treatment (grey screen:  $p=0.705$ ; stimulus presentation:  $p=0.257$ ), indicating that CNO via I.P. injection had limited effect on delta power.

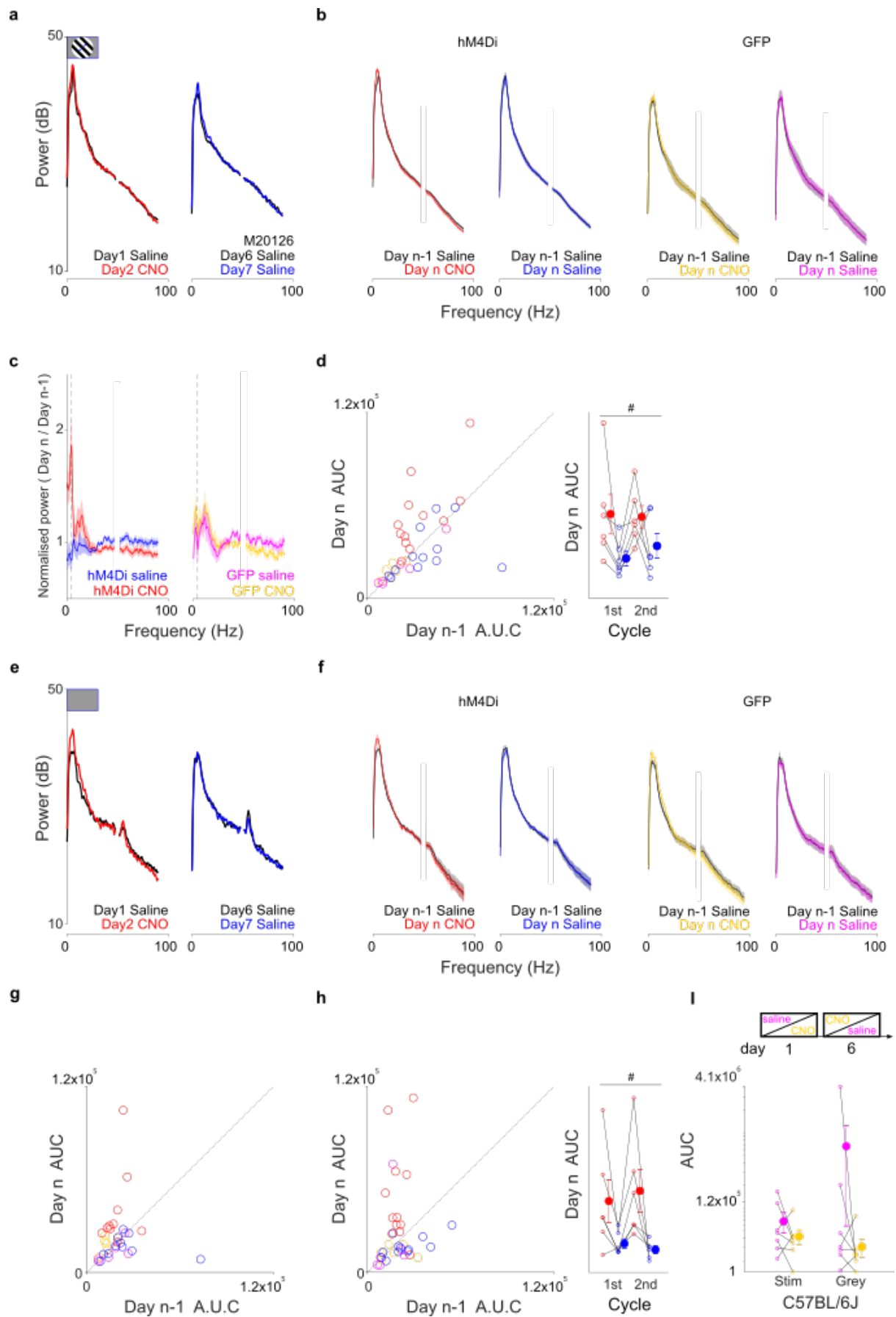


**Fig. 5: hM4Di inactivation of V1 increases low-frequency oscillation.**

**a.** Examples of power spectra during phase-reversing (2Hz) grating stimuli from one mouse. Power spectrum around 50 Hz was removed from the graph due to outliers caused by line noise (50 Hz interference). **b.** Group data of power spectra in the hM4Di mice (n=6, 48 sessions) and GFP mice (n=3, 24 sessions). **c.** Normalised power spectrum from Day n sessions. Dashed lines indicate 4 Hz. Data are shown as mean  $\pm$  S.E.M. **d.** Delta power for 2Hz gratings during Day n-1 and Day n sessions. *Left:* Scatter plot of the delta power. Each data point represents a pair of sessions. *Right:* Trajectory of each hM4Di mice's delta power in Day n sessions. Different dotted lines represent different mice. Open circles denote individual mouse's response. Closed circles denote the average response. Data are shown as mean  $\pm$  S.E.M. ( $p=0.080$ , main effect: CNO vs. saline, repeated measure ANOVA). **e-f.** Same as **a-b** for grey screen response. **g-h.** Delta power for grey screen during Day n-1 and Day n sessions. Delta power obtained from inter-block grey screen and pre-TF grey screen are shown in **g** and **h** respectively. Trajectory of each hM4Di mice's delta power in Day n sessions is shown at the right of **h**. Different dotted lines represent different mice. Open circles denote individual mouse's response. Closed circles denote the average response. Data are shown as mean  $\pm$  S.E.M. ( $p=0.055$ , main effect: CNO vs. saline, repeated measure ANOVA). **i.** Delta power of AP's C57BL/6J mice during CNO and saline sessions (n=7). Magenta circles denote saline treatment. Yellow circles denote CNO treatment. Different dotted lines represent different mice. Open circles denote individual mouse's response. Closed circles denote the average response. Data are shown as mean  $\pm$  S.E.M. Y-axis is set as logarithmic scale.

### *3.3 Discussion*

In this study, we investigated the efficacy of hM4Di manipulation in V1. While we observed little effect of hM4Di manipulation on VEP amplitude and contrast sensitivity, we found an increase in visual response to low-frequency grating stimuli, and a tentative increase in spontaneous oscillations under delta band (1.5-4 Hz).

#### *3.3.1 Impact of locomotion on VEP amplitude*

In our measurements, running VEP amplitude was smaller than the stationary VEP amplitude (Fig. 3d). This result seems in contrast with recent work where a reduction in VEP was found during stationary state (Rasmussen et al., 2019). This discrepancy might be due to different depth of recording, which has been observed in spiking activity from other studies: increases in layer 4/5 during locomotion (Ayaz et al., 2013) but decrease in upper layer (<0.4 mm, in Bennett et al., 2013). In our study, LFP electrode was inserted 0.6mm below the surface to target layer 5 whereas Rasmussen and colleagues were recording from 0.15 mm -0.3 mm below the surface to target layer 2/3. Notably, other studies recording in between these two depths, such as 0.5 mm from the skull (Grønli et al., 2018) or 0.4 mm-0.45mm from the surface (Papanikolaou et al., 2021) found smaller VEP in active awake state (characterised by EEG muscle tone) or during running. These data suggested that behavioural state might modulate VEP amplitude in a layer specific manner.

#### *3.3.2 Influence of contrast on VEP amplitude and latency*

We found that low-contrast stimuli produced VEPs of smaller amplitude and longer latency (Fig. 4b-c). This is consistent with previous literature (Parker et al., 1982; Porciatti et al., 1999; Cooke & Bear, 2010; Speed et al., 2019), suggesting a

normalization mechanism in V1 (or earlier) that reduces latency at high contrast. The cellular mechanism underlying this normalisation is thought to be due to cross-orientation intra-cortical inhibition (Carandini et al., 1997), and adaptive mechanism at the synaptic level (Carandini et al., 2002).

### *3.3.3 Limited effects of hM4Di manipulation on VEP amplitude and contrast sensitivity*

We found limited impact of hM4Di on VEP amplitude (Fig. 3) and contrast sensitivity (Fig. 4). This finding appears inconsistent with previous findings using optogenetics or drugs to reduce VEP (Cooke et al., 2015; Gu & Cang, 2016). However, the difference in methods used to inhibit V1 might explain this discrepancy. Cooke and colleagues inhibited V1 with muscimol, a GABA $\alpha$  receptor agonist that hyperpolarises the cell via the influx of chloride ions. Inhibitory DREADDs instead hyperpolarises neurons via activation of GIRKs. Similar machinery to hyperpolarises neurons is to use baclofen, a GABA $\beta$  receptor agonist activating a potassium conductance via G-protein coupled receptors (Ulrich & Huguenard, 1995; Sodickson & Bean, 1996). Administrating baclofen to visual cortex reduced the spontaneous activity in cats (Baumfalk & Albus, 1987) but its effect on visual-evoked potentials is not clear: baclofen seemed to slightly increase VEP amplitude in awake rats' (Hetzler & Ondracek, 2007), but reduced VEP amplitude in anesthetized mice (Gu & Cang, 2016). In addition, slice recording has showed that GABA agonists may influence both pre-synaptic and post-synaptic neurons (Porter & Nieves, 2004; L. Wang et al., 2019). Hence, the efficacy of baclofen or muscimol on VEP amplitude may largely depend on the modulation of thalamo-cortical inputs. Expressing DREADDs in V1

with AAV virus should prevent a direct influence on the thalamo-cortical inputs, limiting the effect of hM4Di manipulation on VEP amplitude.

We also found that hM4Di manipulation has limited effects on latency of positive peak and negative trough. These results are in concert with Hetzler and Ondracek's findings, suggesting that hM4Di manipulation might have subtle changes in VEP amplitude, but does not affect the overall shape. As we calculated contrast sensitivity based on the AUC value of VEP amplitude at different contrast levels, our finding about limited effects on contrast sensitivity is consistent with the limited effects on VEP amplitude.

#### *3.3.4 TF tuning and baseline harmonic signals in hM4Di mice*

In both DREADD and control mice, we observed V1's low-pass properties for TFs. This finding is consistency with others defining the low-pass properties through single-unit recording (Niell & Stryker, 2008). The 2-Hz peak in our studies is in line with peak responses found in those V1 studies (1-2 Hz: Niell & Stryker, 2008; Gao et al., 2010; 2.8 Hz: Durand et al., 2016; Camillo et al., 2020). V1 is known to have peak responses at lower frequency than dLGN (Grubb & Thompson, 2003; Durand et al., 2016), presumably due to its synaptic conductance slower than thalamic inputs and intra-cortical inhibition (Krukowski & Miller, 2001). We noted that the baseline harmonic signals were different in hM4Di and GFP mice (Fig. 4b), which might be due to CNO-independent effects of hM4Di expression. Although such an off-target effect has only been reported in peripheral nerves (Saloman et al., 2016), it seems that high expression of hM4Di may induce a compensatory mechanism that reduces the conductance of voltage-gated calcium channel and sodium channel. Sodium

current is considered the key current to initiate and maintain slow-frequency oscillation (Hill & Tononi, 2005) in a computational model of thalamocortical system, underpinning the importance of intrinsic neuronal properties in regulating slow oscillation. It would be intriguing to verify whether hM4Di-expressing neurons leads to a long-term increase in baseline harmonic signals without CNO.

### *3.3.5 Effects of hM4Di manipulation on harmonic signals and delta power*

We saw an increase in 1<sup>st</sup> harmonic signals when hM4Di/CNO mice were presented with 1- or 2-Hz flickering gratings. The increase in 1<sup>st</sup> harmonic signals, reflecting a synchronous activity in the cortex, might be due to an increase in intra-cortical inhibition caused by hM4Di manipulation. To further understand the mechanism of increase in harmonic signals, we analysed mice's power spectra and found a tentative increase in hM4Di mice's delta power during both stimulus presentation and grey screen. As hM4Di/CNO mice showed increased delta power in both pre-TF grey screen and inter-block grey screen, it is less likely that the presentation of 1- and 2-Hz grating stimuli caused the increase in delta power. Instead, the enhancement of delta power may influence hM4Di/CNO mice's response to low-frequency gratings.

Delta power, a result from the low-frequency oscillatory activity in the brain, is associated with animal's vigilance. The mechanism of delta power is believed to be caused by a combination of subcortical, thalamic inputs and intra-cortical activity, making the membrane potential of cortical neurons a rhythmic alternation between depolarized states (neurons sustain firing) and hyperpolarized state (neurons stop firing). In cortex, an initial surge of spiking activity during the depolarised state was found in L5 neurons (Chauvette et al., 2010; Krone et al., 2021). Activating layer 5

excitatory neurons with optogenetics can generate depolarised-like state whereas inhibiting L5 neurons reduces spiking activity during the depolarised state (Beltramo et al., 2013), supporting the idea that L5 neurons play an important role in regulating low-frequency oscillation (Sanchez-Vives & McCormick, 2000; Chauvette et al., 2010). Precise circuit mechanisms of L5 for low-frequency oscillation remains a great challenge due to L5 neuron's diverse corticothalamic and corticocortical connectivity(Harris et al., 2019). One possibility is that low-frequency oscillation in cortex is modulated by L5 via cortico-thalamic neurons. Another possibility can be that L5 cortico-cortical neurons might influence the oscillation in the rest of the cortex, perhaps in a manner that similar to how L6 neurons enhance superficial layers' response(Olsen et al., 2012). Dissecting this mechanism requires axon-specific manipulation of deep layer neurons such as using axon-selective hM4Di variants to locally inhibit a particular projection of L5 neurons, while measuring the low-frequency oscillation in cortex.

In addition, I note that a recent report identified a subset of inhibitory fast-spiking neurons expressing CaMKIIa<sup>+</sup> markers(Keaveney et al., 2020). The number of that CaMKIIa<sup>+</sup> inhibitory neurons is low (less than 8% of the CaMKIIa<sup>+</sup> neurons), but we do not know to what extent they affect cortical computation. Hence, future work on this issue should consider using Cre<sup>+</sup> mouse lines that exclusively target on excitatory neurons(Harris et al., 2019), or providing anatomical analysis of how much hM4Di-expressing neurons is excitatory neurons.

### 3.3.6 Experimental limitations

Temporal dynamics and pharmacokinetics of I.P administrated CNO are critical factors when examining hM4Di efficacy. Previous studies on excitatory DREADDs, hM3Dq, showed that it takes around 10 minutes (measured by extracellular recording: Alexander et al., 2009) or 30 minutes (measured by calcium imaging: Nagai et al., 2020) for CNO to kick in. The CNO effect was observed until around 120 minutes after injection (Nagai et al., 2020). Our 50-minute recording session started from 60 minute after injection. Therefore, if hM4Di's efficacy lasts as long as hM3Dq's efficacy, we shall expect the hM4Di manipulation in V1 throughout the recording. Future work focusing on detailed time course of hM4Di efficacy *in vivo* may fill that gap in knowledge.

The number of mice was not balanced for the treatment sequence. 4 hM4Di mice and 3 GFP mice received saline-CNO in the first two sessions, followed by saline-saline treatment in the 3rd and 4th sessions. By contrast, only 2 hM4Di mice received saline-saline treatment in the first 2 sessions, and saline-CNO sessions in the 3rd and 4th session. As we did not have enough number of mice for both designs, we pooled the data together for analysis. In terms of VEP amplitude, harmonic signals and delta power, we note a between-group variance in GFP and hM4Di mice. This result might be due to an imbalance of hM4Di and GFP virus in each batch of mice (1<sup>st</sup> batch: 4 hM4Di mice, 2<sup>nd</sup> batch: 2 hM4Di mice, 3 GFP mice), or long-term effects of high levels of virally mediated hM4Di expression in neurons (Roth, 2016). The difference in baseline activity as well as limited number of mice in each group (6 hM4Di mice vs. 3 GFP mice) affected our statistical analysis. For example, for the analysis on 1<sup>st</sup> harmonic signals, we saw the main effect of

treatment when analysing the two groups separately but failed to detect a significant interaction between virus and treatment. Although it seems unlikely that CNO affected the harmonic signals of GFP mice, more samples are needed to draw a stronger conclusion of the effect of hM4Di manipulation on cortex.

Lastly, we note that the analysis pipeline applied a high pass filter (1.5 Hz to 150Hz) to remove D.C. artefacts. This can mask the contribution of 1 Hz harmonic signals to delta power. Therefore, further analysis on the correlation between delta power and harmonic signals might provide us with other insight of hM4Di manipulation in V1.

### 3.7 Summary

Unlike previous literature using muscimol or optogenetics to inhibit V1, we showed that hM4Di manipulation has limited effect on VEP amplitude, which points out an unclear role of GABA receptors in visual-evoked activity. More importantly, we showed that hM4Di/CNO condition had stronger delta power and stronger 1st harmonic signals to low-frequency stimuli than the control conditions (hM4Di/Saline). These changes are presumably due to efficacy of hM4Di manipulation on cortical cells, causing a synchronous neural activity. Future studies including *ex vivo* slice recording on hM4D-expressing cortical neurons and functional analysis of cortical circuits with axon-selective hM4Di variants might improve our understanding about the mechanism of hM4Di manipulation in cortex.

## *Chapter 4: Behavioural impact of hM4Di manipulation in visual discrimination*

### *4.1 Introduction*

For visually-guided behaviours, animals need to both detect the presence of objects and to identify them. Identifying objects requires discriminating among potential options, for example, whether an object is an animal or a rock. Given neurons within V1 encode orientation and direction, most of the studies have focused on the context of discriminating between orientation (tilt) of visual scenes or shapes of objects. However, earlier studies reported that rats could still respond to grating stimuli after V1 ablation (Dean, 1978 & 1981; Oakley, 1981). It remains unclear whether there are other contexts of visual discrimination that require V1.

As I briefly reviewed in Chapter 1, there are at least two directions to think about the function of V1. One direction focuses on learning and that V1 might be required under conditions where discrimination is expressed through learned actions: e.g. licking for one orientation but not another to gain reward. This role involves linking the features of objects to particular behavioural contingencies. Another direction focuses on visual acuity. Whether V1 is required for coarse discrimination or fine discrimination, which is often defined based on the spatial frequency of grating stimuli. The two directions are not contradictory as animals might need to learn to report differences in visual stimuli if the features of visual stimuli are not usually relevant to them. One way to address this issue and explore other contexts of visual discrimination is to investigate V1's contribution to innate visually guided behaviours, where ethologically relevant stimuli can trigger certain behaviours without learning.

Some studies have shown how potentially aversive visual stimuli may drive defensive behaviours, including studies on the aforementioned looming stimulus, virtual cliffs (Del Grosso et al., 2017), as well as responses to images of snakes (Watanabe et al., 2021). A previous study in our laboratory demonstrated that mice display different defensive responses to overhead looming stimulus and sweeping stimuli (De Franceschi et al., 2016). A sweeping stimulus was defined as a dot moving along a direction tangential to the mouse, possibly representing a distant threat to the animal (Wallace et al., 2013; De Franceschi et al., 2016). A looming stimulus was instead an overhead stimulus simulating the appearance of an object moving towards the mouse: a potentially more imminent threat. V1 may be important for (a) distinguishing between sweeping and looming stimuli, and (b) adjusting behavioural responses based on prior experiences.

In this chapter, we tested the hypothesis that V1 is required for discrimination between potential visual threats. We used virally-mediated expression of hM4Di to perturb V1 in freely moving mice while mice are exposed to a sweep-loom assay (Fig. 1a). We found limited evidence that V1 is required for this discrimination. In addition, we tested the hypothesis that V1 is required for discrimination in a non-aversive context, for which we develop a new visual object recognition (VOR) assay. We found limited evidence that hM4Di manipulation of V1 affected performance in VOR assay, either.

## 4.2 Results

### 4.2.1 *hM4Di manipulation in Sweep-Loom assay*

To assess the effect of hM4Di manipulation on visual discrimination, AAV8-CaMKIIa-hM4Di virus or AAV8-CaMKIIa-GFP virus was injected bilaterally into V1 (Fig. 1a). Mice expressing GFP served as controls to observe any off-target effect of surgical procedure or CNO injection. Six weeks post-surgery, mice were introduced to a sweep-loom assay (Fig. 1b). The hM4Di and GFP mice were given CNO or saline via I.P. injection 1 hour before the experiment and were then allowed to acclimatise to the arena for 8 mins (Fig. 1d). After the acclimation phase, visual or auditory stimuli were delivered when the animal entered the centre of the arena (excluding epochs when the animal ran through that region). 6 sessions were conducted: 3 sessions in which the animal received CNO beforehand, and 3 sessions in which they received saline. Within each session, visual stimuli were delivered in a Sweep-Loom-Sweep-Loom order (Fig. 1d). After mice received the 4 visual stimuli, a high-frequency auditory stimulus was presented.

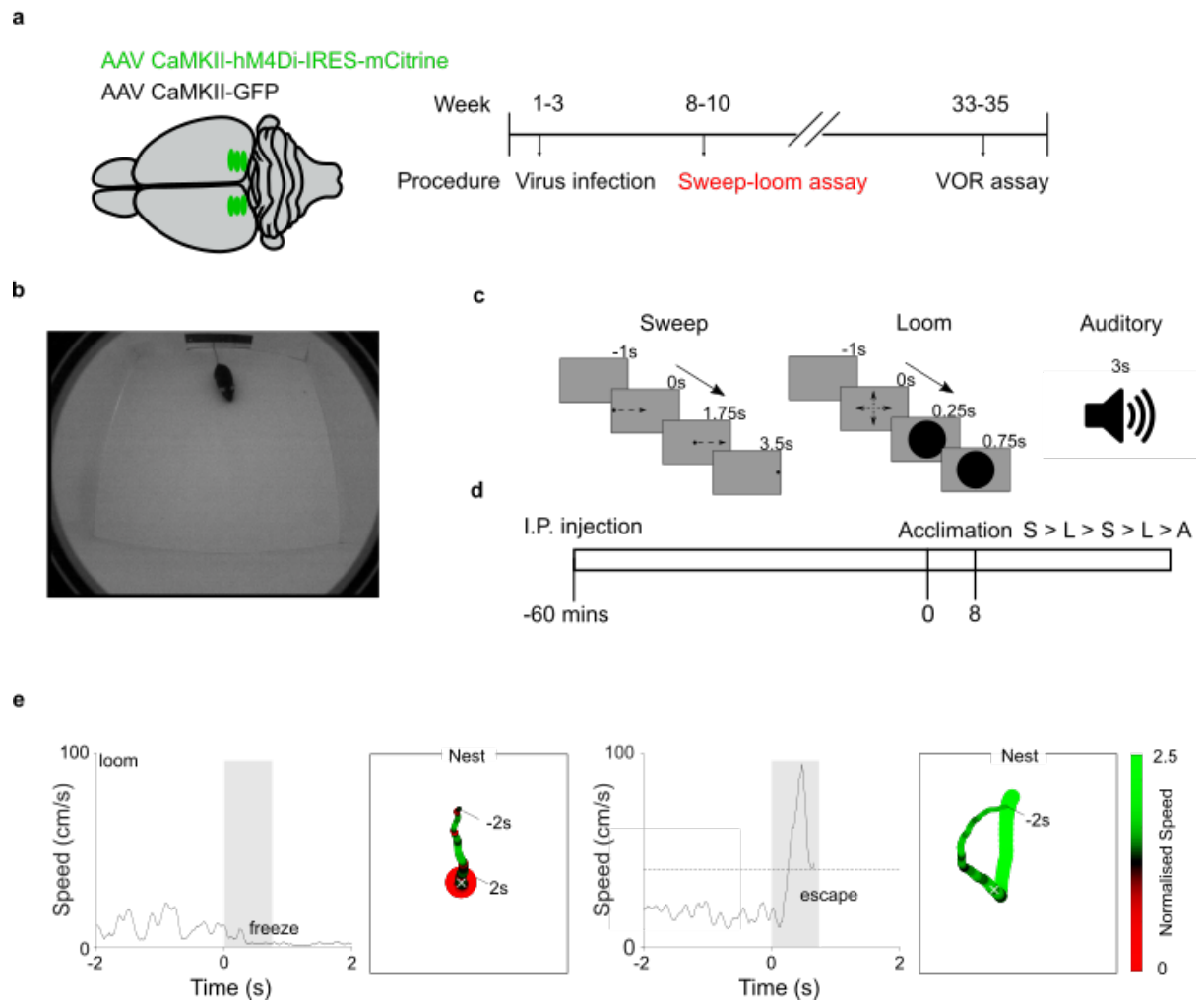


**Fig. 1: hM4Di manipulation in sweep-loom assay.**

**a. Left:** Schematic illustration of the virus injection. **Right:** Overall timeline of virus injection and behavioural sessions. **b.** View of the arena from the perspective of the camera, showing a mouse leaving the nest. **c.** Schematic illustration of the stimuli used in the assay. **d.** Schematic illustration of the timeline of a single session in the sweep-loom assay. **e.** Example freeze (left two panels) and escape (right two panels) events. In each pair, the left panel shows the movement speed of the animal before, during and after presentation of a looming stimulus. Grey areas indicate the time at which the looming stimulus was present on the overhead screen. Dashed line

indicates the threshold of escape speed (40 cm/s). In each pair, the right panel shows the mouse trajectories over the same time period. Spot colour indicates the logarithm of movement speed of the animal and saturates at the threshold of escape speed. Spot size indicates the time of the frame relative to the stimulus onset (larger spot indicates later time frame, the white X marks the location at time of stimulus onset).

#### 4.2.2 Limited effects of hM4Di manipulation on exploratory behaviours

We first asked whether CNO treatment affected exploratory behaviours in the arena by analysing behaviour during the acclimatisation period of each session. In the 1<sup>st</sup> session (CNO session), mice spent around 40% of the time in the arena, and the rest of the time in the nest. There was variability within and between each mouse and a general reduction in the arena time over sessions (Fig. 2a-b). To examine if CNO treatment affected time spent in the arena, a repeated measures ANOVA with treatment type (CNO or saline) and session number (T1: 1<sup>st</sup> CNO or saline session, T2: 2<sup>nd</sup> CNO or saline session, T3: 3<sup>rd</sup> CNO or saline session) as fixed factors was used. The ANOVA revealed that no significant main effect of treatment type ( $F=1.361$ ,  $p=0.271$ ), but a significant main effect of arena time in both groups ( $F=10.309$ ,  $p<0.001$ ). To capture the relationship between arena time and session number, the arena time of individual mice was subjected a repeated measure correlation (Bakdash & Marusich, 2017). Both hM4Di and GFP mice showed a negative correlation between the arena time and session number (GFP mice:  $r(28) = -0.46$ ,  $p = 0.011$ ; hM4Di mice:  $r(38) = -0.52$ ,  $p < 0.001$ ). The occupancy of open field is often used to access mice's anxiety level. As mice spent different times in the arena, I calculated the ratio of mice's time by the wall to mice's time in the arena (Fig. 2b). Regardless of treatment type, both groups of mice spent more and more time by the wall while they were in the arena over sessions. Similar to previous analysis, the corner time ratios were subjected to a repeated measure correlation, showing a positive correlation between the corner time ratios and sessions (GFP mice:  $r(27) = 0.50$ ,  $p = 0.006$ ; hM4Di mice:  $r(38) = 0.71$ ,  $p < 0.001$ ). Mice sometimes pause during exploration, or run back to the nest, even in absence of any overt stimulus. We therefore asked if CNO treatment affected these

spontaneous freezes and escapes. We defined freeze response if the animal was stationary (moving less than 2cm/s) for at least 0.2 s (Fig. 1e); escape response if the animal ran over 40cm/s and returned to the nest in less than 2s (Fig. 1f). Fig. 2c shows the results of these analyses. In the 1<sup>st</sup> session, hM4Di and GFP mice showed similar spontaneous escape and freeze rate. Inspection of spontaneous escape and freeze rate showed some variability in each mouse but there is no clear trend over sessions. Similar to analysis on the arena time, each mouse's spontaneous freeze and escape rates were subjected to a repeated measured ANOVA with treatment type and session number as fixed factors. The ANOVA suggested there were neither main effects of treatment type nor of session number on the spontaneous freeze (treatment:  $F=1.184$ ,  $p=0.302$ ; time:  $F=0.693$   $p=0.477$ ) and escape (treatment:  $F=2.72$ ,  $p=0.130$ ; time:  $F=0.411$   $p=0.668$ ).

We conclude that hM4Di and GFP mice spent similar amounts of time in the arena, and similar spontaneous escape and freeze rate regardless of treatment type. These results suggest (1) there is no clear effect of hM4Di manipulation on mice exploratory and spontaneous escape/freeze behaviours, and (2) while mice spent less and less time exploring the arena over sessions, their spontaneous escape/freeze behaviours seemed to be unchanged.

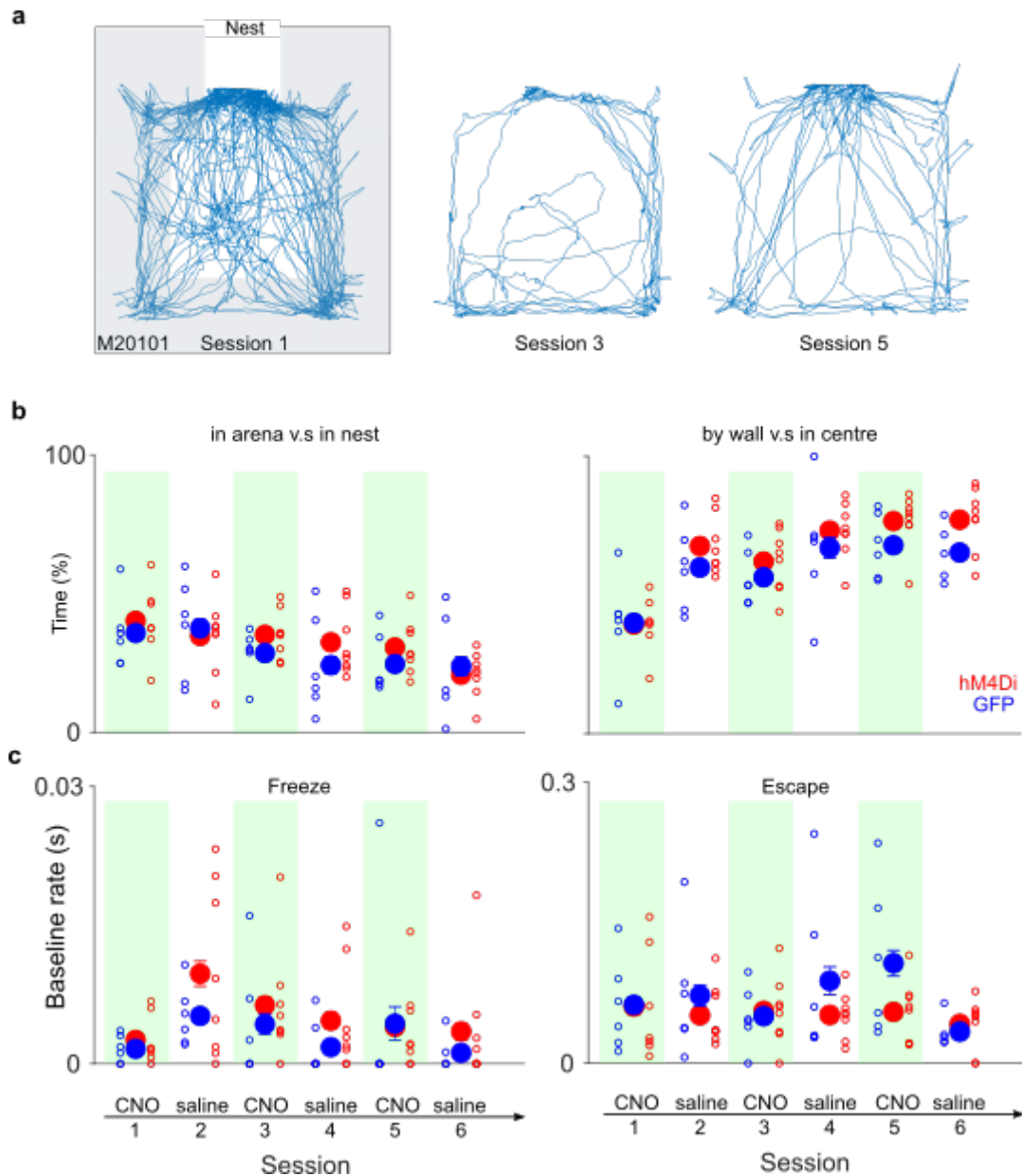


**Fig. 2: Mice exploration in the acclimation phase.**

**a.** Example traces showing a mouse's trajectory in the arena during the acclimatisation phase over sessions. Shaded area indicates wall area in contrast to centre of the arena for subsequent analysis. **b. Left:** Fraction of time spent exploring arena. *Right:* fraction of that exploration time spent near the walls of the arena across sessions. Open circles indicate individual animals. Closed circles indicate average across animals. Data are shown as mean  $\pm$ S.E.M (often too small to be seen). **c. Left:** Spontaneous freeze rate. *Right:* Spontaneous escape rate during exploration. Conventions as in (b).

#### *4.2.3 Limited effects of hM4Di manipulation on visual detection*

To establish the impact of hM4Di manipulation on visual detection I analysed behaviour in a 5-s window after each stimulus was presented. I used the ratio of freezes and escapes to establish detection and discrimination. I defined detection probability as the number of defensive behaviours (including both escape and freeze) divided by the number of stimuli in each group (Fig. 3a). I found around 70% of the sweeping stimuli and 60% of the looming stimuli were detected in both hM4Di and GFP mice in the 1<sup>st</sup> session (sweep: 71% in 8 hM4Di mice, 75% in 6 GFP mice; loom: 57% in 8 hM4Di mice, 64% in 6 GFP mice). The detection probability of both groups gradually decreased throughout the sessions, except for the last saline session. Although there was variance in the detection probability in both groups across sessions, there was no clear difference in the detection probability of hM4Di and GFP under CNO treatment (Fig. 3a). This suggests that visual detection was not impaired by hM4Di manipulation.

#### *4.2.4 Mice freeze more often than escape in sweep-loom assay.*

To investigate if mice responded differently to sweeping and looming stimuli, we investigated the occurrence of freeze and escape responses in each trial (Fig. 3b). We first focused on the responses to sweeping stimuli. In the 1<sup>st</sup> session, hM4Di mice showed similar freeze rate with GFP mice but a lower escape rate than GFP mice (hM4Di freeze: 71%, escape: 0.07%; GFP freeze: 66%, escape: 25%). To observe if these responses were due to small trial size in a session, we also compared the freeze and escape rate across different sessions. By pooling the responses under the same treatment together, similar to the responses in the 1<sup>st</sup> session, we found out both GFP and hM4Di mice were more likely to freeze than

escape (hM4Di freeze: 66% in CNO, 63% in saline; hM4Di escape: 10% in CNO, 10% in saline; GFP freeze: 63% in both CNO and saline; GFP escape: 21% in CNO, 13% in saline). The freeze rate was similar in both groups under both treatments. hM4Di mice had similar escape rate under saline and CNO treatment, but hM4Di/CNO condition's escape rate was slightly lower than GFP/CNO condition.

We then analysed the responses to looming stimuli. In the first session, both groups' responses to looming stimuli showed similar freeze rate but hM4Di mice had a lower escape rate than GFP mice (hM4Di freeze: 57%, escape: 0%; GFP freeze: 63%, escape: 18%), which was surprisingly similar to their responses to sweeping stimuli. Across sessions, both groups were more likely to freeze than to escape in response to looming stimuli (hM4Di freeze: 55% in CNO, 52% in saline; hM4Di escape: 10% in CNO, 10% in saline; GFP freeze: 61% in CNO, 69% in saline; GFP escape: 11% in CNO, 6.3% in saline). Importantly, looming stimuli triggered similar escape rates in both groups. These results show that both groups of mice were more likely to freeze than escape, irrespective of visual stimulus type and treatment type.

We found a greater escape probability when the stimulus was auditory. In the 1<sup>st</sup> session, both groups of mice responded vigorously to auditory stimulus (hM4Di freeze: 71%, escape: 43%; GFP freeze: 80%, escape: 60%). These freeze rates were slightly higher than their corresponding freeze rate in response to visual stimuli. We saw the main difference between visual and auditory stimuli is that auditory stimulus evoked a large increase in the escape rate of both hM4Di and GFP groups. To examine if these responses varied over sessions, we also analysed mice's responses to auditory stimuli over sessions (Fig. 3b). There was no clear difference

in their responses under CNO and saline treatment (hM4Di freeze: 38% in CNO, 36% in saline; hM4Di escape: 38% in CNO, 43% in saline; GFP freeze: 71% in CNO, 25% in saline; GFP escape: 43% in CNO, 38% in saline).

Group analysis showed a general trend of defensive strategies in mice: a higher ratio of freeze to escape in response to visual stimuli. To reduce between subject variance, I conducted a within-subject analysis to seek for any behavioural change in hM4Di mice due to CNO treatment. As some mice stayed in the nest until the end of the session after receiving the first visual stimulus (data not shown but can be captured by a reduction in delivery rate over sessions in Fig.3a), I narrowed the analysis to 4 hM4Di mice that received all the visual stimuli across sessions (Fig. 3c). These 4 mice showed fewer escape events than freeze events. Inspection of the escape speed and of freeze duration showed some variance in each mouse but no obvious difference under saline and CNO treatment. Similar to previous analysis, the freeze duration of each mice in response to both sweeping and looming stimuli was subjected to a repeated measured ANOVA with treatment type and session number as fixed factors. The ANOVA showed that there was no difference in the freeze response under different treatments ( $F=0.772$ ,  $p=0.444$ ).

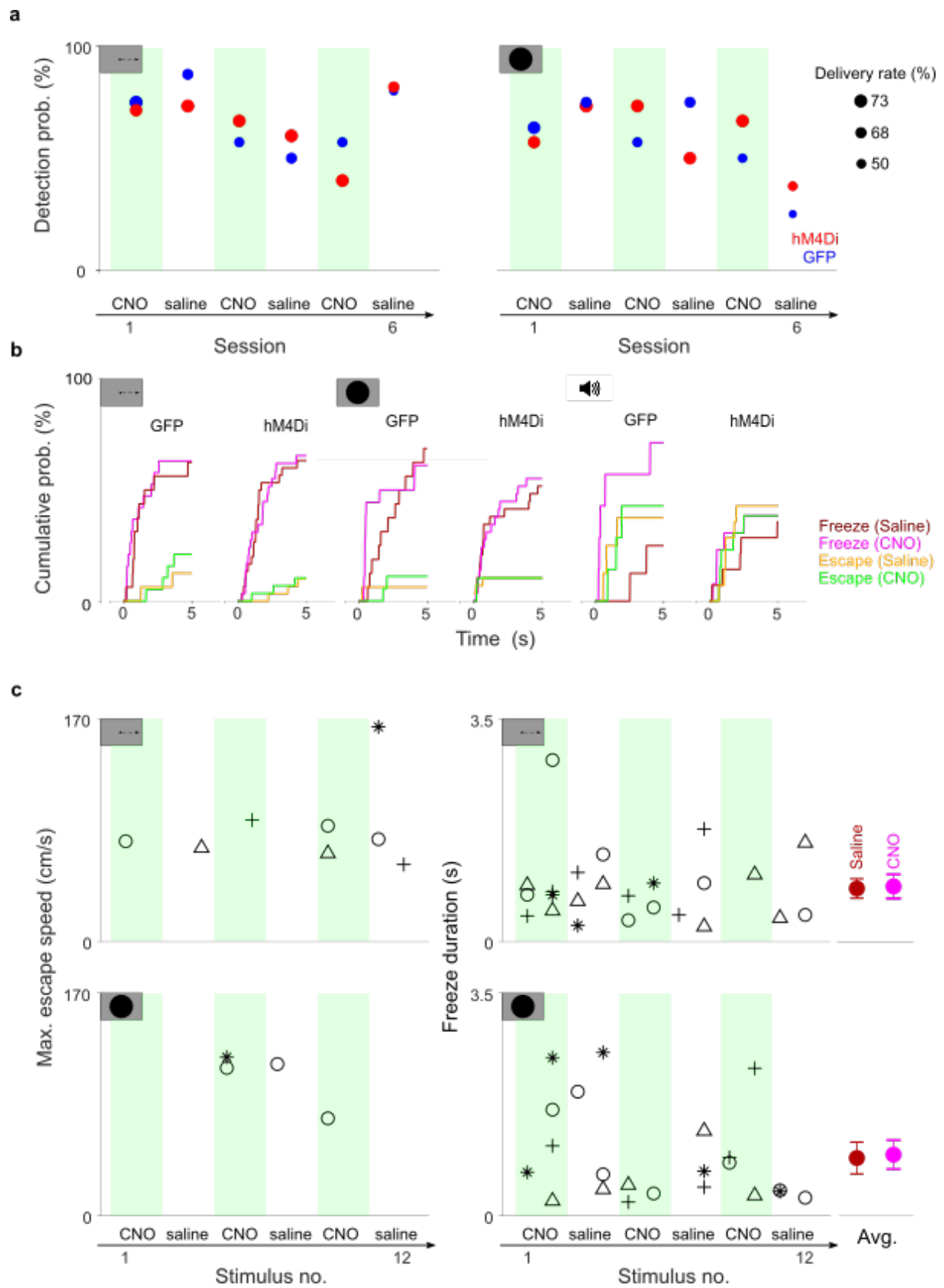


**Fig. 3: Limited effect of hM4Di manipulation on visually guided behaviours.**

**a.** Detection probability of mice in response to sweeping and looming stimuli. Spot indicates mean for each group of mice. Spot size indicates stimulus delivery rate. At maximum, hM4Di and GFP group respectively receive 32 and 24 visual stimuli in a session. **b.** Cumulative probability of mice in response to sweeping, looming and auditory stimuli. Line colour indicates type of virus (GFP or hM4Di) and treatment (saline or CNO). X axis indicates the time from the stimulus onset **c.** Intensity of defensive behaviours in hM4Di mice. Different markers are different mice. The average freeze duration of these mice is presented at the right of **(c)**. Data are mean  $\pm$ S.E.M.

#### 4.2.5 A new visual object recognition assay

We sought other assays to examine the effect of hM4Di manipulation on visual discrimination, to test the hypothesis that visual cortex is required for discrimination in a non-aversive context. To test this hypothesis, we developed a visual object recognition (VOR) assay. In the classic novel object recognition (NOR) task, mice are placed into an arena and are allowed to explore two identical objects. These are real but inanimate objects, and the mouse may use vision, olfaction and/or somatosensation (whisking) to explore them. After mice familiarise with the objects, one of the objects is replaced with a new object and mice are allowed to explore the objects again. The time mice exploring the novel and familiar objects is a proxy for whether mice remember the familiar object, and therefore whether mice are capable of discriminating the familiar and novel objects. As laboratory mice show neophilic behaviours after they become habituated with the assay, they are more likely to spend more time exploring the novel object.

To provide a visual-only version of this task, we enclosed each of the two objects in the arena with transparent cylinders (Fig. 4a). A previous study classified white triangle and square as difficult-to-discriminate images in mice (Braida et al., 2013), suggesting that that objects in the same colour might not be distinct enough for mice in this type of assay. Therefore, I started the assay with a black cube and wooden cone to ensure not only shape, but colour could be used to discriminate the object (Fig. 4b). The two objects were placed on the same side of the arena so that whether mice prefer to approach or avoid any objects could be estimated by measuring the time spent on the side where the two objects were placed (Object side). I was concerned that the new objects may be different in salience to the animals. In

standard NOR tests this is often resolved by screening the innate preference of mice for an array of objects in pilot experiments, prior to the NOR assay (for a review, see Leger et al., 2013). However, that form of screening does not account for individual variance in mice's innate preference among the sampled objects. I reckoned that individual innate preference may be problematic when using new, arbitrary combinations of objects and perturbing visual cortex with DREADDs. I therefore first measured mouse behaviour during two VOR assays. One followed the standard timeline of the classic NOR assay (Condition A). The other (Condition B) was the same as Condition A, except that a pre-familiarisation test was used to sample individual mouse's preference over the two objects prior to familiarisation (Fig. 4a). I used two groups of mice to examine how mice explore objects in the Condition A and B. The two groups showed similar travel distance per session but some variance (Fig. 4c). Their travel distance during familiarisation phase was subjected to a one-way repeated measure ANOVA, which was not significant ( $F=1.88$ ,  $p=0.075$ ). During the post-familiarisation test, both groups spent more time on the Object side (Fig. 4d-e).

I used DeepLabCut (Mathis et al., 2018) to estimate the position of each mouse's nose and ears, and defined object exploration as when the animal entered a region of interest (ROI) around the object, based on the distance between the mouse's nose and the centroid of the cylinder. I calculated an object preference index as the difference in exploration time for the new object and that for the familiar object, normalized by the sum of the two. This preference index was negative at each of several ROI distances (Fig. 4f), suggesting that mice in both groups preferred exploration around the novel object. For a 5-cm ROI, all mice spent more time around the novel object. The preference index from post-familiarisation test in

Condition A was subjected to a one sample T-test against chance level and the preference index from pre- and post-familiarisation tests in Condition B was subjected to a paired T-test to examine the effect of familiarisation phase on the preference index. The statistical analysis revealed that all mice showed higher preferences for novel objects (Condition A:  $p=0.005$ ; Condition B:  $p<0.001$ ; Fig. 4f-h). There was no obvious preference toward objects placed on the left or right in either Condition (one-sample t-test, Condition A:  $p=0.756$ ; Condition B:  $p=0.916$  to chance level; Fig. 4f). In addition, Condition B yielded a slight larger preference index than Condition A, but the difference was not significant (two-tailed Student's T-test,  $p=0.096$ ). Overall, these results suggest that mice were able to discriminate the novel object from the familiar object with visual information only, and that the pre-familiarisation test does not prevent the expression of novelty seeking.

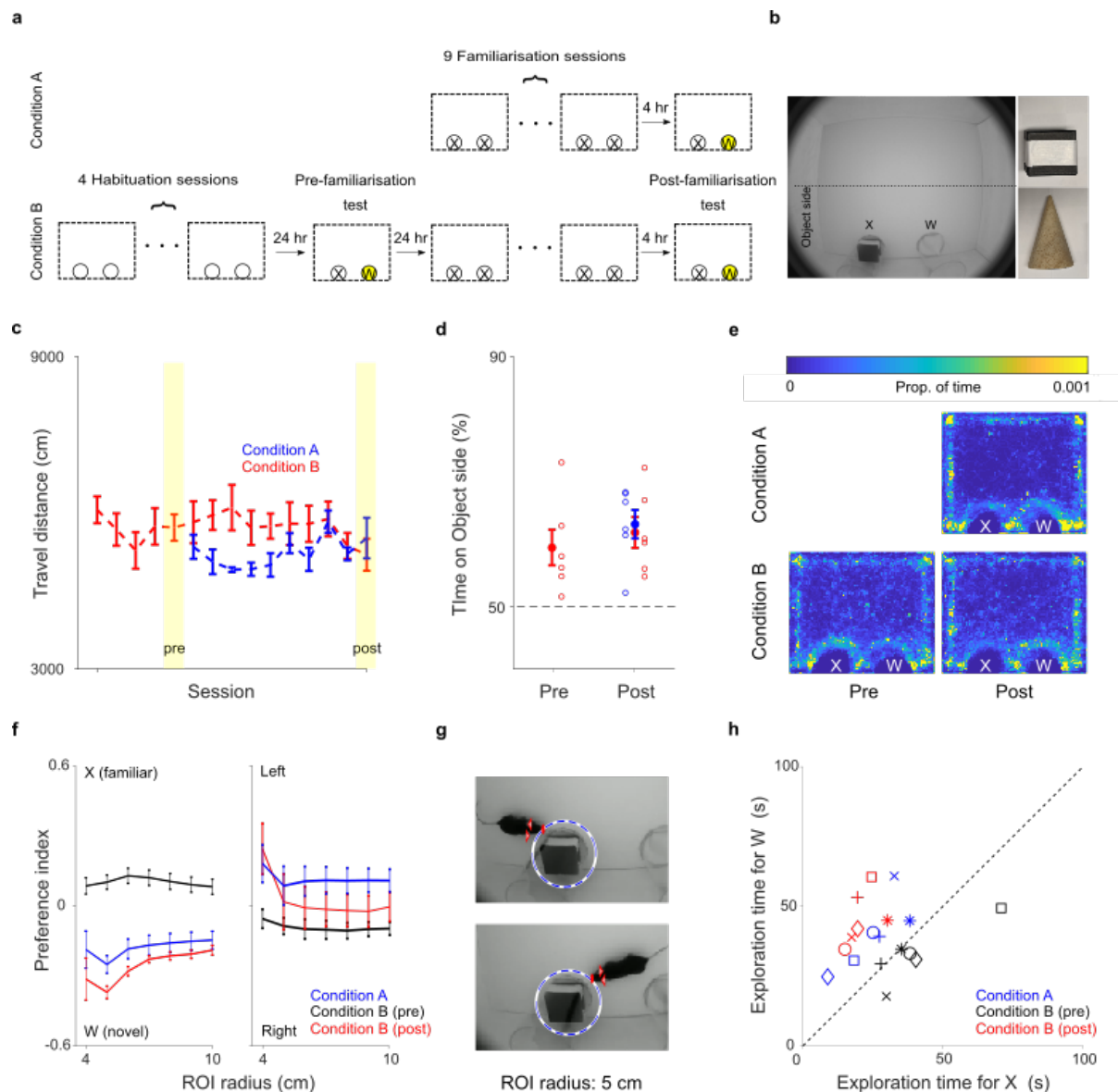


**Fig. 4: A visual object recognition assay.**

**a.** Schematic illustration of the timeline of the assays. X and W indicates object identity. Condition A shows the standard VOR assay timeline. In Condition B, mice were provided with a pre-familiarisation test to establish their innate object preference. **b. Left:** View of the arena from the perspective of the camera, Object side indicates the area where the two objects were placed. *Top right:* black cube (object X); *Bottom right:* wooden cone (object W). **c.** Average travel distance in the arena across sessions. Yellow area indicates pre- and post-familiarisation tests (Condition A: n=6 mice, Condition B: n=6 mice). Data are mean  $\pm$ S.E.M. **d.**

Occupancy time on Object side during pre- and post-familiarisation tests. Open circles indicate individual response. Closed circles indicate average response. Data are mean  $\pm$ S.E.M. Dotted line indicates chance level (50%). **e.** Average occupancy map during pre- and post-familiarisation tests. Dotted line indicates no preference (50%). **f.** Average preference index across different ROI size during pre- and post-familiarisation tests. Data are mean  $\pm$ S.E.M. **g.** Example image of exploration behaviours. Blue circles indicate ROI. Triangles indicate ears. Filled oval indicates nose. **h.** Scatter plot of mice exploration time for both objects. Different markers are different mice.

#### 4.2.6 Limited effects of hM4Di manipulation in the VOR assay

Having developed a new VOR assay, we asked whether hM4Di manipulation of V1 affected visual discrimination using this assay. I conducted the assay on the same mice used previously in the sweep-loom assay and included 4 additional mice from the LFP recording sessions (Fig. 4a, LFP recording mice not shown). I used Condition B and injected CNO 1 hour prior to the post-familiarisation tests. The exploratory behaviours of mice were analysed in the same way as before (Fig. 5b-d). Mice from the sweep-loom assay and from LFP recording showed similar exploratory behaviours so they were pooled together for statistical analysis.

During the pre-familiarisation test, neither hM4Di nor GFP mice showed obvious preference for one of the objects (hM4Di:  $p=0.726$ ; GFP:  $p=0.166$  to chance level; Fig. 5e-f). Comparison of pre- and post-familiarisation preference index showed that both hM4Di and GFP group spent more time exploring the novel object during the post-familiarisation test (one-tailed Student's T-test, hM4Di:  $p=0.015$ ; GFP:  $p=0.037$ ). Although we found GFP mice had some overall bias toward the left objects during the last session in the familiarisation phase (Fig. 5g), these data suggested that both groups were able to discriminate between the two objects. To establish whether hM4Di manipulation affected visual discrimination, the preference index of hM4Di and GFP mice at pre- and post-familiarisation tests was subjected to a one-way repeated measure ANOVA with session number as the fixed factors. There was no significant interaction effect between the session number and virus type (pre- or post-familiarisation tests X hM4Di or GFP interaction:  $F=5.87e^{-4}$ ,  $p=0.981$ ), suggesting that the change in preference index from pre to post-familiarisation tests

was similar in both groups of mice. This analysis indicated that hM4Di manipulation did not influence visual discrimination between the wooden cone and black cube.

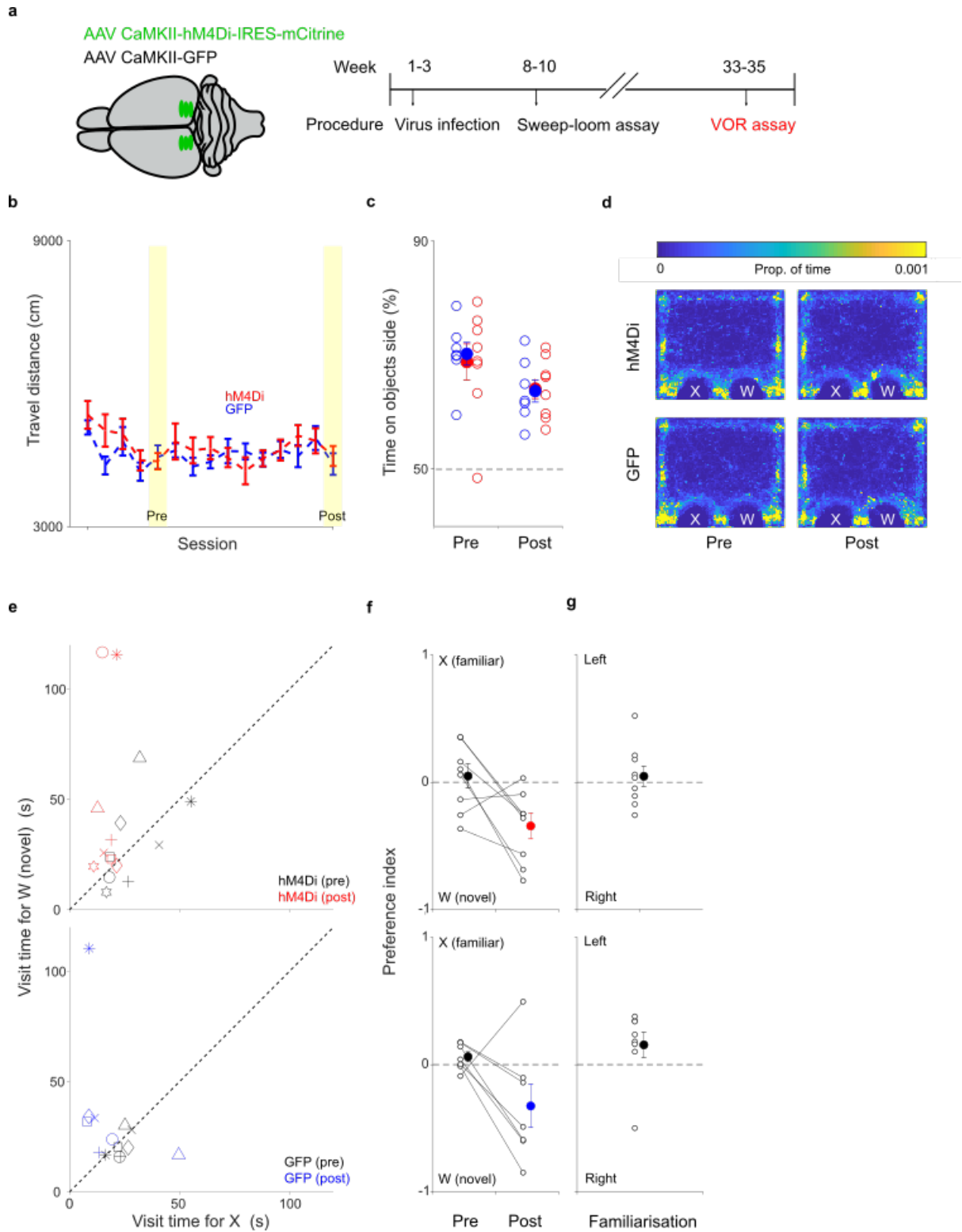


**Fig. 5: Limited effect of hM4Di manipulation on visual object recognition.**

**a.** *Left:* Schematic illustration of the virus injections. *Right:* Timeline of virus injection and behavioural assays. **b.** Average travel distance in the arena across sessions. Yellow area indicates pre- and post-familiarisation tests (hM4Di: n=8 mice, GFP: n=7 mice). Data are mean  $\pm$ S.E.M. **c.** Occupancy time on Object side during pre- and post-familiarisation tests. Open circles indicate individual response. Closed circles indicate average response. Data are mean  $\pm$ S.E.M. **d.** Average occupancy map during pre- and post-familiarisation tests. **e.** Scatter plot of mouse exploration time for both objects during pre- and post-familiarisation tests. Different markers are different mice. **f.** Object preference index of hM4Di and GFP mice during pre- and post-familiarisation tests. Negative value indicates preference for novel objects. Open circles indicate individual response. Closed circles indicate average response. Data are mean  $\pm$ S.E.M. Dotted line indicates no preference. **g.** Left/right preference index of hM4Di and GFP mice during the last familiarisation session. Negative value indicates preference for objects placed on the right. Open circles indicate individual response. Closed circles indicate average response. Data are mean  $\pm$ S.E.M. Dotted line indicates no preference.

### *4.3 Discussion*

In this study, we attempted to test hypotheses about the role of V1 in visual discrimination. Firstly, we presented sweeping and looming stimuli to freely moving mice in a sweep-loom assay. Mice tended to freeze regardless of the type of visual stimuli, and both sweeping and looming stimulus evoked similar freeze rate. Hence, we had no evidence that hM4Di manipulation affected animal's ability to discriminate the two different visual threats. In addition, we established a new VOR assay by using transparent cylinder covering objects of different shapes and colour. Both hM4Di and GFP mice spent more time on the novel objects, suggesting that visual discrimination was not disrupted by hM4Di manipulation.

#### *4.3.1 Variable responses to looming stimulus*

We first measured responses to sweeping and looming stimuli in hM4Di and GFP mice. Previous work from our laboratory showed that mice discriminated between these potential and imminent visual threats by freezing and escaping respectively. In the current experiments, however, mice were more likely to freeze than to escape regardless of the type of visual stimulus. The probability of freezing responses to sweeping stimulus was similar to the previous work, but the probability of escape responses to looming stimulus was lower (De Franceschi et al., 2016).

It is not obvious why mice were less likely to escape than expected. However, we modified this behavioural assay to be compatible with hM4Di perturbation, and there are potential consequences of these changes. First, instead of delivering 1 or 2 visual stimuli in a session (De Franceschi et al., 2016), we delivered 4 visual stimuli in a session. This adjustment was meant to reduce the number of I.P. injections mice

received. Although we did not observe a clear difference between GFP mice's first response and averaged responses to sweeping and looming stimuli, receiving 4 visual stimuli and an auditory stimulus might make encourage mice to habituate to the stimuli earlier, reducing their motivation to escape. In addition, instead of using a monitor to deliver the stimulus in the previous study (De Franceschi et al., 2016), a projector was used. Although several studies have used projectors to deliver looming stimulus, and we approximately mimicked the luminance level of previous work (30~40 candela/m<sup>2</sup>) there may be subtle differences between the looming stimuli presented by projectors and monitors respectively.

Escape behaviour is not merely a simple reflex but subject to internal state. Stress can enhance mouse escape speed (Li et al., 2018). It is also known that mice housed in two different animal facilities may respond to looming stimuli differently (Yilmaz & Meister, 2013), suggesting that housing conditions can affect defensive behaviour. We conducted the behavioural experiments during the coronavirus pandemic in 2020, when the access to animal facility was restricted. The reduced capacity of the animal facility might reduce sensorial enrichment and affect the internal state of the mice. In addition, mice were not tail-carried into the arena, possibly reducing stress levels prior to the behavioural assay. In our experiments, auditory stimuli were more likely to trigger escape than visual looming stimuli. Nevertheless, the probability of auditory-induced escape was still somewhat lower than in other reports (Evans et al., 2018; Vale et al., 2017). It is possible that due to a combination of environmental factors this batch of mice did not escape as extensively as other published work.

#### *4.3.2 Limited effects of hM4Di manipulation in visual detection and defensive behaviours*

We found no clear discrimination in GFP control mice: behavioural responses to sweeping and looming stimulus were similar, making it difficult to interpret if the visual discrimination in hM4Di manipulation was intact. We therefore focused on the probability of visual detection. In the 1<sup>st</sup> session, both hM4Di mice and GFP mice froze in response to sweeping and looming stimuli, and in both the first and subsequent sessions there was no clear effect of treatment on visual detection. Failure to disrupt visual detection is consistent with a previous study where mice receiving muscimol in V1 could still respond to looming stimuli (Evans et al., 2018). Sweeping and looming stimuli might be able to activate defence pathways without the V1. It is likely that the SC, which receives strong input from the retina, may play a major role in detecting visual threats.

In addition, both hM4Di mice and GFP showed reduced response probability over sessions. The reduction in response (albeit ignoring the last session) suggests that mice habituate to sweeping and looming stimuli (Tafreshiha et al., 2021; Yilmaz & Meister, 2013). Given the limited number of mice and stimuli in this assay, it was difficult to determine if this habituation was independent from hM4Di manipulation.

Finally, previous work has found that muscimol inhibition of V1 might slightly reduce maximum escape speed (Evans et al., 2018). However, in our studies, we did not find an obvious change in escape speed between treatments. A straightforward explanation arises from different methods of V1 perturbation. On the one hand, hM4Di manipulation and muscimol inhibition in V1 may have different effect on VEP

(see Chapter 3 for further discussion), which may explain the different responses in mice to looming stimulus. On the other hand, some studies have shown that one mechanism of hM4Di manipulation is through inhibiting synaptic release (Stachniak et al., 2014). Therefore, it is may be that the limited effect of hM4Di on VEP in V1 does not reveal whether V1's downstream regions such as SC are effected by the hM4Di manipulation or not.

Other factors might help explain the discrepancy between the results presented in this thesis and previous work. The environmental factors potentially affecting defensive behaviours in mice was described above. Additional differences between Evans et al and this work may also play a role. First, the escape rate in our mice was much lower than in previous studies and loom-evoked escape responses were mainly found in the later experimental sessions (3<sup>rd</sup> to 6<sup>th</sup> sessions) when mice had received CNO multiple times. Therefore, mice might have adapted to the effect hM4Di manipulation brought. We do not have hM4Di mice's escape response prior to the 1<sup>st</sup> session, so we cannot examine if any reduction in escape speed was due to the first CNO administration. Secondly, the maximum escape speed in our mice (around 80-90 cm/s) was slightly lower than Evans and other colleagues' findings (around 100 cm/s). This could be explained by (a) more behavioural sessions in the assay: Evans and others' looming assay is a single-session assay whereas we ran several sessions of CNO to manipulate V1 activity. In our assay, hM4Di mice showed a general reduction in escape speed in response to looming and auditory stimuli over sessions (data not shown), which might lower the averaged escape speed; (b) shorter travel distance between stimuli-delivery site to shelter: at least 30

cm away from the shelter in Evans et al whereas around 21 cm away from the shelter in our assay.

Overall, these environmental factors may explain why our mice escape less extensively than the previous work. Therefore, it was difficult to speculate if the limited effect of hM4Di manipulation on visually evoked defensive behaviours is due to those environmental factors or hM4Di manipulation itself.

#### *4.3.3 Establishment of a new VOR assay*

The NOR assay is a popular memory test that exploits animals' innate neophilia. It is straightforward to set up and able to yield comparative memory performance across species. Our results, which show that vision is sufficient for NOR, are consistent with previous studies displaying visual patterns on screens in mice (Braida et al., 2013; Romberg et al., 2013; Cooke et al., 2015) or in rats (Forwood et al., 2007; Del Grosso et al., 2017). These studies together argue that it is possible to study visually guided behaviours in mice under such a context (monitoring mice's spontaneous behaviours without the use of external reward/punishment). The use of visual objects instead of patterns, opens an opportunity to study object recognition in mice, which has been studied in mainly rats (for rats: Zoccolan et al., 2009; Djurdjevic et al., 2018; for mice: Froudarakis et al., 2020) with the use of associated reward. The inclusion of a pre-familiarisation test in this study allowed assessment of novelty-independent object preferences while preserving the effect of familiarity on subsequent behaviour. Previous work also suggests that objects lose their novelty cumulatively, not instantaneously (Genzel et al., 2019). Applying the framework of

this experimental design to future studies may improve our understanding of how individual's visual discrimination changes due to prior experiences.

#### *4.3.4 Limited effect of hM4Di on visual discrimination*

We found similar VOR in hM4Di and GFP mice. Both groups showed similar occupancy patterns in the arena, with more time on the Object side, suggesting that their capacity to detect the presence of visual objects was not affected by the hM4Di manipulation. In addition, both groups showed a preference for novel objects, after long-term familiarisation with the other object, suggesting that the visual discrimination was not affected by hM4Di manipulation. As our objects are distinct in luminance level, this result is aligned with classic lesion studies that rats' striate cortex is not required for luminance discrimination (Lashley, 1935). However, the neural mechanism behind that remains unclear.

Firstly, we need to consider is whether V1 is sufficiently disrupted by hM4Di manipulation or not. Cooke et al., 2015 found that SRP in V1 is required for visual discrimination between novel and familiar grating stimuli, but we failed to detect any disruption in SRP in hM4Di-expressing mice (see Chapter 3 for more details). Therefore, failing to disrupt visual discrimination in the VOR assay might simply reflect the fact that the SRP was intact. To address this concern, we can use positive controls such as grating stimuli of different orientation in the VOR assay. As VEP was intact by hM4Di manipulation, mice shall be able to discriminate grating stimuli of different orientation.

Secondly, mice can use other visual pathways such as SC to detect the difference in the two objects. Similar to V1 neurons, SC neurons also display tuning for orientation and direction (Inayat et al., 2015), and thus may permit similar involvement in visual discrimination. In addition, there are parallel pathways reaching higher visual areas via SC only (Beltramo & Scanziani, 2019), so it is possible that the hM4Di-induced V1 disruption is compensated by other visual pathways. To separate the role of V1 and SC in visual discrimination, one must combine multiple perturbation methods to selectively inhibit SC, V1 or both.

#### *4.3.5 Experimental limitations*

The behavioural categories we used as a proxy of visual discrimination (freeze/escape ratio; occupancy time around objects) were based on previous studies. It is possible that other behavioural categories might be affected by hM4Di manipulation in V1. For instance, rearing behaviour (a type of exploratory behaviour) and tail rattling (a type of aggressive behaviour) have been described in looming assay to capture the emotional state of mice during the test (Salay et al., 2018). Biting behaviour was described in NOR assay as another behavioural measure of exploration in mice (Ahmadlou et al., 2021). These behavioural epochs require further analysis to identify their occurrence.

#### *4.4 Summary*

In this chapter, we attempted to use two different behavioural assays to identify the impact of hM4Di manipulation on visual discrimination. I ran multiple sessions of the existing sweep-looming assay in the lab and developed a new VOR assay to study visual discrimination in different contexts. In both behavioural assays, hM4Di mice

showed limited differences in visual detection. hM4Di mice had similar detection rate as GFP mice in sweep-loom assay, and they spent similar time in the Object side as GFP mice did in the VOR assay. Beyond *detection*, we also attempted to test if visual *discrimination* was impaired by hM4Di manipulation. Unfortunately, in the sweep-loom assay mice did not behaviourally discriminate between sweeping and looming stimuli. In the VOR assay, whilst mice did discriminate the novel object, this was true of both hM4Di and GFP mice, suggesting that hM4Di manipulation does not impair the visual discrimination between the cube and the cone.

## *Chapter 5: Conclusion*

How cerebral cortex integrates signals about sensory stimuli with signals about other non-sensory factors such as locomotion and prior experience is one of the key open questions in neuroscience. Pioneering studies on primates and cats have shown how sensory information is represented and transformed in the visual system and have started to explore how cortical layers or cell types contribute to behaviours.

In this thesis, I sought to better understand the role of V1 in visual discrimination by manipulating neural activity of excitatory neurons in V1 with DREADDs.

Electrophysiological work examined the efficacy of hM4Di manipulation *in vivo*. The VEP amplitude was not affected by the hM4Di manipulation. Instead, the hM4Di manipulation was associated with a tentative enhancement in low-frequency oscillations during grey screen, and in the first harmonic signals during low-temporal frequency grating stimuli. As I injected the hM4Di virus into the deeper layers of V1, and it is known that layer 5 pyramidal neurons play a role in low-frequency oscillation (Beltramo et al., 2013; Krone et al., 2021), the enhanced oscillations could be due to effects caused by those neurons. Nevertheless, interpreting the effects of these kinds of manipulations remains a challenge in the field, and to what extent V1 function is disrupted by hM4Di manipulation remains unclear. It would be more convincing to see that V1's firing rate is reduced and/or the cortical output is suppressed. In Chapter 3, I discussed potential reasons of limited effects of hM4Di manipulation on VEP amplitude. In Section 5.1, I consider future experiments that could help validate and interpret the effect of hM4Di manipulations in V1.

At the behavioural level, I found no evidence that the hM4Di manipulation in V1 affected (untrained) visual detection and discrimination in freely moving mice. This lack of effect might be due to a lack of impact of the hM4Di manipulation on V1 activity (for example, the hM4Di manipulation did not obviously affect VEP amplitude). Alternatively, the lack of effect may indicate that V1 is not required to discriminate visual stimuli in the behavioural assays used (for example, sweeping vs. looming stimuli). In Section 5.3, I consider the potential role of V1 in these innate visually-guided behaviours.

### *5.1 Experiments to validate the impact of hM4Di manipulation on V1 function*

hM4Di is advertised to inhibit neuronal activity via the induction of neuronal hyperpolarisation and inhibition of presynaptic release. Several methods can show the efficacy of hM4Di manipulation in both *in vivo* and *ex vivo*. *Ex vivo* whole cell recordings have shown that, upon application of CNO, hM4Di-expressing neurons are hyperpolarised and/or their spiking activity is inhibited (Richards et al., 2014; Robinson et al., 2014; Sano et al., 2014; Chiou et al., 2016; Viskaitis et al., 2017; Sheng et al., 2020; Vale et al., 2020; Y.-C. Wang et al., 2020; Devienne et al., 2021; Wu et al., 2021). *In vivo* studies have shown that hM4Di-expression is associated with the reduction of spiking activity in neural populations in subcortical areas (Viskaitis et al., 2017) and in neocortex (Sano et al., 2014; Vale et al., 2020). Evidence for a role of hM4Di in preventing synaptic release comes mainly from *ex vivo* experiments, where a reduction of evoked postsynaptic current was measured upon administration of CNO (Bock et al., 2013; Stachniak et al., 2014; Evans et al., 2018; Doron et al., 2020). However, *in vivo* experiments, where post-synaptic neurons' field potential was measured upon application of electrical stimuli to presynaptic neurons (field excitatory postsynaptic potential, fEPSP), have yield

mixed results. hM4Di manipulation can cause an increase in fEPSP in motor cortex (Natale et al., 2021) and entorhinal cortex (Madroñal et al., 2016), but other work has shown that hM4Di manipulation causes a decrease in fEPSP in motor cortex (Y.-C. Wang et al., 2020).

I used the VEP as a measure of neural activity but failed to find a consistent effect of hM4Di manipulation on VEP amplitude in V1. In Chapter 3, I discussed possible mechanisms of that and argued that unlike pharmacological approaches, expressing DREADDs in V1 with AAV virus should prevent a direct influence on the thalamo-cortical inputs, limiting the effect on VEP amplitude. Therefore, other measures should be used when validating the impact of hM4Di manipulation on V1 neurons. *Ex vivo* slice recordings would allow me to measure the resting membrane potential of hM4Di-expressing neurons; and in combination with electrical stimulation of thalamocortical or intracortical axons would allow me to also assess stimulus-evoked membrane potential and spiking activity. By comparing hM4Di-expressing neurons' response in the presence to CNO and during the wash-out period, I expect that CNO would induce hM4Di-mediated hyperpolarisation, and that the stimulus-evoked response would also be reduced. *In vivo* extracellular recording with laminar probes can then be used to measure the spiking activity in hM4Di-expressing layers of V1, before and during systemic injection of CNO. If the effect of hM4Di manipulation is similar to the aforementioned *in vivo* measurements, or similar measurements using baclofen (a GABA-B receptor agonist in Baumfalk & Albus, 1987), I expect a reduction in stimulus-evoked spiking activity during CNO administration.

hM4Di-induced hyperpolarisation itself may not be enough to prevent synaptic release in cortical neurons (Stachniak et al., 2014). This suggests that hM4Di may exert its effect by dampening synaptic release, and thereby reducing neuronal population activity. Thus, showing hyperpolarisation of hM4Di-expressing neurons may not be sufficient to infer that V1's output is lost. *Ex vivo* paired recordings from synaptically coupled neurons can be used to assess hM4Di's capability to suppress synaptic release. By co-expressing excitatory optogenetic proteins and hM4Di in the pre-synaptic neurons, and measuring post-synaptic currents evoked by photostimulation in the presence and absence of CNO, I would use the post-synaptic currents to evaluate to what extent hM4Di dampens synaptic release. One concern with paired recording is that long-term activation of hM4Di with CNO may induce homeostatic plasticity in hM4Di-expressing neurons, in turn leading to an increase in miniature EPSCs between the paired neurons (Wen & Turrigiano, 2021; Wu et al., 2021). To circumvent this issue, I could either limit the CNO wash-in time during recording, or co-express hM4Di with exogenous synaptic scaling hallmarks in the cortical neurons to prevent further synaptic scaling (Lambo & Turrigiano, 2013) while conducting the slice recording.

## *5.2 Alternative methods to inhibit V1 output*

In Section 5.1, I discuss future works to validate the efficacy of hM4Di manipulation. However, experiments such as *ex vivo* paired recording and *in vivo* recording can be technically challenging. For example, if the electrode is not inserted to the correct area or neuron, it would be still difficult to examine the efficacy of hM4Di manipulation. If this is the case, other methods may be used as a substitution to inhibit V1 output.

Alternative optogenetic- and chemogenetic approaches are possible. Previous studies have shown that activating PV+ inhibitory neurons via optogenetics leads to a reduction in VEP amplitude (Cooke et al., 2015; Kaplan et al., 2016). I did not choose optogenetic approaches in the experiments described here, because its sustained activation can be problematic during behavioural studies, especially in VOR assay where visual stimuli are not locked to particular behavioural events. Stronger control over V1 activity might nevertheless be provided by introducing hM3Dq, an excitatory DREADD, into inhibitory neurons, thereby reducing the activity of excitatory neurons. Electrophysiological work shows that manipulating PV+ neurons with hM3Dq reduces spontaneous cortical firing and slow wave activity during NREM sleep (Funk et al., 2017), and behavioural studies show that chemogenic activation of cortical PV+ neurons can lead to behavioural change in mouse disease models (Chen et al., 2018; Goel et al., 2018; Lupien-Meilleur et al., 2021). Thus, if manipulating PV+ neurons with hM3Dq reduced VEP amplitude or other visual responses, this would suggest an alternative way to manipulate V1 activity during behaviours.

### *5.3 Potential role of V1 in innate visually-guided behaviours*

In this thesis, I used two behavioural assays to probe the potential function of V1 in innate behaviours. These two assays feature different contexts, stimuli of interest, and analysis methods. In the sweep-loom assay, I used ethologically relevant stimuli and observed mice's responses to the stimuli. To study visual discrimination in the VOR assay, I exploited neophilia, expressed after mice habituate to a familiar object. In both assays, I used stimuli distinct in shape and size, and found no clear evidence that V1 is involved in either visual discrimination.

Two concerns need to be addressed when investigating V1's role in innate visually guided behaviours. Technically, the parallel visual pathways from retina to higher visual cortical areas (e.g. via SC and pulvinar, or via LGN and V1) makes it difficult to identify the role of V1 in behaviours. Failing to find behavioural deficits while perturbing one of the pathways does not mean that pathway is not involved in the behaviour. Instead, the other pathway might react to compensate for that circuit perturbation. Hence, applying multiple perturbation methods to these two areas would be the key to clarify the role of V1 (and SC) in visually guided behaviours.

Conceptually, our understanding of how V1 might be involved in visually guided behaviours is largely based on learned behaviours with orientation/direction selective stimuli. Hence, little is known how V1 responds to intrinsically salient visual stimuli. Recent behavioural studies simulating prey capture (Hoy et al., 2016) or predator avoidance (Yilmaz & Meister, 2013; Salay et al., 2018) have provided clues to what intrinsically salient visual stimuli are in mice. It is likely that mice prefer small stimuli on the ground and avoid approaching stimuli from above. In addition, another behavioural study has showed that mice's sensitivity to total luminance change or wavelength-specific luminance change is not uniform across visual fields (Denman et al., 2018). Would it be possible that some salient stimuli are only encoded in some parts of the visual field? This question has been addressed by electrophysiological recording in different parts of V1. For example, V1 neurons with receptive fields in the upper visual field have higher spatial frequency tuning than neurons in the lower visual field (Zhang et al., 2015). Concurrent *in vivo* electrophysiological recording and behavioural testing may shed light on whether different tuning/detection features in upper and lower visual field contribute to innate behaviours.

Interestingly, motor signals in V1 may also play a role in innate behaviours (Saleem et al., 2013). V1 projects to several brain regions including SC, and inhibiting SC disrupts escape responses to looming stimuli (Evans et al., 2018). Hence, one potential role for V1 motor signals during navigation may be to differentiate looming stimuli that are driven by self-generated actions, from those driven by the movement of other agents. Since both approaching an object and being approached by an object causes an expansion of the object in the field of view, such a predictive motor-to-sensory signalling seems necessary for navigation. Similar mechanisms for saccadic eye movements are known to be present in SC (Crapse & Sommer, 2008). How the motor signals in V1 are used to predict the appearance of subsequent visual stimuli is still an active line of research.

#### *5.4 Summary*

While previous studies on cortex often use behavioural paradigms developed in human psychological studies to investigate how a neutral stimulus is associated with a positive or negative outcome, recent studies have started to address the cortical contribution to innate behaviours. These studies suggest a broader role that cortex may serve. For instance, auditory cortex is known to process complex auditory signals (Carruthers et al., 2015) and inhibiting auditory cortex with muscimol disrupts pup retrieval in female mice (Marlin et al., 2015). More importantly, maternal experience can facilitate maternal events by shaping the sound-tuning for pup vocalisation in auditory cortex (Schiavo et al., 2020). In addition, retrosplenial cortex (RSP) has been extensively studied in space-action representation including head direction (Chen et al., 1994), reward locations (Vedder et al., 2017) and goal locations (Miller et al., 2019). A recent study showed that chemogenetic inactivation

of SC-projecting RSP neurons disrupted escape trajectories (Vale et al., 2020).

Ethologically relevant stimuli, such as pup and female conspecifics, looming stimulus and shelter, may pinpoint what features are important for behaviours, and for the cortex to process.

This thesis aimed to open up a new role of V1 in behaviours. While exploring the rich behavioural repertoire animals display, it seems that interplay between learned and innate behaviours is more complicated than expected. In addition, technical concerns remain an issue when perturbing neural activity. In this thesis, I have raised examples of what experiments to do to tackle those technical issues. As the functional and anatomical organisation of mouse V1 become clearer, future studies may even test the role of laminar computations, or how inputs from other cortical areas affects the computation performed within V1, to provide new insights into how the cerebral cortex influences behaviours.

## Chapter 6: Bibliography

- Ahmadlou, M., Houba, J. H. W., van Vierbergen, J. F. M., Giannouli, M., Gimenez, G.-A., van Weeghel, C., ... Heimel, J. A. (2021). A cell type-specific cortico-subcortical brain circuit for investigatory and novelty-seeking behavior. *Science (New York, N.Y.)*, 372(6543). <https://doi.org/10.1126/science.abe9681>
- Ahmadlou, M., Zweifel, L. S., & Heimel, J. A. (2018). Functional modulation of primary visual cortex by the superior colliculus in the mouse. *Nature Communications*, 9(1), 1–13. <https://doi.org/10.1038/s41467-018-06389-6>
- Alexander, G. M., Rogan, S. C., Abbas, A. I., Armbruster, B. N., Pei, Y., Allen, J. A., ... Roth, B. L. (2009). Remote control of neuronal activity in transgenic mice expressing evolved G protein-coupled receptors. *Neuron*, 63(1), 27–39. <https://doi.org/10.1016/j.neuron.2009.06.014>
- Allen, T. A., Narayanan, N. S., Kholodar-smith, D. B., Laubach, M., & Brown, T. H. (2009). Imaging the spread of reversible brain inactivations using fluorescent muscimol. *Journal of Neuroscience Methods*, 171(1), 30–38.
- Armbruster, B. N., Li, X., Pausch, M. H., Herlitze, S., & Roth, B. L. (2007). Evolving the lock to fit the key to create a family of G protein-coupled receptors potently activated by an inert ligand. *Proceedings of the National Academy of Sciences of the United States of America*, 104(12), 5163–5168. <https://doi.org/10.1073/pnas.0700293104>
- Ayaz, A., Saleem, A. B., Schölvinc, M. L., & Carandini, M. (2013). Locomotion controls spatial integration in mouse visual cortex. *Current Biology*, 23(10), 890–894. <https://doi.org/10.1016/j.cub.2013.04.012>
- Bakdash, J. Z., & Marusich, L. R. (2017). Repeated Measures Correlation . *Frontiers in Psychology* . Retrieved from

<https://www.frontiersin.org/article/10.3389/fpsyg.2017.00456>

Ball, W., & Tronick, E. (1971). Infant responses to impending collision: optical and real. *Science (New York, N.Y.)*, *171*(3973), 818–820.

<https://doi.org/10.1126/science.171.3973.818>

Baumfalk, U., & Albus, K. (1987). Baclofen inhibits the spontaneous and visually evoked responses of neurones in the striate cortex of the cat. *Neuroscience Letters*, *75*(2), 187–192. [https://doi.org/10.1016/0304-3940\(87\)90295-3](https://doi.org/10.1016/0304-3940(87)90295-3)

Beltramo, R., D'Urso, G., Maschio, M. D., Farisello, P., Bovetti, S., Clovis, Y., ... Fellin, T. (2013). Layer-specific excitatory circuits differentially control recurrent network dynamics in the neocortex. *Nature Neuroscience*, *16*(2), 227–234.

<https://doi.org/10.1038/nn.3306>

Beltramo, R., & Scanziani, M. (2019). A collicular visual cortex: Neocortical space for an ancient midbrain visual structure. *Science*, *363*(6422), 64–69.

<https://doi.org/10.1126/science.aau7052>

Bennett, C., Arroyo, S., & Hestrin, S. (2013). Subthreshold Mechanisms Underlying State-Dependent Modulation of Visual Responses. *Neuron*, *80*(2), 350–357.

<https://doi.org/https://doi.org/10.1016/j.neuron.2013.08.007>

Bock, R., Hoon Shin, J., Kaplan, A. R., Dobi, A., Markey, E., Kramer, P. F., ...

Alvarez, V. A. (2013). Strengthening the accumbal indirect pathway promotes resilience to compulsive cocaine use. *Nature Neuroscience*, *16*(5), 632–638.

<https://doi.org/10.1038/nn.3369>

Bokil, H., Andrews, P., Kulkarni, J. E., Mehta, S., & Mitra, P. P. (2010). Chronux: a platform for analyzing neural signals. *Journal of Neuroscience Methods*, *192*(1),

146–151. <https://doi.org/10.1016/j.jneumeth.2010.06.020>

Braida, D., Donzelli, A., Martucci, R., Ponzoni, L., Pauletti, A., Langus, A., & Sala, M.

- (2013). Mice discriminate between stationary and moving 2D shapes: Application to the object recognition task to increase attention. *Behavioural Brain Research*, 242(1), 95–101. <https://doi.org/10.1016/j.bbr.2012.12.040>
- Bubb, E. J., Aggleton, J. P., O'Mara, S. M., & Nelson, A. J. D. (2021). Chemogenetics Reveal an Anterior Cingulate–Thalamic Pathway for Attending to Task-Relevant Information. *Cerebral Cortex*, 31(4), 2169–2186. <https://doi.org/10.1093/cercor/bhaa353>
- Camillo, D., Ahmadlou, M., & Heimel, J. A. (2020). Contrast-Dependence of Temporal Frequency Tuning in Mouse V1. *Frontiers in Neuroscience*. Retrieved from <https://www.frontiersin.org/article/10.3389/fnins.2020.00868>
- Campbell, E. J., & Marchant, N. J. (2018). The use of chemogenetics in behavioural neuroscience: receptor variants, targeting approaches and caveats. *British Journal of Pharmacology*, 175(7), 994–1003. <https://doi.org/10.1111/bph.14146>
- Carandini, M., Heeger, D. J., & Movshon, J. A. (1997). Linearity and Normalization in Simple Cells of the Macaque Primary. *The Journal of Neuroscience*, 17(21), 8621–8644.
- Carandini, M., Heeger, D. J., & Senn, W. (2002). A synaptic explanation of suppression in visual cortex. *Journal of Neuroscience*, 22(22), 10053–10065. <https://doi.org/10.1523/jneurosci.22-22-10053.2002>
- Carruthers, I. M., Laplagne, D. A., Jaegle, A., Briguglio, J. J., Mwilambwe-Tshilobo, L., Natan, R. G., & Geffen, M. N. (2015). Emergence of invariant representation of vocalizations in the auditory cortex. *Journal of Neurophysiology*, 114(5), 2726–2740. <https://doi.org/10.1152/jn.00095.2015>
- Chauvette, S., Volgushev, M., & Timofeev, I. (2010). Origin of active states in local neocortical networks during slow sleep oscillation. *Cerebral Cortex*, 20(11),

2660–2674. <https://doi.org/10.1093/cercor/bhq009>

Chen, C. C., Lu, J., Yang, R., Ding, J. B., & Zuo, Y. (2018). Selective activation of parvalbumin interneurons prevents stress-induced synapse loss and perceptual defects. *Molecular Psychiatry*, *23*(7), 1614–1625.

<https://doi.org/10.1038/mp.2017.159>

Chen, L. L., Lin, L.-H., Barnes, C. A., & McNaughton, B. L. (1994). Head-direction cells in the rat posterior cortex. *Experimental Brain Research*, *101*(1), 24–34.

<https://doi.org/10.1007/BF00243213>

Chen, T. W., Wardill, T. J., Sun, Y., Pulver, S. R., Renninger, S. L., Baohan, A., ... Kim, D. S. (2013). Ultrasensitive fluorescent proteins for imaging neuronal activity. *Nature*, *499*(7458), 295–300. <https://doi.org/10.1038/nature12354>

Chiou, C. S., Chen, C. C., Tsai, T. C., Huang, C. C., Chou, D., & Hsu, K. Sen. (2016). Alleviating Bone Cancer-induced Mechanical Hypersensitivity by Inhibiting Neuronal Activity in the Anterior Cingulate Cortex. *Anesthesiology*, *125*(4), 779–792. <https://doi.org/10.1097/ALN.0000000000001237>

Cooke, S. F., & Bear, M. F. (2010). Visual Experience Induces Long-Term Potentiation in the Primary Visual Cortex. *Journal of Neuroscience*, *30*(48), 16304–16313. <https://doi.org/10.1523/jneurosci.4333-10.2010>

Cooke, Sam F., Komorowski, R. W., Kaplan, E. S., Gavornik, J. P., & Bear, M. F. (2015). Visual recognition memory, manifested as long-term habituation, requires synaptic plasticity in V1. *Nature Neuroscience*, *18*(2), 262–271. <https://doi.org/10.1038/nn.3920>

Crapse, T. B., & Sommer, M. A. (2008). Corollary discharge across the animal kingdom. *Nature Reviews Neuroscience*, *9*(8), 587–600.

<https://doi.org/10.1038/nrn2457>

- De Franceschi, G., Vivattanasarn, T., Saleem, A. B., & Solomon, S. G. (2016). Vision Guides Selection of Freeze or Flight Defense Strategies in Mice. *Current Biology*, 26(16), 2150–2154. <https://doi.org/10.1016/j.cub.2016.06.006>
- Dean, P., Mitchell, I. J., & Redgrave, P. (1988). Responses resembling defensive behaviour produced by microinjection of glutamate into superior colliculus of rats. *Neuroscience*, 24(2), 501–510. [https://doi.org/10.1016/0306-4522\(88\)90345-4](https://doi.org/10.1016/0306-4522(88)90345-4)
- Dean, P. (1981). Grating detection and visual acuity after lesions of striate cortex in hooded rats. *Experimental Brain Research*, 43(2), 145–153. <https://doi.org/10.1007/BF00237758>
- Dean, Paul. (1978). Visual acuity in hooded rats: Effects of superior collicular or posterior neocortical lesions. *Brain Research*, 156(1), 17–31. [https://doi.org/https://doi.org/10.1016/0006-8993\(78\)90076-8](https://doi.org/https://doi.org/10.1016/0006-8993(78)90076-8)
- Deisseroth, K. (2015). Optogenetics: 10 years of microbial opsins in neuroscience. *Nature Neuroscience*, 18(9), 1213–1225. <https://doi.org/10.1038/nn.4091>
- Del Grosso, N. A., Graboski, J. J., Chen, W., Blanco-Hernández, E., & Sirota, A. (2017). Virtual reality system for freely-moving rodents. *BioRxiv*, 161232. <https://doi.org/10.1101/161232>
- Denman, D. J., Luviano, J. A., Ollerenshaw, D. R., Cross, S., Williams, D., Buice, M. A., ... Reid, R. C. (2018). Mouse color and wavelength-specific luminance contrast sensitivity are non- uniform across visual space. *ELife*, 7, 1–16. <https://doi.org/10.7554/eLife.31209>
- Devienne, G., Picaud, S., Cohen, I., Piquet, J., Tricoire, L., Testa, D., ... Lambolez, B. (2021). Regulation of perineuronal nets in the adult cortex by the activity of the cortical network. *Journal of Neuroscience*, 41(27), 5779–5790.

<https://doi.org/10.1523/JNEUROSCI.0434-21.2021>

Ditterich, J., Mazurek, M. E., & Shadlen, M. N. (2003). Microstimulation of visual cortex affects the speed of perceptual decisions. *Nature Neuroscience*, 6(8), 891–898. <https://doi.org/10.1038/nn1094>

Djurdjevic, V., Ansuini, A., Bertolini, D., Macke, J. H., & Zoccolan, D. (2018). Accuracy of Rats in Discriminating Visual Objects Is Explained by the Complexity of Their Perceptual Strategy. *Current Biology*, 28(1007), 1005–1015. <https://doi.org/10.1016/j.cub.2018.02.037>

Dobrzanski, G., Lukomska, A., Zakrzewska, R., Posluszny, A., Kanigowski, D., Urban-Ciecko, J., ... Kossut, M. (2020). Learning-induced plasticity in the barrel cortex is disrupted by inhibition of layer 4 somatostatin-containing interneurons. *BioRxiv*, 1–40.

Doron, G., Shin, J. N., Takahashi, N., Drüke, M., Bocklisch, C., Skenderi, S., ... Larkum, M. E. (2020). Perirhinal input to neocortical layer 1 controls learning. *Science (New York, N.Y.)*, 370(6523). <https://doi.org/10.1126/science.aaz3136>

Durand, S., Iyer, R., Mizuseki, K., De Vries, S., Mihalas, S., & Reid, R. C. (2016). A comparison of visual response properties in the lateral geniculate nucleus and primary visual cortex of awake and anesthetized mice. *Journal of Neuroscience*, 36(48), 12144–12156. <https://doi.org/10.1523/JNEUROSCI.1741-16.2016>

Ennaceur, A. (2010). One-trial object recognition in rats and mice: Methodological and theoretical issues. *Behavioural Brain Research*, 215(2), 244–254. <https://doi.org/10.1016/j.bbr.2009.12.036>

Evans, D., Stempel, V., Vale, R., Ruehle, S., Lefler, Y., & Branco, T. (2018). A synaptic threshold mechanism for computing escape decisions. *Nature*, 558(7711), 590–594. <https://doi.org/10.1038/s41586-018-0244-6>

- Fantz, R. L. (1964). Visual Experience in Infants: Decreased Attention to Familiar Patterns Relative to Novel Ones. *Science*, *146*(3644), 668–670.  
<https://doi.org/10.1126/science.146.3644.668>
- Feinberg, T. E., Pasik, T., & Pasik, P. (1978). Extrageniculostriate vision in the monkey. VI. Visually guided accurate reaching behavior. *Brain Research*, *152*(2), 422–428. [https://doi.org/10.1016/0006-8993\(78\)90276-7](https://doi.org/10.1016/0006-8993(78)90276-7)
- Ferster, D., Chung, S., & Wheat, H. (1996). Orientation selectivity of thalamic input to simple cells of cat visual cortex. *Nature*, *380*(6571), 249–252.  
<https://doi.org/10.1038/380249a0>
- Forwood, S. E., Bartko, S. J., Saksida, L. M., & Bussey, T. J. (2007). Rats Spontaneously Discriminate Purely Visual, Two-Dimensional Stimuli in Tests of Recognition Memory and Perceptual Oddity. *Behavioral Neuroscience*, *121*(5), 1032–1042. <https://doi.org/10.1037/0735-7044.121.5.1032>
- Froudarakis, E., Cohen, U., Diamantaki, M., Walker, E. Y., Reimer, J., Berens, P., ... Tolias, A. S. (2020). Object manifold geometry across the mouse cortical visual hierarchy. *BioRxiv*, 2020.08.20.258798. Retrieved from  
<https://doi.org/10.1101/2020.08.20.258798>
- Fucich, E. A., Paredes, D., Saunders, M. O., & Morilak, D. A. (2018). Activity in the ventral medial prefrontal cortex is necessary for the therapeutic effects of extinction in rats. *Journal of Neuroscience*, *38*(6), 1408–1417.  
<https://doi.org/10.1523/JNEUROSCI.0635-17.2017>
- Funk, C. M., Peelman, K., Bellesi, M., Marshall, W., Cirelli, C., & Tononi, G. (2017). Role of somatostatin-positive cortical interneurons in the generation of sleep slow waves. *Journal of Neuroscience*, *37*(38), 9132–9148.  
<https://doi.org/10.1523/JNEUROSCI.1303-17.2017>

- Gallup Jr., G. G. (1969). Chimpanzees : Self-Recognition. *Science*, 167(1968), 86–87.
- Gao, E., DeAngelis, G. C., & Burkhalter, A. (2010). Parallel input channels to mouse primary visual cortex. *Journal of Neuroscience*, 30(17), 5912–5926.  
<https://doi.org/10.1523/JNEUROSCI.6456-09.2010>
- Genzel, L., Schut, E., Schröder, T., Eichler, R., Khamassi, M., Gomez, A., ... Battaglia, F. (2019). The object space task shows cumulative memory expression in both mice and rats. *PLoS Biology*, 17(6), 1–25.  
<https://doi.org/10.1371/journal.pbio.3000322>
- Goel, A., Cantu, D. A., Guilfoyle, J., Chaudhari, G. R., Newadkar, A., Todisco, B., ... Portera-Cailliau, C. (2018). Impaired perceptual learning in a mouse model of Fragile X syndrome is mediated by parvalbumin neuron dysfunction and is reversible. *Nature Neuroscience*, 21(10), 1404–1411.  
<https://doi.org/10.1038/s41593-018-0231-0>
- Gremel, C. M., & Costa, R. M. (2013). Orbitofrontal and striatal circuits dynamically encode the shift between goal-directed and habitual actions. *Nature Communications*, 4(May), 2264. <https://doi.org/10.1038/ncomms3264>
- Grønli, J., Schmidt, M. A., & Wisor, J. P. (2018). State-Dependent Modulation of Visual Evoked Potentials in a Rodent Genetic Model of Electroencephalographic Instability. *Frontiers in Systems Neuroscience*, 12, 36.  
<https://doi.org/10.3389/fnsys.2018.00036>
- Grubb, M. S., & Thompson, I. D. (2003). Quantitative Characterization of Visual Response Properties in the Mouse Dorsal Lateral Geniculate Nucleus. *Journal of Neurophysiology*, 90(6), 3594–3607. <https://doi.org/10.1152/jn.00699.2003>
- Gu, Y., & Cang, J. (2016). Binocular matching of thalamocortical and intracortical

- circuits in the mouse visual cortex. *ELife*, 5(DECEMBER2016), 1–14.  
<https://doi.org/10.7554/eLife.22032>
- Hallman, L. E., Schofield, B. R., & Lin, C. -S. (1988). Dendritic morphology and axon collaterals of corticotectal, corticopontine, and callosal neurons in layer V of primary visual cortex of the hooded rat. *Journal of Comparative Neurology*, 272(1), 149–160. <https://doi.org/10.1002/cne.902720111>
- Harris, J. A., Mihalas, S., Hirokawa, K. E., Whitesell, J. D., Choi, H., Bernard, A., ... Zeng, H. (2019). Hierarchical organization of cortical and thalamic connectivity. *Nature*, 575(7781), 195–202. <https://doi.org/10.1038/s41586-019-1716-z>
- Hein, A. M., Altshuler, D. L., Cade, D. E., Liao, J. C., Martin, B. T., & Taylor, G. K. (2020). An Algorithmic Approach to Natural Behavior. *Current Biology*, 30(11), R663–R675. <https://doi.org/10.1016/j.cub.2020.04.018>
- Hetzler, B. E., & Ondracek, J. M. (2007). Baclofen alters flash-evoked potentials in Long-Evans rats. *Pharmacology, Biochemistry, and Behavior*, 86(4), 727–740. <https://doi.org/10.1016/j.pbb.2007.02.020>
- Heyser, C. J., & Chemero, A. (2012). Novel object exploration in mice: Not all objects are created equal. *Behavioural Processes*, 89(3), 232–238. <https://doi.org/10.1016/j.beproc.2011.12.004>
- Hill, S., & Tononi, G. (2005). Modeling sleep and wakefulness in the thalamocortical system. *Journal of Neurophysiology*, 93(3), 1671–1698. <https://doi.org/10.1152/jn.00915.2004>
- Holmgren, C. D., Stahr, P., Wallace, D. J., Voit, K., Matheson, E. J., & Sawinski, J. (2021). Freely-moving mice visually pursue prey using a retinal area with least optic flow. *BioRxiv*.
- Hoy, J. L., Yavorska, I., Wehr, M., & Niell, C. M. (2016). Vision Drives Accurate

- Approach Behavior during Prey Capture in Laboratory Mice. *Current Biology*, 26(22), 3046–3052. <https://doi.org/10.1016/j.cub.2016.09.009>
- Hubel, D. H., & Wiesel, T. N. (1963). Shape and arrangement of columns in cat's striate cortex. *The Journal of Physiology*, 165(3), 559–568. <https://doi.org/10.1113/jphysiol.1963.sp007079>
- Hubel, D. H., & Wiesel, T. N. (1968). Receptive fields and functional architecture of monkey striate cortex. *The Journal of Physiology*, 195(1), 215–243. <https://doi.org/10.1113/jphysiol.1968.sp008455>
- Huberman, A. D., & Niell, C. M. (2011). What can mice tell us about how vision works? *Trends in Neurosciences*, 34(9), 464–473. <https://doi.org/10.1016/j.tins.2011.07.002>
- Inayat, S., Barchini, J., Chen, H., Feng, L., Liu, X., & Cang, J. (2015). Neurons in the most superficial lamina of the mouse superior colliculus are highly selective for stimulus direction. *The Journal of Neuroscience : The Official Journal of the Society for Neuroscience*, 35(20), 7992–8003. <https://doi.org/10.1523/JNEUROSCI.0173-15.2015>
- Juavinett, A. L., Erlich, J. C., & Churchland, A. K. (2018). Decision-making behaviors: weighing ethology, complexity, and sensorimotor compatibility. *Current Opinion in Neurobiology*, 49, 42–50. <https://doi.org/10.1016/j.conb.2017.11.001>
- Jun, J. J., Steinmetz, N. A., Siegle, J. H., Denman, D. J., Bauza, M., Barbarits, B., ... Harris, T. D. (2017). Fully integrated silicon probes for high-density recording of neural activity. *Nature*, 551(7679), 232–236. <https://doi.org/10.1038/nature24636>
- Kaplan, E. S., Cooke, S. F., Komorowski, R. W., Chubykin, A. A., Thomazeau, A.,

- Khibnik, L. A., ... Bear, M. F. (2016). Contrasting roles for parvalbumin-expressing inhibitory neurons in two forms of adult visual cortical plasticity. *ELife*, 5, 1–27. <https://doi.org/10.7554/eLife.11450>
- Kasper, E. M., Larkman, A. U., Lübke, J., & Blakemore, C. (1994). Pyramidal neurons in layer 5 of the rat visual cortex. II. Development of electrophysiological properties. *Journal of Comparative Neurology*, 339(4), 475–494. <https://doi.org/10.1002/cne.903390403>
- Keaveney, M. K., Rahsepar, B., Tseng, H. A., Fernandez, F. R., Mount, R. A., Ta, T., ... Han, X. (2020). CaMKIIa-positive interneurons identified via a microrna-based viral gene targeting strategy. *Journal of Neuroscience*, 40(50), 9576–9588. <https://doi.org/10.1523/JNEUROSCI.2570-19.2020>
- Knott, V., Labelle, A., Jones, B., & Mahoney, C. (2001). Quantitative EEG in schizophrenia and in response to acute and chronic clozapine treatment. *Schizophrenia Research*, 50(1–2), 41–53. [https://doi.org/10.1016/S0920-9964\(00\)00165-1](https://doi.org/10.1016/S0920-9964(00)00165-1)
- Koike, H., Demars, M. P., Short, J. A., Nabel, E. M., Akbarian, S., Baxter, M. G., & Morishita, H. (2016). Chemogenetic Inactivation of Dorsal Anterior Cingulate Cortex Neurons Disrupts Attentional Behavior in Mouse. *Neuropsychopharmacology*, 41(4), 1014–1023. <https://doi.org/10.1038/npp.2015.229>
- Krone, L. B., Yamagata, T., Blanco-Duque, C., Guillaumin, M. C. C., Kahn, M. C., van der Vinne, V., ... Vyazovskiy, V. V. (2021). A role for the cortex in sleep–wake regulation. *Nature Neuroscience*, 24(September). <https://doi.org/10.1038/s41593-021-00894-6>
- Krukowski, A. E., & Miller, K. D. (2001). Thalamocortical NMDA conductances and

- intracortical inhibition can explain cortical temporal tuning. *Nature Neuroscience*, 4(4), 424–430. <https://doi.org/10.1038/86084>
- Lambo, M. E., & Turrigiano, G. G. (2013). Synaptic and intrinsic homeostatic mechanisms cooperate to increase L2/3 pyramidal neuron excitability during a late phase of critical period plasticity. *Journal of Neuroscience*, 33(20), 8810–8819. <https://doi.org/10.1523/JNEUROSCI.4502-12.2013>
- Lashley, K. S. (1935). The mechanism of vision. XII. Nervous structures concerned in the acquisition and retention of habits based on reactions to light. *Comparative Psychology Monographs*, 11, 2, 43–79.
- Leger, M., Quiedeville, A., Bouet, V., Haelewyn, B., Boulouard, M., Schumann-Bard, P., & Freret, T. (2013). Object recognition test in mice. *Nature Protocols*, 8(12), 2531–2537. <https://doi.org/10.1038/nprot.2013.155>
- Leventhal, A. G., Wang, Y., Pu, M., Zhou, Y., & Ma, Y. (2003). GABA and its agonists improved visual cortical function in senescent monkeys. *Science*, 300(5620), 812–815. <https://doi.org/10.1126/science.1082874>
- Li, L., Feng, X., Zhou, Z., Zhang, H., Shi, Q., Lei, Z., ... Wang, L. (2018). Stress Accelerates Defensive Responses to Looming in Mice and Involves a Locus Coeruleus-Superior Colliculus Projection. *Current Biology*, 28(6), 859-871.e5. <https://doi.org/10.1016/j.cub.2018.02.005>
- Liang, F., Xiong, X. R., Zingg, B., Ji, X. ying, Zhang, L. I., & Tao, H. W. (2015). Sensory Cortical Control of a Visually Induced Arrest Behavior via Corticotectal Projections. *Neuron*, 86(3), 755–767. <https://doi.org/10.1016/j.neuron.2015.03.048>
- Livingstone, M. S., & Hubel, D. H. (1984). Anatomy and physiology of a color system in the primate visual cortex. *Journal of Neuroscience*, 4(1), 309–356.

<https://doi.org/10.1523/jneurosci.04-01-00309.1984>

Lopes, G., Bonacchi, N., Frazão, J., Neto, J. P., Atallah, B. V., Soares, S., ... Kampff, A. R. (2015). Bonsai: an event-based framework for processing and controlling data streams. *Frontiers in Neuroinformatics*, 9, 7.

<https://doi.org/10.3389/fninf.2015.00007>

Lopes, G., Farrell, K., Horrocks, E. A., Lee, C.-Y., Morimoto, M. M., Muzzu, T., ... Saleem, A. B. (2021). Creating and controlling visual environments using BonVision. *ELife*, 10, 1–17. <https://doi.org/10.7554/elife.65541>

Lupien-Meilleur, A., Jiang, X., Lachance, M., Taschereau-Dumouchel, V., Gagnon, L., Vanasse, C., ... Rossignol, E. (2021). Reversing frontal disinhibition rescues behavioural deficits in models of CACNA1A-associated neurodevelopment disorders. *Molecular Psychiatry*. <https://doi.org/10.1038/s41380-021-01175-1>

MacCrimmon, D., Brunet, D., Criollo, M., Galin, H., & Lawson, J. S. (2012). Clozapine Augments Delta, Theta, and Right Frontal EEG Alpha Power in Schizophrenic Patients. *ISRN Psychiatry*, 2012, 596486.

<https://doi.org/10.5402/2012/596486>

Madroñal, N., Delgado-García, J. M., Fernández-Guizán, A., Chatterjee, J., Köhn, M., Mattucci, C., ... Gruart, A. (2016). Rapid erasure of hippocampal memory following inhibition of dentate gyrus granule cells. *Nature Communications*, 7(1), 10923. <https://doi.org/10.1038/ncomms10923>

Manns, J. R., Stark, C. E. L., & Squire, L. R. (2000). The visual paired-comparison task as a measure of declarative memory. *Proceedings of the National Academy of Sciences of the United States of America*, 97(22), 12375–12379.

<https://doi.org/10.1073/pnas.220398097>

Manvich, D. F., Webster, K. A., Foster, S. L., Farrell, M. S., Ritchie, J. C., Porter, J.

- H., & Weinschenker, D. (2018). The DREADD agonist clozapine N-oxide (CNO) is reverse-metabolized to clozapine and produces clozapine-like interoceptive stimulus effects in rats and mice. *Scientific Reports*, *8*(1), 1–10.  
<https://doi.org/10.1038/s41598-018-22116-z>
- Marlin, B. J., Mitre, M., D'Amour, J. A., Chao, M. V., & Froemke, R. C. (2015). Oxytocin enables maternal behaviour by balancing cortical inhibition. *Nature*, *520*(7548), 499–504. <https://doi.org/10.1038/nature14402>
- Marques, T., Summers, M. T., Fioreze, G., Fridman, M., Dias, R. F., Feller, M. B., & Petreanu, L. (2018). A Role for Mouse Primary Visual Cortex in Motion Perception. *Current Biology*, *28*(11), 1703-1713.e6.  
<https://doi.org/10.1016/j.cub.2018.04.012>
- Martin, J. H. (1991). Autoradiographic estimation of the extent of reversible inactivation produced by microinjection of lidocaine and muscimol in the rat. *Neuroscience Letters*, *127*(2), 160–164. [https://doi.org/10.1016/0304-3940\(91\)90784-Q](https://doi.org/10.1016/0304-3940(91)90784-Q)
- Marusich, L. R., & Bakdash, J. Z. (2021). rmcrrShiny: A web and standalone application for repeated measures correlation. *F1000Research*, *10*, 697.  
<https://doi.org/10.12688/f1000research.55027.1>
- Mathis, A., Mamidanna, P., Cury, K. M., Abe, T., Murthy, V. N., Mathis, M. W., & Bethge, M. (2018). DeepLabCut: markerless pose estimation of user-defined body parts with deep learning. *Nature Neuroscience*, *21*(9), 1281–1289.  
<https://doi.org/10.1038/s41593-018-0209-y>
- May, P. J. (2006). The mammalian superior colliculus: Laminar structure and connections. *Progress in Brain Research*, *151*, 321–378.  
[https://doi.org/10.1016/S0079-6123\(05\)51011-2](https://doi.org/10.1016/S0079-6123(05)51011-2)

- Meltzer, H. Y. (1994). An overview of the mechanism of action of clozapine. *The Journal of Clinical Psychiatry*, 55 Suppl B, 47–52.
- Meyer, A. F., O'Keefe, J., & Poort, J. (2020). Two Distinct Types of Eye-Head Coupling in Freely Moving Mice. *Current Biology*, 30(11), 2116-2130.e6. <https://doi.org/10.1016/j.cub.2020.04.042>
- Meyer, A. F., Poort, J., O'Keefe, J., Sahani, M., & Linden, J. F. (2018). A Head-Mounted Camera System Integrates Detailed Behavioral Monitoring with Multichannel Electrophysiology in Freely Moving Mice. *Neuron*, 100(1), 46-60.e7. <https://doi.org/10.1016/j.neuron.2018.09.020>
- Meyer, H. C., & Bucci, D. J. (2016). Imbalanced Activity in the Orbitofrontal Cortex and Nucleus Accumbens Impairs Behavioral Inhibition. *Current Biology*, 26(20), 2834–2839. <https://doi.org/10.1016/j.cub.2016.08.034>
- Miao, C., Cao, Q., Ito, H. T., Yamahachi, H., Witter, M. P., Moser, M. B., & Moser, E. I. (2015). Hippocampal Remapping after Partial Inactivation of the Medial Entorhinal Cortex. *Neuron*, 88(3), 590–603. <https://doi.org/10.1016/j.neuron.2015.09.051>
- Miller, A. M. P., Mau, W., & Smith, D. M. (2019). Retrosplenial Cortical Representations of Space and Future Goal Locations Develop with Learning. *Current Biology*, 29(12), 2083-2090.e4. <https://doi.org/https://doi.org/10.1016/j.cub.2019.05.034>
- Mishkin, M., Ungerleider, L. G., & Macko, K. A. (1983). Object vision and spatial vision: two cortical pathways. *Trends in Neurosciences*, 6(C), 414–417. [https://doi.org/10.1016/0166-2236\(83\)90190-X](https://doi.org/10.1016/0166-2236(83)90190-X)
- Mohler, C. W., & Wurtz, R. H. (1977). Role of striate cortex and superior colliculus in visual guidance of saccadic eye movements in monkeys. *Journal of*

- Neurophysiology*, 40(1), 74–94. <https://doi.org/10.1152/jn.1977.40.1.74>
- Morris, R. (1984). Developments of a water-maze procedure for studying spatial learning in the rat. *Journal of Neuroscience Methods*, 11(1), 47–60. [https://doi.org/10.1016/0165-0270\(84\)90007-4](https://doi.org/10.1016/0165-0270(84)90007-4)
- Munk, H. (1881). *Über die Funktionen der Grosshirnrinde. A Hirschwald (On the Functions of the Cortex)*.
- Nagai, Y., Miyakawa, N., Takuwa, H., Hori, Y., Oyama, K., Ji, B., ... Minamimoto, T. (2020). Deschloroclozapine, a potent and selective chemogenetic actuator enables rapid neuronal and behavioral modulations in mice and monkeys. *Nature Neuroscience*, 23(9), 1157–1167. <https://doi.org/10.1038/s41593-020-0661-3>
- Natale, S., Masferrer, M. E., Deivasigamani, S., & Gross, C. T. (2021). A role for cerebral cortex in the suppression of innate defensive behavior. *European Journal of Neuroscience*, (August), 1–16. <https://doi.org/10.1111/ejn.15426>
- Nathanson, J. L., Yanagawa, Y., Obata, K., & Callaway, E. M. (2009). Preferential labeling of inhibitory and excitatory cortical neurons by endogenous tropism of adeno-associated virus and lentivirus vectors. *Neuroscience*, 161(2), 441–450. <https://doi.org/10.1016/j.neuroscience.2009.03.032>
- Newcombe, F., & Russell, W. R. (1969). Dissociated visual perceptual and spatial deficits in focal lesions of the right hemisphere. *Journal of Neurology, Neurosurgery & Psychiatry*, 32(2), 73–81. <https://doi.org/10.1136/jnnp.32.2.73>
- Newsome, W. T., & Pare, E. B. (1988). A selective impairment of motion perception following lesions of the middle temporal visual area (MT). *Journal of Neuroscience*, 8(6), 2201–2211. <https://doi.org/10.1523/JNEUROSCI.08-06-02201.1988>

- Nieder, A., Freedman, D. J., & Miller, E. K. (2002). Representation of the quantity of visual items in the primate prefrontal cortex. *Science*, 297(5587), 1708–1711.  
<https://doi.org/10.1126/science.1072493>
- Niell, C. M., & Stryker, M. P. (2008). Highly selective receptive fields in mouse visual cortex. *Journal of Neuroscience*, 28(30), 7520–7536.  
<https://doi.org/10.1523/JNEUROSCI.0623-08.2008>
- Niell, C. M., & Stryker, M. P. (2010). Modulation of Visual Responses by Behavioral State in Mouse Visual Cortex. *Neuron*, 65(4), 472–479.  
<https://doi.org/10.1016/j.neuron.2010.01.033>
- Oakley, D. A. (1981). Performance of decorticated rats in a two-choice visual discrimination apparatus. *Behavioural Brain Research*, 3(1), 55–69.  
[https://doi.org/https://doi.org/10.1016/0166-4328\(81\)90028-0](https://doi.org/https://doi.org/10.1016/0166-4328(81)90028-0)
- Olsen, S. R., Bortone, D. S., Adesnik, H., & Scanziani, M. (2012). Gain control by layer six in cortical circuits of vision. *Nature*, 483(7387), 47–52.  
<https://doi.org/10.1038/nature10835>
- Papanikolaou, A., Rodrigues, F. R., Holeniewska, J., Phillips, K., Saleem, A. B., & Solomon, S. G. (2021). Disrupted visual cortical plasticity in early neurodegeneration. *BioRxiv*, 2020.11.02.365767.  
<https://doi.org/10.1101/2020.11.02.365767>
- Parker, D. M., Salzen, E. A., & Lishman, J. R. (1982). Visual-evoked responses elicited by the onset and offset of sinusoidal gratings: Latency, waveform, and topographic characteristics. *Investigative Ophthalmology and Visual Science*, 22(5), 675–680.
- Parker, P. R. L., Abe, E. T. T., Beatie, N. T., Leonard, E. S. P., Martins, D. M., Sharp, S. L., ... Niell, C. M. (2021). Distance estimation from monocular cues in an

- ethological visuomotor task. *BioRxiv*, 5–24. Retrieved from <https://doi.org/10.1101/2021.09.29.462468>
- Parker, P. R. L., Abe, E. T. T., Leonard, E. S. P., Martins, D. M., & Niell, C. M. (2022). Joint coding of visual input and eye/head position in V1 of freely moving mice. *BioRxiv*.
- Peirce, J. W. (2009). Generating stimuli for neuroscience using PsychoPy. *Frontiers in Neuroinformatics*, 2(JAN), 1–8. <https://doi.org/10.3389/neuro.11.010.2008>
- Petruno, S. K., Clark, R. E., & Reinagel, P. (2013). Evidence That Primary Visual Cortex Is Required for Image, Orientation, and Motion Discrimination by Rats. *PLOS ONE*, 8(2), e56543. Retrieved from <https://doi.org/10.1371/journal.pone.0056543>
- Porciatti, V., Pizzorusso, T., & Maffei, L. (1999). The visual physiology of the wild type mouse determined with pattern VEPs. *Vision Research*, 39(18), 3071–3081. [https://doi.org/10.1016/S0042-6989\(99\)00022-X](https://doi.org/10.1016/S0042-6989(99)00022-X)
- Porter, J. T., & Nieves, D. (2004). Presynaptic GABAB receptors modulate thalamic excitation of inhibitory and excitatory neurons in the mouse barrel cortex. *Journal of Neurophysiology*, 92(5), 2762–2770. <https://doi.org/10.1152/jn.00196.2004>
- Prusky, G. T., West, P. W. R., & Douglas, R. M. (2000). Behavioral assessment of visual acuity in mice and rats. *Vision Research*, 40(16), 2201–2209. [https://doi.org/10.1016/S0042-6989\(00\)00081-X](https://doi.org/10.1016/S0042-6989(00)00081-X)
- Przybylski, A. W., Gaska, J. P., Foote, W., & Pollen, D. A. (2000). Striate cortex increases contrast gain of macaque LGN neurons. *Visual Neuroscience*, 17(4), 485–494. <https://doi.org/10.1017/S0952523800174012>
- Purushothaman, G., Marion, R., Li, K., & Casagrande, V. A. (2012). Gating and

- control of primary visual cortex by pulvinar. *Nature Neuroscience*, 15(6), 905–912. <https://doi.org/10.1038/nn.3106>
- Rasmussen, R., Nicholas, E., Petersen, N. C., Dietz, A. G., Xu, Q., Sun, Q., & Nedergaard, M. (2019). Cortex-wide Changes in Extracellular Potassium Ions Parallel Brain State Transitions in Awake Behaving Mice. *Cell Reports*, 28(5), 1182–1194.e4. <https://doi.org/10.1016/j.celrep.2019.06.082>
- Reimer, J., Froudarakis, E., Cadwell, C. R., Yatsenko, D., Denfield, G. H., & Tolias, A. S. (2014). Pupil Fluctuations Track Fast Switching of Cortical States during Quiet Wakefulness. *Neuron*, 84(2), 355–362. <https://doi.org/10.1016/j.neuron.2014.09.033>
- Richards, B. A., Xia, F., Santoro, A., Husse, J., Woodin, M. A., Josselyn, S. A., & Frankland, P. W. (2014). Patterns across multiple memories are identified over time. *Nature Neuroscience*, 17(7), 981–986. <https://doi.org/10.1038/nn.3736>
- Robinson, S., Todd, T. P., Pasternak, A. R., Luikart, B. W., Skelton, P. D., Urban, D. J., & Bucci, D. J. (2014). Chemogenetic silencing of neurons in retrosplenial cortex disrupts sensory preconditioning. *The Journal of Neuroscience : The Official Journal of the Society for Neuroscience*, 34(33), 10982–10988. <https://doi.org/10.1523/JNEUROSCI.1349-14.2014>
- Romberg, C., Horner, A. E., Bussey, T. J., & Saksida, L. M. (2013). A touch screen-automated cognitive test battery reveals impaired attention, memory abnormalities, and increased response inhibition in the TgCRND8 mouse model of Alzheimer's disease. *Neurobiology of Aging*, 34(3), 731–744. <https://doi.org/10.1016/j.neurobiolaging.2012.08.006>
- Roth, B. L. (2016). DREADDs for Neuroscientists. *Neuron*, 89(4), 683–694. <https://doi.org/10.1016/j.neuron.2016.01.040>

- Roth, B. L. (2017). Use of DREADDS. *Neuron*, 89(4), 683–694.  
<https://doi.org/10.1016/j.neuron.2016.01.040>.DREADDs
- Sahibzada, N., Dean, P., & Redgrave, P. (1986). Movements resembling orientation or avoidance elicited by electrical stimulation of the superior colliculus in rats. *Journal of Neuroscience*, 6(3), 723–733. <https://doi.org/10.1523/jneurosci.06-03-00723.1986>
- Salay, L. D., Ishiko, N., & Huberman, A. D. (2018). A midline thalamic circuit determines reactions to visual threat. *Nature*, 557(7704).  
<https://doi.org/10.1038/s41586-018-0078-2>
- Saleem, A. B., Ayaz, A. I., Jeffery, K. J., Harris, K. D., & Carandini, M. (2013). Integration of visual motion and locomotion in mouse visual cortex. *Nature Neuroscience*, 16(12), 1864–1869. <https://doi.org/10.1038/nn.3567>
- Saloman, J. L., Scheff, N. N., Snyder, L. M., Ross, S. E., Davis, B. M., & Gold, M. S. (2016). Gi-DREADD expression in peripheral nerves produces ligand-dependent analgesia, as well as ligand-independent functional changes in sensory neurons. *Journal of Neuroscience*, 36(42), 10769–10781.  
<https://doi.org/10.1523/JNEUROSCI.3480-15.2016>
- Sanchez-Vives, M. V., & McCormick, D. A. (2000). Cellular and network mechanisms of rhythmic recurrent activity in neocortex. *Nature Neuroscience*, 3(10), 1027–1034. <https://doi.org/10.1038/79848>
- Sano, Y., Shobe, J. L., Zhou, M., Huang, S., Shuman, T., Cai, D. J., ... Silva, A. J. (2014). CREB regulates memory allocation in the insular cortex. *Current Biology*, 24(23), 2833–2837. <https://doi.org/10.1016/j.cub.2014.10.018>
- Sattler, N., & Wehr, M. (2020). A head-mounted multi-camera system for electrophysiology and behavior in freely-moving mice Results :

- Schiavo, J. K., Valtcheva, S., Bair-Marshall, C. J., Song, S. C., Martin, K. A., & Froemke, R. C. (2020). Innate and plastic mechanisms for maternal behaviour in auditory cortex. *Nature*, *587*(7834), 426–431. <https://doi.org/10.1038/s41586-020-2807-6>
- Schiff, W., Caviness, J. A., & Gibson, J. J. (1962). Persistent Fear Responses in Rhesus Monkeys to the Optical Stimulus of “Looming.” *Science*, *136*(3520), 982–983. <https://doi.org/10.1126/science.136.3520.982>
- Sebban, C., Tesolin-Decros, B., Millan, M. J., & Spedding, M. (1999). Contrasting EEG profiles elicited by antipsychotic agents in the prefrontal cortex of the conscious rat: Antagonism of the effects of clozapine by modafinil. *British Journal of Pharmacology*, *128*(5), 1055–1063. <https://doi.org/10.1038/sj.bjp.0702893>
- Shang, C., Liu, Z., Chen, Z., Shi, Y., Wang, Q., Liu, S., ... Cao, P. (2015). A parvalbumin-positive excitatory visual pathway to trigger fear responses in mice. *Science*, *348*(6242), 1472 LP – 1477. <https://doi.org/10.1126/science.aaa8694>
- Sheng, H.-Y., Lv, S.-S., Cai, Y.-Q., Shi, W., Lin, W., Liu, T.-T., ... Zhang, Y.-Q. (2020). Activation of ventrolateral orbital cortex improves mouse neuropathic pain-induced anxiodepression. *JCI Insight*, *5*(19), e133625. <https://doi.org/10.1172/jci.insight.133625>
- Siegle, J. H., Jia, X., Durand, S., Gale, S., Bennett, C., Graddis, N., ... Koch, C. (2021). Survey of spiking in the mouse visual system reveals functional hierarchy. *Nature*, *592*(7852), 86–92. <https://doi.org/10.1038/s41586-020-03171-x>
- Sodickson, D. L., & Bean, B. P. (1996). GABA(B) receptor-activated inwardly rectifying potassium current in dissociated hippocampal CA3 neurons. *Journal of*

*Neuroscience*, 16(20), 6374–6385. <https://doi.org/10.1523/jneurosci.16-20-06374.1996>

Speed, A., Del Rosario, J., Burgess, C. P., & Haider, B. (2019). Cortical State Fluctuations across Layers of V1 during Visual Spatial Perception. *Cell Reports*, 26(11), 2868–2874.e3. <https://doi.org/10.1016/j.celrep.2019.02.045>

Stachniak, T. J., Ghosh, A., & Sternson, S. M. (2014). Chemogenetic Synaptic Silencing of Neural Circuits Localizes a Hypothalamus→Midbrain Pathway for Feeding Behavior. *Neuron*, 82(4), 797–808. <https://doi.org/10.1016/j.neuron.2014.04.008>

Stanford, T. R., Quessy, S., & Stein, B. E. (2005). Evaluating the operations underlying multisensory integration in the cat superior colliculus. *Journal of Neuroscience*, 25(28), 6499–6508. <https://doi.org/10.1523/JNEUROSCI.5095-04.2005>

Štih, V., Petrucco, L., Kist, A. M., & Portugues, R. (2019). Stytra: An open-source, integrated system for stimulation, tracking and closed-loop behavioral experiments. *PLoS Computational Biology*, 15(4), 1–19. <https://doi.org/10.1371/journal.pcbi.1006699>

Tafreshiha, A., Burg, S. A. V., Smits, K., Blomer, L. A., & Heimel, J. A. (2021). Visual stimulus-specific habituation of innate defensive behaviour in mice. *Journal of Experimental Biology*, 224(6). <https://doi.org/10.1242/jeb.230433>

Tang, L., & Higley, M. J. (2020). Layer 5 Circuits in V1 Differentially Control Visuomotor Behavior. *Neuron*, 105(2), 346–354.e5. <https://doi.org/10.1016/j.neuron.2019.10.014>

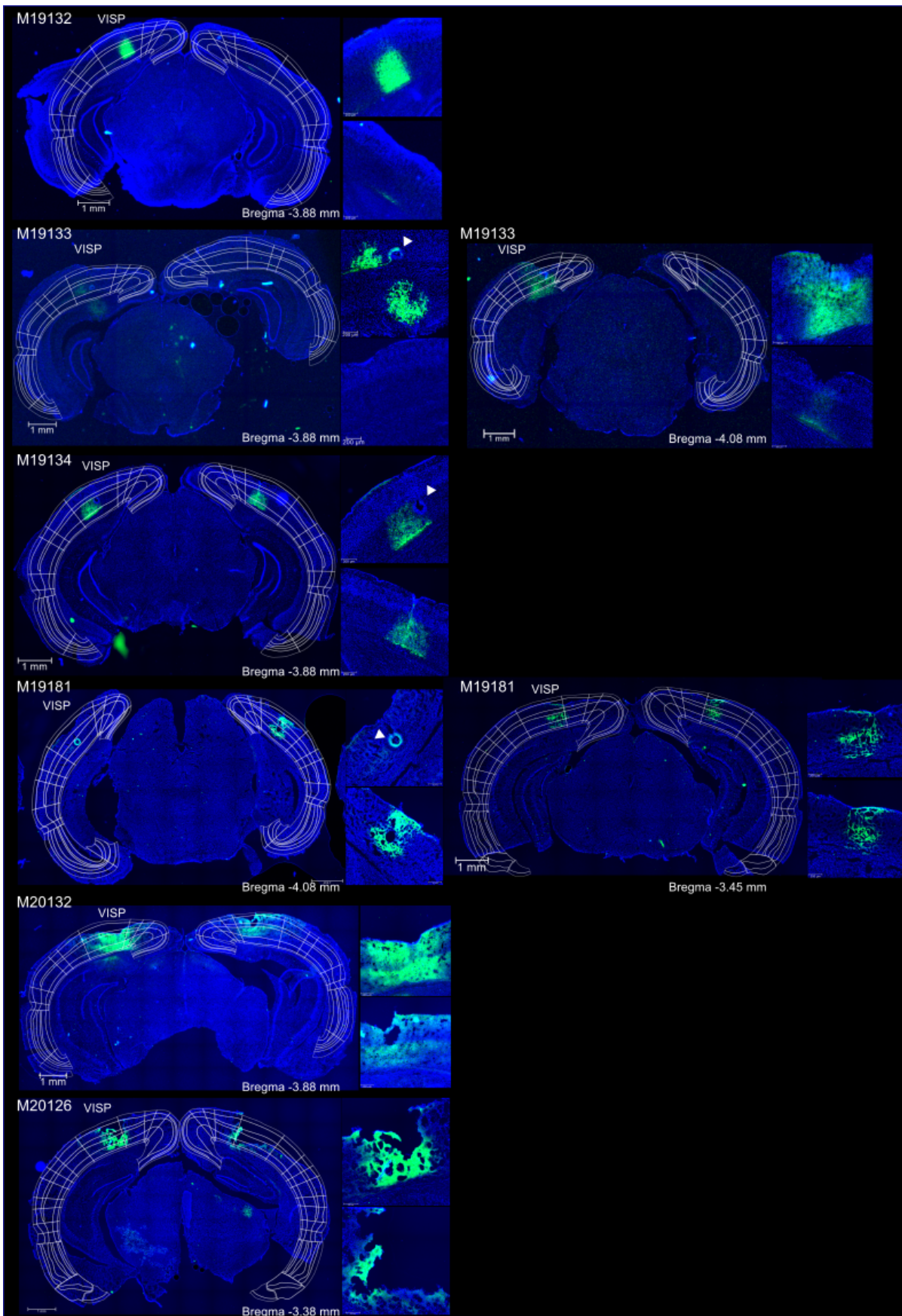
Thompson, K. J., Khajehali, E., Bradley, S. J., Navarrete, J. S., Huang, X. P., Slocum, S., ... Tobin, A. B. (2018). DREADD Agonist 21 Is an Effective Agonist

- for Muscarinic-Based DREADDs in Vitro and in Vivo. *ACS Pharmacology & Translational Science*, 1(1), 61–72. <https://doi.org/10.1021/acsptsci.8b00012>
- Tinbergen, N. (1951). *The study of instinct. The study of instinct*. New York, NY, US: Clarendon Press/Oxford University Press.
- Treviño, M., Fregoso, E., Sahagún, C., & Lezama, E. (2018). An automated water task to test visual discrimination performance, adaptive strategies and stereotyped choices in freely moving mice. *Frontiers in Behavioral Neuroscience*, 12(November), 1–14. <https://doi.org/10.3389/fnbeh.2018.00251>
- Treviño, M., Oviedo, T., Jendritza, P., Li, S. Bin, Köhr, G., & De Marco, R. J. (2013). Controlled variations in stimulus similarity during learning determine visual discrimination capacity in freely moving mice. *Scientific Reports*, 3, 1–13. <https://doi.org/10.1038/srep01048>
- Uka, T., & DeAngelis, G. C. (2004). Contribution of area MT to stereoscopic depth perception: Choice-related response modulations reflect task strategy. *Neuron*, 42(2), 297–310. [https://doi.org/10.1016/S0896-6273\(04\)00186-2](https://doi.org/10.1016/S0896-6273(04)00186-2)
- Ulrich, D., & Huguenard, J. R. (1995). Purinergic inhibition of GABA and glutamate release in the thalamus: implications for thalamic network activity. *Neuron*, 15(4), 909–918. [https://doi.org/10.1016/0896-6273\(95\)90181-7](https://doi.org/10.1016/0896-6273(95)90181-7)
- Vale, R., Campagner, D., Iordanidou, P., Arocas, O. P., Tan, Y. L., & Stempel, A. V. (2020). A cortico-collicular circuit for accurate orientation to shelter during escape.
- Vale, R., Evans, D. A., & Branco, T. (2017). Rapid Spatial Learning Controls Instinctive Defensive Behavior in Mice. *Current Biology*, 27(9), 1342–1349. <https://doi.org/10.1016/j.cub.2017.03.031>
- Vedder, L. C., Miller, A. M. P., Harrison, M. B., & Smith, D. M. (2017). Retrosplenial

- Cortical Neurons Encode Navigational Cues, Trajectories and Reward Locations During Goal Directed Navigation. *Cerebral Cortex (New York, N.Y. : 1991)*, 27(7), 3713–3723. <https://doi.org/10.1093/cercor/bhw192>
- Vetere, G., Kenney, J. W., Tran, L. M., Xia, F., Steadman, P. E., Parkinson, J., ... Frankland, P. W. (2017). Chemogenetic Interrogation of a Brain-wide Fear Memory Network in Mice. *Neuron*, 94(2), 363-374.e4. <https://doi.org/10.1016/j.neuron.2017.03.037>
- Viskaitis, P., Irvine, E. E., Smith, M. A., Choudhury, A. I., Alvarez-Curto, E., Glegola, J. A., ... Withers, D. J. (2017). Modulation of SF1 Neuron Activity Coordinately Regulates Both Feeding Behavior and Associated Emotional States. *Cell Reports*, 21(12), 3559–3572. <https://doi.org/10.1016/j.celrep.2017.11.089>
- Vorhees, C. V., & Williams, M. T. (2006). Morris water maze: Procedures for assessing spatial and related forms of learning and memory. *Nature Protocols*, 1(2), 848–858. <https://doi.org/10.1038/nprot.2006.116>
- Wallace, D. J., Greenberg, D. S., Sawinski, J., Rulla, S., Notaro, G., & Kerr, J. N. D. (2013). Rats maintain an overhead binocular field at the expense of constant fusion. *Nature*, 498(7452), 65–69. <https://doi.org/10.1038/nature12153>
- Wang, C., Yue, H., Hu, Z., Shen, Y., Ma, J., Li, J., ... Gu, Y. (2020). Microglia mediate forgetting via complement-dependent synaptic elimination. *Science*, 367(6478), 688–694. <https://doi.org/10.1126/science.aaz2288>
- Wang, L., Kloc, M., Maher, E., Erisir, A., & Maffei, A. (2019). Presynaptic GABAA receptors modulate thalamocortical inputs in layer 4 of Rat V1. *Cerebral Cortex*, 29(3), 921–936. <https://doi.org/10.1093/cercor/bhx364>
- Wang, Q., & Burkhalter, A. (2013). Stream-Related Preferences of Inputs to the Superior Colliculus from Areas of Dorsal and Ventral Streams of Mouse Visual

- Cortex. *Journal of Neuroscience*, 33(4), 1696–1705.  
<https://doi.org/10.1523/jneurosci.3067-12.2013>
- Wang, Y.-C., Galeffi, F., Wang, W., Li, X., Lu, L., Sheng, H., ... Yang, W. (2020). Chemogenetics-mediated acute inhibition of excitatory neuronal activity improves stroke outcome. *Experimental Neurology*, 326, 113206.  
<https://doi.org/10.1016/j.expneurol.2020.113206>
- Ward, R. D., Winiger, V., Kandel, E. R., Balsam, P. D., & Simpson, E. H. (2015). Orbitofrontal cortex mediates the differential impact of signaled-reward probability on discrimination accuracy. *Frontiers in Neuroscience*, 9(JUN), 1–9.  
<https://doi.org/10.3389/fnins.2015.00230>
- Watanabe, S., Scheich, H., Braun, K., & Shinozuka, K. (2021). Visual snake aversion in Octodon degus and C57BL/6 mice. *Animal Cognition*.  
<https://doi.org/10.1007/s10071-021-01527-y>
- Wei, P., Liu, N., Zhang, Z., Liu, X., Tang, Y., He, X., ... Wang, L. (2015). Processing of visually evoked innate fear by a non-canonical thalamic pathway. *Nature Communications*, 6, 6756. <https://doi.org/10.1038/ncomms7756>
- Weiskrantz, L. (2009). Is blindsight just degraded normal vision? *Experimental Brain Research*, 192(3), 413–416. <https://doi.org/10.1007/s00221-008-1388-7>
- Wen, W., & Turrigiano, G. G. (2021). Developmental Regulation of Homeostatic Plasticity in Mouse Primary Visual Cortex. *The Journal of Neuroscience*, 41(48), 9891–9905. <https://doi.org/10.1523/jneurosci.1200-21.2021>
- Weston, M., Kaserer, T., Wu, A., Mouravlev, A., Carpenter, J. C., Snowball, A., ... Lieb, A. (2019). Olanzapine: A potent agonist at the hM4D(Gi) DREADD amenable to clinical translation of chemogenetics. *Science Advances*, 5(4), 1–7.  
<https://doi.org/10.1126/sciadv.aaw1567>

- Wu, C. H., Ramos, R., Katz, D. B., & Turrigiano, G. G. (2021). Homeostatic synaptic scaling establishes the specificity of an associative memory. *Current Biology*, 31(11), 2274-2285.e5. <https://doi.org/10.1016/j.cub.2021.03.024>
- Yilmaz, M., & Meister, M. (2013). Rapid innate defensive responses of mice to looming visual stimuli. *Current Biology*, 23(20), 2011–2015. <https://doi.org/10.1016/j.cub.2013.08.015>
- Zhang, X., An, X., Liu, H., Peng, J., Cai, S., Wang, W., ... Yang, Y. (2015). The Topographical Arrangement of Cutoff Spatial Frequencies across Lower and Upper Visual Fields in Mouse V1. *Scientific Reports*, 5, 1–9. <https://doi.org/10.1038/srep07734>
- Zhao, X., Liu, M., & Cang, J. (2014). Visual cortex modulates the magnitude but not the selectivity of looming-evoked responses in the superior colliculus of awake mice. *Neuron*, 84(1), 202–213. <https://doi.org/10.1016/j.neuron.2014.08.037>
- Zingg, B., Chou, X. lin, Zhang, Z. gang, Mesik, L., Liang, F., Tao, H. W., & Zhang, L. I. (2017). AAV-Mediated Anterograde Transsynaptic Tagging: Mapping Corticocollicular Input-Defined Neural Pathways for Defense Behaviors. *Neuron*, 93(1), 33–47. <https://doi.org/10.1016/j.neuron.2016.11.045>
- Zoccolan, D., Oertelt, N., DiCarlo, J. J., & Cox, D. D. (2009). A rodent model for the study of invariant visual object recognition. *Proceedings of the National Academy of Sciences*, 106(21), 8748–8753. <https://doi.org/10.1073/pnas.0811583106>



## **Appendix I. hM4Di expression and the location of LFP electrode in different mice.**

Example images of the hM4Di mouse in LFP recording were included in the panel. hM4Di expression (in green) was found in all of the mice. LFP electrodes were identified in M19133, M19134 and M19181. In M19133 and M19181, maximum hM4Di expression and LFP electrode were found at different slices, hence both slices were included. DAPI expression is marked in blue. White triangles denote the location of LFP electrode. No obvious electrode site was identified in M19133, M20126 and M20132. VISP is shorted for primary visual cortex. White lines denote cortical areas, modified from Allen Brain Atlas 2011 version. The distance from Bregma (shown at the bottom right of each image) is referred from similar images in the 2008 version of the reference atlas.